University of Alberta Library
0 1620 2918375 1

Digitized by the Internet Archive
in 2026 with funding from
University of Alberta Library

https://archive.org/details/0162029183751

University of Alberta

Cys-Loop Receptor Pharmacology: Alterations in Agonist or Receptor Structure may Provide Insight into Receptor Function

by

Christian Carter

Special Collections Library

A thesis submitted to the Faculty of Graduate Studies and Research
in partial fulfillment of the requirements for the degree of

Doctor of Philosophy

Department of Pharmacology

©Christian Carter
Fall 2010
Edmonton, Alberta

Permission is hereby granted to the University of Alberta Libraries to reproduce single copies of this thesis and to lend or sell such copies for private, scholarly or scientific research purposes only. Where the thesis is converted to, or otherwise made available in digital form, the University of Alberta will advise potential users of the thesis of these terms.

The author reserves all other publication and other rights in association with the copyright in the thesis and, except as herein before provided, neither the thesis nor any substantial portion thereof may be printed or otherwise reproduced in any material form whatsoever without the author's prior written permission.

Examining Committee

Dr. Peter Light, Pharmacology

Dr. John Peters, Pharmacoloogy

Dr. Susan Dunn, Pharmacology

Dr. Peter Smith, Pharmacology

Dr. William Dryden, Pharmacology

Dr. Marek Duszyk, Physiology

ABSTRACT

The Cys-loop family of LGICs plays a crucial role in chemical synaptic transmission throughout the CNS and includes receptors that are activated by acetylcholine (Ach), serotonin (5-HT), γ-aminobutyric acid (GABA) and glycine (Gly). The Cys-loop family of LGICs were named after a characteristic highly conserved signature sequence of 13 amino acid residues flanked by cysteines that is present in each family member. This receptor family is an area of great interest for multiple disease processes and are targets for clinically significant pharmacotherapies.

Recent advances in the elucidation of receptor structure have led to an abundance of work attempting to describe the dynamic properties responsible for receptor activation. To investigate receptor-agonist interactions, alterations in the structure of the agonist or receptor may be introduced. Here we manipulate the structure of the ligand while observing the binding and functional properties of a series of bischoline agonists at recombinant *Torpedo* nAChRs expressed in *Xenopus* oocytes. Bischoline compounds show an increase in apparent affinity and potency with increasing interonium length. However, bischoline compounds shorter than 16 Å display weak partial agonist properties at the *Torpedo* nAChR.

Alternatively, by changing the receptor's structure via site-directed mutagenesis it is possible to elucidate the role that individual amino acids may play in agonist interactions. Cys-loop receptors are dynamic proteins that undergo agonist-induced conformational changes. Predictions from

homology models of the α1β2γ2 $GABA_AR$ suggest binding loops C and F come into close proximity upon interaction with agonist. We performed site-directed mutagenesis creating the mutant receptor α1V205Cβ2V223Cγ2, predicting that, upon interaction with agonist, these two cysteine residues would come into close proximity to form a disulphide bond locking the C-loop in the capped position. Recombinant receptors were expressed in *Xenopus* oocytes but we were unsuccessful in trapping the C-loop in the capped conformation, suggesting our predictions of residue location or residue motion may be inaccurate.

In addition, we investigated the role of a conserved arginine residue in binding loop D at the synaptic α1β2γ2 and extrasynaptic α4β3δ $GABA_ARs$. Homology modeling and ligand docking studies predict the residue α1R94 may play a larger role in stabilizing GABA than THIP in the binding pocket whereas the homologues residue α4R100 may play a larger role in stabilizing THIP than GABA. We performed the charge conserving α1R94K and α4R100K mutations and carried out functional studies of the effect of GABA and THIP on recombinant wild-type and mutant receptors expressed in *Xenopus* oocytes. Our data suggest that this arginine residue plays a larger role in the stabilization of THIP than GABA in the binding pocket of each receptor. In addition, there is a decrease in the efficacy of THIP observed in the α1R94Kβ2γ2 receptor relative to its wild-type. However, there is no decrease in the efficacy of THIP observed at the α4R100Kβ3δ receptor relative to its wild-type receptor.

ACKNOWLEDGEMENTS

There are so many people to thank for their support throughout my research and study in this degree program, that to be honest, I have no idea where to start. I am very grateful to my supervisor, Dr. Susan Dunn for taking me in to her lab and allowing me to carry out my work, as well as the many afternoon drinks discussing science, life, the past, the present and the future. I would also like to thank my co-supervisor Dr. Peter Smith, who has offered encouragement at every stage of this long process as well as his wife Mrs. Anne Smith who has taken me under her wing as well. I would also like to thank Dr. William Dryden, who although is titled as a committee member played the role of 2nd co-supervisor on many occasions and first accepted me into his lab as a young naïve, excited undergraduate student looking to explore the world of science. To Susan, Bill and Peter, I thank you for all your time and patience, as well as many hours discussing science over many beverages. I would also like to thank Dr. Ian Martin, who has assisted me in more ways than I am sure I am aware of, from scientific to just calming me down and providing a laugh, you've helped me out at times that really matter and for that I am grateful.

There have been many faces to come through the 9th floor of MSB and many of these I have called friends. Thank you to Isabelle Paulsen for her guidance, friendship and patience. The same can be said for Dr. Janna Kozuska who has really come through for me on more than one occasion, and has been a good friend since the beginning of my grad studies. Sheldon Michaelson, thank you too, for making me smile and your friendship, though you were a late addition you are appreciated. Thank you to Dr. William Colmers for all the wonderful conversations and drinks, its been a pleasure. Thank you to Mr. Ray Kozak, without you I would have been lost in computer failure and would have never gotten out, and thank you for being entertaining though I may not remember all the specifics.

Thank you to all the many friends I've had and held on to over the years. All the people from Edson, the bar industry, school and the gym with whom I've had the pleasure of being friends with (Switzer, Kaz, Willy, Tang, Zaptown, Chad, Fil, Codey, Joey, Jono, Robbie, Kwai, Evan, James, Plumer, Wes, Quinlan, Lonny, Jarvis, Dr. Wang too many to list), many of whom have seen me at my best and my worst. If we've shared a table and a drink in the last decade then you have played a role in my education that requires acknowledgement. You know who you are.

Last but not least, thank you to my family, my parents John and Gail Carter for raising me, as well as my brother Clayton and sister Carrie-Lynn, as much as you may not want to admit it you two played a part in making me who I am. Thank you to my second family, Charles, Parkash and Tony for welcoming me with open arms and treating me like one of their own. And finally thank you to the love of my life, my wife Sheena, for all that you have done for me and put up with you deserve an honorary degree, I love you and appreciate all that you do. In addition, I would like to thank the compound ethanol for being present in so many delicious beverages and helping me cope with school and life for over a decade, as well as a special thanks to George Lucas for telling the second best story ever told, Star Wars, second only to the pages you are about to read.

TABLE OF CONTENTS

Page

CHAPTER 1- Introduction 1

Introduction..... 2

Structural Insights..... 4

Extracellular/Ligand Binding Domain..... 8

TMDs and Channel Gate..... 9

Intracellular Loops and MA Helixies..... 12

Channel Function..... 14

C-Loop and Pre-M1 Region..... 16

The Cys-loop, Loops 2 and 9..... 18

M2-M3 Linker..... 20

nAChRs..... 20

Neuronal nAChRs..... 23

Neuronal nAChRs and Calcium Regulation..... 24

Subcellular Localization of Neuronal nAChRs..... 25

nAChR Regulation of Gene Expression..... 26

$GABA_AR$s..... 27

$GABA_AR$ Genes..... 27

$GABA_AR$ Heterogeneity..... 29

Phasic and Tonic Inhibition..... 30

Synaptic Targeting of $GABA_AR$s 33

$GABA_AR$ Pharmacology 34

Agonists 34

Antagonists 36

Allosteric Modulators 37

The Benzodiazepines 37

Barbiturates 39

Neurosteroids 40

Aims of Present Study 41

References 59

CHAPTER 2 – Chain Length Dependence of Interactions of Bisquaternary Ligands with the *Torpedo* nAChR 81

Introduction 82

Materials and Methods 85

Materials 85

Preparation of nAChR-Enriched Membrane Fragments 86

Equilibrium Binding of [^{3}H]ACh and [^{3}H]SbCh to Membrane-Bound nAChR 87

Competition Assays 88

Thallium (1) Flux Assays 88

In Vitro Transcription 89

Expression in *Xenopus* Oocytes and Electrophysiology 90

Data Analysis 91

Results 93

Binding of [^{3}H]ACh and [^{3}H]SbCh to *Torpedo* Membrane Preparations 93

Apparent Affinities of the Bischoline Esters Measured in Competition Assays 94

The Effects of ACh and SbCh on Activation of *Torpedo* Expressed in *Xenopus* Oocytes 95

Potency of Bischoline Esters 96

Efficacies of the Bischoline Ligands 97

Discussion 98

References 114

CHAPTER 3 – C-Loop Trapping 119

Introduction 120

Materials and Methods 125

Materials 125

Comparative Modeling 125

Mutagenesis 126

In Vitro Transcription 127

Expression in *Xenopus* Oocytes and Electrophysiology 127

C-Loop Trapping and Alkylating Experiments 128

Data and Statistical Analysis 129

Results..... 130

Structural Modeling..... 130

Potency of GABA on Wild-Type and Mutant Receptors..... 130

C-Loop Trapping/Steric Hindrance Experiments..... 131

Discussion..... 132

References..... 150

CHAPTER 4 - D-Loop Arginine and its Role in Receptor Function in the α1β2γ2 and α4β3δ $GABA_A$Rs 155

Introduction..... 156

Materials and Methods..... 160

Materials..... 160

Comparative Modeling..... 160

Ligand Docking..... 161

Mutagenesis..... 162

In Vitro Transcription..... 163

Expression in *Xenopus* Oocytes and Electrophysiology..... 163

Statistical Analysis..... 164

Results..... 165

In silico Modeling of the α1β2γ2 and α4β3δ $GABA_A$Rs Docked with GABA and THIP..... 165

Potency of GABA on Wild-Type and Mutant Receptors..... 165

Potency of THIP on Wild-Type and Mutant Receptors..... 166

Efficacy of THIP at Wild-Type and Mutant Receptors..... 167

Discussion..... 168

References..... 187

CHAPTER 5 – General Discussion 193

General Discussion..... 194

Conclusions and Future Directions..... 202

References..... 206

LIST OF TABLES

		Page
Table 2-1	Summary of binding and functional data for the effects of bischoline esters using native *Torpedo* membrane vesicles or recombinant *Torpedo* nAChRs expressed in *Xenopus* oocytes	113
Table 4-1	Summary of functional data for the effects of GABA and THIP at recombinant α1β2γ2, α1R94Kβ2γ2, α4β3δ and α4R100Kβ3δ $GABA_A$Rs expressed in *Xenopus* oocytes	186

LIST OF FIGURES

		Page
Figure 1-1	A cartoon representation of a Cys-loop receptor.	44
Figure 1-2	A cartoon representation of single subunit from a Cys-loop receptor.	45
Figure 1-3	Profile view of *Torpedo* nAChR channel associated with the membrane.	46
Figure 1-4	A depiction of a *Torpedo* nAChR in the lipid bilayer spanning (TMD) region.	47
Figure 1-5	(A) A synaptic view of the AChBP pentamer. (B) A view of AChBP perpendicular to its five-fold axis.	48
Figure 1-6	(A) Ribbon diagram of the *Torpedo* nAChR as viewed from the synaptic cleft and (B) parallel with the membrane plain.	49
Figure 1-7	Ribbon diagram of a single nAChR α subunit viewed viewed parallel with the membrane plane in an orientation such that the central axis of the pentamer is at the back (A) and to the side.	50
Figure 1-8	A schematic representation of the 'six loop' binding model.	51
Figure 1-9	Schematic representation of the open state conformation of two M2 segments from Cys-loop receptors	52

Figure 1-10 Electrostatic potential surface representations showing portals for cation conductance between MA helices in the *Torpedo* nAChR. 53

Figure 1-11 Ribbon diagrams of AChBP in the presence and absence of ligand (A) and of Loop C movement in the presence of various ligands (B). 54

Figure 1-12 (A) Ribbon diagram of the pentameric structure of the *Torpedo* nAChR. (B) Close up view of coupling of the pre-M1 and loop 2 domains. 55

Figure 1-13 (A) Ribbon diagram of the side view of an α subunit from the *Torpedo* nAChR. (B) Close up view of the binding-channel interface. 56

Figure 1-14 Dendrogram showing the sequence relationships of 19 human genes encoding $GABA_AR$ subunits. 57

Figure 1-15 Cartoon depiction of phasic and tonic inhibition. 58

Figure 2-1 The structure of the bischoline analogues. 107

Figure 2-2 A model illustrating how SbCh may cross-link two subsites in the *Torpedo* nAChR 108

Figure 2-3 (A) Representative data for equilibrium binding of [^{3}H]ACh and [^{3}H]SbCh to *Torpedo* nAChR enriched membrane fragments. (B) Representative data for bischoline displacement of [^{3}H]ACh. 109

Figure 2-4 The relative affinities of bischoline analogues for

the membrane bound *Torpedo* nAChR measured in competitive binding assays. 110

Figure 2-5 Functional responses of ACh and SbCh. (A) Thallium flux assays performed at the native *Torpedo* nAChR. (B) Concentration-effect curves from recombinant *Torpedo* nAChR expressed in *Xenopus* oocytes. 111

Figure 2-6 Potency (A) and efficacy (B) studies of the bischoline analogues performed at recombinant *Torpedo* nAChRs expressed in *Xenopus* oocytes. 112

Figure 3-1 Ribbon diagram of the α1β2γ2 $GABA_AR$ adapted from Unwin's structure of the *Torpedo* nAChR. 137

Figure 3-2 Protocol for C-loop trapping experiments. 138

Figure 3-3 Protocol for steric hindrance experiments. 139

Figure 3-4 Molecular model of C and F loops and their proximity in the apo- and agonist-bound state. 140

Figure 3-5 Concentration-effect curves for GABA acting on the wild-type α1β2γ2 $GABA_AR$. 141

Figure 3-6 Concentration-effect curves for GABA at the wild-type α1β2γ2 and mutant α1V205Cβ2γ2 $GABA_ARs$. 142

Figure 3-7 Concentration-effect curves for GABA at the wild-type α1β2γ2 and mutant α1β2V223Cγ2 $GABA_ARs$. 143

Figure 3-8 Concentration-effect curves for GABA at the wild-type α1β2γ2 and mutant α1V205Cβ2V223Cγ2

	$GABA_AR$s.	144
Figure 3-9	Compilation of concentration-effect curves of GABA at the wild-type α1β2γ2 and mutant α1V205Cβ2γ2, α1Cβ2V223Cγ2 and α1V205Cβ2V223Cγ2 $GABA_AR$s.	145
Figure 3-10	Representative current traces following a 100 μM GABA challenge.	146
Figure 3-11	Statistical analysis of the effect of Cu:Phen and DPDPB.	147
Figure 3-12	Statistical analysis of the effect of iodoacetamide and DTNB.	148
Figure 3-13	Protein sequence alignments of various AChBPs and $GABA_AR$ subunits.	149
Figure 4-1	Protein sequence alignments of $GABA_AR$ α subunits.	175
Figure 4-2	Docked cluster of the agonists GABA and THIP in the in the binding pocket of the α1β2γ2 $GABA_AR$.	176
Figure 4-3	Docked cluster of the agonists GABA and THIP in the in the binding pocket of the α4β3δ $GABA_AR$.	177
Figure 4-4	Concentration-effect curves for GABA at the wild-type α1β2γ2 and α4β3δ $GABA_AR$s.	178
Figure 4-5	Concentration-effect curves for GABA at the wild-type α1β2γ2 and mutant α1R94Kβ2γ2 $GABA_AR$s.	179
Figure 4-6	Concentration-effect curves for GABA at the wild-type α4β3δ and mutant α4R100Kβ3δ $GABA_AR$s.	180
Figure 4-7	Concentration-effect curves for THIP at the wild-	

type α1β2γ2 and α4β3δ $GABA_A$Rs. 181

Figure 4-8 Concentration-effect curves for THIP at the wild-type α1β2γ2 and mutant α1R94Kβ2γ2 $GABA_A$Rs. 182

Figure 4-9 Concentration-effect curves for THIP at the wild-type α4β3δ and mutant α4R100Kβ3δ $GABA_A$Rs. 183

Figure 4-10 Statistical analysis of the potency of the agonists GABA and THIP at wild-type and mutant $GABA_A$Rs. 184

Figure 4-11 Statistical analysis of the efficacy of THIP at wild-type $GABA_A$Rs compared to their respective mutants. 185

LIST OF ABBREVIATIONS AND SYMBOLS

14AA	imidazole-4-acetic acid
ACh	acetylcholine
AMP	adenosine monophosphate
ANOVA	analysis of variance
ANTS	8-amino-1,3,6-naphthalene trisulfonic acid
α-BgTx	α-bungarotoxin
AChBP	acetylcholine binding protein
BIG2	brefeldin A-inhibited GDP'GTP exchange factor 2
Bis-Q	cis-3,3'-bis[α-(trimethylammonium)methyl]azobenzene dibromide
cDNA	complementary deoxyribonucleic acid
CICR	calcium-induced calcium release
CNS	central nervous system
CREB	phospho-cyclic AMP response element-binding protein
cRNA	complementary ribonucleic acid
Cu:Phen	Cu:Phenanthroline
DMSO	dimethyl sulfoxide
DNPP	diethyl-p-nitrophenyl phosphate
DPDPB	1,4-d[3'-(2'pyridyldithio)-propionamido]butane
DTNB	5,5'-dithiobis(2-nitrobenzoic acid)
DTT	dithiothreitol

EC_{50}	half-maximal concentration required for channel activation
ECD	extracellular domain
ELIC	prokaryotic Cys-loop receptor homologue from *Erwinia chrysanthemi*
GABA	γ-aminobutyric acid
$GABA_AR$	γ-aminobutyric acid type-A receptor
$GABA_BR$	γ-aminobutyric acid type-B receptor
$GABA_CR$	γ-aminobutyric acid type-C receptor
GABARAP	$GABA_AR$-associated protein
GLIC	prokaryotic Cys-loop receptor homologue from *Globebacter violaceus*
Gly	glycine
GlyR	glycine receptor
GRIF-1	$GABA_AR$ interacting factor-1
HEPES	4-(hydroxyethyl)-1-piperazineethanesulfonic acid
5-HT	5-hydroxytryptamine
$5\text{-}HT_3R$	5-hydroxytryptamine type-3 receptor
IANBD	4-[N-[(2-iodoacetoxy)ethyl]-N-methylamine]-7-nitrobenzene-2-oxa-1,3-diazole
IC_{50}	concentration of unlabeled ligand that causes 50% displacement
I_{Max}	maximal response
K_D	equilibrium ligand dissociation constant

K_I	equilibrium inhibitor dissociation constant
KNF	Koshland-Nemethy-Filmer
LBD	ligand binding domain
LGIC	ligand-gated ion channel
mAChR	muscarinic acetylcholine receptor
MWC	Monod-Wyman-Changeux
nAChR	nicotinic acetylcholine receptor
NMJ	neuromuscular junction
NTP	nucleotide triphosphate
P4S	piperidine-4-sulphonic acid
PC12	pheochromocytoma cell line
PNS	peripheral nervous system
RNA	ribonucleic acid
SbCh	suberyldicholine
SEM	standard error of the mean
Thio-4-PIOL	5-(4-piperidyl)-3-isothiazolol
THIP	4,5,6,7-tetrahydroisoxazolo[5,4]pyridin-3-ol
VOCC	voltage-operated calcium channel
ZAPA	Z-3-[(aminoiminomethyl)thio]prop-2-enoic acid

CHAPTER 1

Introduction

INTRODUCTION

The mammalian central nervous system (CNS) is an extremely complex network comprised of billions of neurons signaling in a finely tuned interplay to communicate with each other. The main process by which communication between neurons is achieved is by chemical synaptic transmission. This method of communication offers the advantage of signal amplification and a great potential for modulation, both being important properties for higher brain activity. Chemical synaptic transmission takes place when the depolarization of the presynaptic neuron causes the release of neurotransmitter into the synaptic cleft. After the transmitter diffuses across the synaptic cleft, it may interact with receptors on the postsynaptic neuron. Ligand-gated ion channels (LGICs) are a superfamily of receptors responsible for converting the synaptic chemical signal into the alteration of the postsynaptic membrane's electrical activity. This is accomplished via the rapid gating of an ion channel, which allows the flux of ions across the postsynaptic membrane. Another important feature of LGICs is their rapid responses. Channel gating occurs within a few microseconds following transmitter association. Thus a fully functioning CNS is a finely tuned concert of moment-to-moment communication which relies heavily on the rapid gating response of LGICs, leaving no question as to why this is an extremely complicated field of study.

The Cys-loop family of LGICs plays a crucial role in chemical synapses throughout the CNS and includes receptors that are activated by acetylcholine (ACh), serotonin (5-HT), γ-aminobutyric acid (GABA) and glycine (Gly) (Unwin, 1995; Sine and Engel, 2006). The Cys-loop family of LGICs was named after a characteristic, highly conserved, signature sequence of 13 amino acid residues flanked by bridged cysteines which is present in each family member. In the tertiary structure of a correctly folded receptor this loop is situated at the interface between the extracellular ligand-binding domain (LBD) and the transmembrane domains (TMDs). The Cys-loop family of LGICs is an area of great interest for multiple disease processes and the members are targets for clinically significant pharmacotherapies. Cys-loop receptors are an important target for a battery of widely used pharmaceuticals including neuromuscular blockers such as succinylcholine acting at the muscle type nicotinic acetylcholine receptor (nAChR), benzodiazepines and barbiturates at the γ-aminobutyric acid type A receptors ($GABA_A$Rs) and the anti-emetic setrons, acting at the $5\text{-}HT_3$Rs that are used in the treatment of chemotherapy-induced emesis. Recently, there has been a well documented increase in the number of conditions shown to be caused either by defective functioning of Cys-loop receptors, or are susceptible to amelioration by agents acting at these receptors (Lindstrom, 1997; Korpi et al., 2002; Le Novere et al., 2002; Barik and Wonnacott, 2009). These conditions include hereditary epilepsies, hyperactivity disorder, attention-deficit disorder, schizophrenia, autism, autoimmune autonomic

neuropathies, myasthenia gravis, congenital myasthenic syndromes, anxiety disorders, insomnia, obsessive compulsive disorder, alcoholism and emesis (Bera et al., 2002; Sine and Engel, 2006; Kalamida et al., 2007). In vertebrates, the Cys-loop family of receptors can be either cation selective, namely the nAChR and the 5-HT type-three receptors (5-HT_3Rs) or anion selective, i.e., the $GABA_A$Rs and the glycine receptors (GlyRs). There is a larger diversity of Cys-loop receptors in invertebrates where there are 5-HT, glutamate, ACh, histamine and biogenic amine anionic channels and GABA-gated cation channels (Jones and Sattelle, 2008; Ringstad et al., 2009). The ion selectivity of the LGICs for cations or anions in conjunction with the driving force upon the selected ions dictates individual ionic movements, and therefore the type of response. These may be excitatory for cationic channels as they allow membrane depolarization via the influx of Na^+ ions into the cell, and inhibitory for anionic channels as they cause membrane hyperpolarization via the influx of Cl^- ions into the cell.

STRUCTURAL INSIGHTS

Although the primary focus of this work is on the *Torpedo* nAChR and $GABA_A$R, a portion of the structural information is taken from other members of the Cys-loop LGIC family. Homology modeling is based on the observation that structure is much more conserved in protein families than their primary sequences. Using this knowledge, the unknown structure of a protein can be predicted by comparing it sequence to another member of the fold family (i.e.

a family of proteins with a similar folding pattern) of resolved structure (Schonbrun et al., 2002). Before the turn of the century, detailed structural models of the Cys-loop family did not exist (fig 1-1 and 1-2). Only glimpses of the pentameric structure were provided by low resolution images of the *Torpedo* nAChR via cryo-electron microscopy (Unwin, 1993, 1995) (fig 1-3 and 1-4). These low resolution structures provided us with a rudimentary knowledge of the shape and dimensions of the nAChR protein.

In the last decade, two major breakthroughs have occurred which have allowed us to generate models of Cys-loop receptors with increasing accuracy. The first came in 2001 with the crystallization of an acetylcholine binding protein (AChBP). This is a soluble 210 amino acid, glial released protein which forms homopentamers and acts as an ACh buffer in the snail, *Lymnaea stagnalis* (Brejc et al., 2001). The crystal structure of AChBP was first resolved to 2.7 Å (fig 1-5) and this revealed it to be a structural homolog of the extracellular ligand-binding domain of the nAChR. This protein was shown to interact with classical nAChR agonists and antagonists, which displayed similar pharmacological affinities to the full nAChR (Changeux and Edelstein, 2001; Grutter and Changeux, 2001; Karlin, 2002). It should be noted that although the AChBP contains structures homologous to the N-terminal binding domain of a Cys-loop receptor, it lacks the TMD. In 2004, Bouzat et al. generated a homopentameric chimeric complex that combined the N-terminal LBD from AChBP and the TMDs and intracellular domain of a

5-HT3AR subunit (Bouzat et al., 2004). Although this chimeric receptor bound ACh, it could not be activated by ACh. In order to produce a completely functioning chimeric protein, residues from three loops present at the LBD-TMD interface (Cys-loop, loops 2 and 9) had to be mutated in the AChBP to their counterparts in the 5-HT3AR subunit (Bouzat et al., 2004). Such results suggest that the tertiary structure of AChBP provides a functional model to interpret the interaction of ligands with the LBD of the Cys-loop receptors.

The second breakthrough came in 2005 with the further refinement of the *Torpedo* nAChR structure to a resolution of 4Å via cryo-electron microscopy with image reconstruction (Unwin, 2005). This study shed light on the orientation of the protein backbone, location of α-carbons and bulky side chains. However, it gave only a limited resolution of small side chains and their orientation (fig 1-6). Combined with the crystal structure of AChBP, this structure was used to create a refined 4 Å model of the complete receptor in what is proposed to be a channel closed state (Unwin, 2005). Unwin has provided us with the highest resolution structural model of a complete Cys-loop receptor to date. Each of the receptor subunits are of similar size, with the same three-dimensional folding pattern. The heteropentameric receptor was shown to be approximately 160 Å in length and contains three general structural domains: (1) the N-terminal ligand binding domain (LBD), also referred to as the extracellular domain (ECD)

which forms a central vestibule with a diameter of ~20 Å and a length of ~60 Å, (2) the TMD which forms a 40 Å long water filled narrow channel pore and (3) an intracellular domain which contains the membrane associated (MA) helix and forms a smaller intracellular vestibule with narrow lateral openings to allow the flow of ions into the cell (Unwin, 2005). These previous works led the way for a new era in the elucidation of Cys-loop receptor structure as well as the dynamic process linking ligand binding to channel gating. Previous homology modeling and crystallization studies have attempted to elucidate the allosteric changes in the protein mediated by interaction with agonist (Celie et al., 2004; Bourne et al., 2005; Celie et al., 2005a; Hansen et al., 2005; Dellisanti et al., 2007). Crystal structures of AChBP in the presence of α-conotoxins, α-cobratoxin and nAChR agonists (nicotine, carbamylcholine, lobeline and epibatidine) have been resolved (Celie et al., 2004; Bourne et al., 2005; Celie et al., 2005b; Hansen et al., 2005; Ulens et al., 2006). In addition, a crystal structure of a homopentamer comprised of extracellular domains of the α1 nAChR subunit in the presence of α-bungarotoxin (α-BgTx) has also provided structural information (Dellisanti et al., 2007). Such studies have helped to shed light on precisely which residues play a role in the binding pocket, enabling us to create structural models of binding sites in Cys-loop receptors and the docking of ligands within them (see chapter 4).

EXTRACELLULAR/LIGAND BINDING DOMAIN

The extracellular LBD of each Cys-loop receptor subunit contains a short N-terminal α-helix, 10 β-strands and multiple loops. The 10 β-strands are separated into an inner and outer sheet with β-strands 1, 2, 3, 5, 6 and 8 making up the inner sheet while β-strands 4, 7, 9 and 10 comprise the outer sheet. These two sheets are connected by the receptor's characteristic Cys-loop to form a "β-sandwich" which surrounds a hydrophobic inner core (Unwin, 2005) (fig 1-7). Each Cys-loop receptor can contain two to five binding sites for agonist depending on the subunit composition of the receptor. Binding sites are positioned at subunit interfaces where there are six conserved non-contiguous "loops" of amino acids, known as loops A-F (Corringer et al., 2000) (fig 1-8). It should noted that although the loops A-F are referred to as loops this was based on earlier ideas (Galzi et al., 1991) that pre-dated structural refinement of these regions. It is now clear that some of the proposed loops are actually β-sheets. In a simplistic model each subunit donates three of the six loops with loops A (which corresponds to β4-β5 loop), B (β7-β8 loop), and C (β9-β10 loop) coming from the "principal subunit" and loops D, E, and F (β8-β9 loop) provided by the "complementary subunit"(Corringer et al., 2000).

Binding sites are thought to be formed by these loops at subunit interfaces. In the muscle type nAChR, two non-equivalent ACh binding sites occur at the α-γ and α-δ subunit interfaces (Stroud et al., 1990; Changeux et

al., 1992). At these sites, the α subunit plays the role of the principal subunit while the δ or γ subunit act as the complementary subunit. In heteropentameric neuronal nAChRs (e.g. α4β2), the binding sites for ACh are located at the α-β subunit interface, whereas in homopentameric nAChRs (e.g. α7) the binding sites are located at α-α subunit interfaces. GABA binding sites on the $GABA_A$Rs occur at the β-α interface.

TMDS AND CHANNEL GATE

The difficulty of crystallizing large transmembrane proteins such as the members of the Cys-loop family of LGICs has left us void of a complete crystal structure. However, cryo-electron microscopy studies of the *Torpedo* nAChR and recent crystal structures of ancestral prokaryotic LGICs from the organisms *Erwinia chrysanthemi* (ELIC) and *Gloebacter violaceus* (GLIC) have confirmed earlier ideas and have given us new ones regarding Cys-loop receptor pore structure (Unwin, 2005; Hilf and Dutzler, 2008; Bocquet et al., 2009). Each Cys-loop receptor subunit contains four α-helical TMDs of ~20 amino acids designated M1 to M4 that comprise the integral ion conducting central channel. The M4 domain of each subunit lies in the periphery and interacts with membrane lipid and the M1/M3 domains, while M1/M3 domains help to anchor the M2 domain into place. An abundance of experimental evidence indicates that the ion channel is located along the fivefold axis of symmetry of the heteropentamer with each subunit

contributing its M2 domain to the lining of the channel (Unwin et al., 2002; Unwin, 2005; Hilf and Dutzler, 2008; Bocquet et al., 2009; Hilf and Dutzler, 2009b, a). The TMDs are connected via intra- and extra-cellular loops; loops connecting M1 to M2 and M2 to M3 are shorter peptides (approximately 10 amino acids long) while the M3 to M4 linker is considerably larger. Charged amino acid residues flank the M2 segment of most LGIC receptors. Generally a net positive charge is present at the intra and extracellular openings of anion selective channels, whereas there is a net negative charge in cation selective channels (Keramidas et al., 2004) (figure 1-9). One example is found in the $GABA_AR$ $\alpha1$, $\beta2$ and $\gamma2$ subunits. Here there are positively charged arginine residues at both ends of the M2 domains of each subunit. This positive charge at the M2 extracellular end helps to increase the local concentrations of anions and attract them to the pore domain. The intracellular positive charge helps move anions through the lower section of the M2 domain (Lester, 1992). It is suggested that negatively charged residues in the cation selective Cys-loop receptors may play a similar role (Unwin, 2005) (figure 1-9).

While the other three TMDs, M1, M3 and M4 form an outer ring of helices that separate M2 from the surrounding lipid environment, amino acid residues of M2 line the channel pore. In order to facilitate comparisons between different members of the Cys-loop family of LGICs, M2 residues lining the channel are referred to by an index numbering system (Miller,

1989) (see figure 1-9). According to this system 0' is the conserved charged residue located at the intracellular end of M2 and 20' is located at the M2 extracellular ring of charge (Imoto et al., 1988). The channel gate in $GABA_AR$s is thought to lie at the 2' position nearer to the intracellular end of the pore. It has been proposed that the gate is composed of a ring of hydrophobic amino acid residues that in the closed state of the receptor constricts the diameter of the channel to a width making it energetically unfavorable to ion flow (Unwin, 1995). In the closed state of the receptor, the M2 helices tilt towards the central axis, coming together to make a hydrophobic gate. Previous studies have suggested that opening of this gate may be accomplished via a slight rotation of M2, a subtle movement that is consistent with the "hydrophobic gating" model proposed for the nAChR (Miyazawa et al., 2003). In the nAChR, the hydrophobic gate is thought to be located at a more extracellular position than in the $GABA_AR$, these M2 residues act as a desolvation barrier for ions rather than a steric one. In this gating mechanism, the diameter of the pore in the closed state is small enough that an ion must shed a portion of its hydration shell to pass through, though this is energetically unfavorable. At this point we believe an attractive model is that in the Cys-loop receptors, the hydrophobic gate may be an energetic barrier to ion permeation. The binding of agonist signals the opening of the channel gate, but the exact mechanism remains unknown (Unwin, 2005; Bali and Akabas, 2007).

INTRACELLULAR LOOPS AND MA HELIXIES

The large intracellular M3-M4 linker domain, which contains the amphipathic MA helix, also known as the HA-stretch (Unwin, 2005) is likely to play a diverse role in Cys-loop receptor function, which to date has not been fully elucidated. The M3-M4 linker region displays the greatest amount of sequence variation amongst the Cys-loop LGIC receptor subunits and a structural model of this loop is not yet available (Unwin, 2005). An abundance of information as to the role this region may play in receptor function has been generated using 5-HT_3Rs, where it was first found to be involved in the determination of single channel conductance. In 1999 Davies et al. discovered the 5-HT3B subunit (Davies et al., 1999). When this subunit was co-expressed with the 5-HT3A subunit, the investigators were able to resolve single channel currents. These could not be detected previously from the 5-HT3A homomeric receptor due to its sub-pS single channel conductance (Davies et al., 1999). Surprisingly, the 5-HT3B subunit lacked any of the structural features in the M2 domain that were thought to promote channel conductance in the Cys-loop receptors. Later work by Kelley et al. found that the residues responsible for this increase in conductance were located in a stretch of 23 amino acid residues (Kelley et al., 2003). Previous work on the nAChR predicted that these residues would be located within the amphipathic α-helix, within the HA-stretch (Finer-Moore and Stroud, 1984; Miyazawa et al., 1999). A sequence alignment of the 5-HT3A and 5-HT3B subunits with other subunits from cation-selective members of the Cys-loop

receptor family revealed that the 5-HT3A subunit contains four positively charged arginine residues, R426, R432, R436 and R440 (Kelley et al., 2003). It was shown that three of these residues were responsible for the sub-pS single channel conductance of the homomeric 5-HT_3AR, as mutating them to their 5-HT3B subunit counterparts R432Q, R436D and R440A substantially increased the single channel conductance of the receptor (Kelley et al., 2003). Subsequently, based on their mutations the authors coined the term, RRR-QDA mutation (Bouzat et al., 2004). In 2005, Unwin better resolved the structure of the intracellular domain in the *Torpedo* nAChR, suggesting that the MA helical domains of the five subunits form an intracellular vestibule (Unwin, 2005). This vestibule contains portals which provide exit routes by which permeating ions can pass through the receptor and into the cytoplasm (figure 1-10). Residues located in homologous positions to the RRR-QDA domain of the 5-HT3BR subunits in the MA helix of the nAChR and GlyRs have also been shown to play a role in determining channel conductance (Hales et al., 2006; Carland et al., 2009). In 2008, Jansen et al. performed a study of the homomeric 5-HT_3AR in which they replaced the entire M3-M4 linker with a heptapeptide prokaryotic homologue from *Gloeobacter Violaceus* (Jansen et al., 2008). This mutation led to a significant increase in single channel conductance of the mutant receptor (Jansen et al., 2008). This group carried out a similar substitution of the M3-M4 domain of the homomeric ρ1 $GABA_A$R. In this case the pharmacology of the receptor did

not appear to be altered and single channel analysis was not performed (Jansen et al., 2008).

The M3-M4 linker has also been proposed to play a role in receptor assembly, trafficking and cellular distribution. In the $GABA_AR$, it has been suggested to interact with gephyrin, $GABA_AR$ interacting factor-1 (GRIF-1), brefeldin A-inhibited GDP/GTP exchange factor 2 (BIG2) and adaptor protein 2 which plays a role in clathrin mediated receptor endocytosis (Kittler et al., 2000; Beck et al., 2002; Charych et al., 2004). In the nAChRs, it may also interact with chaperone proteins. Some of these have been identified to be calnexin, rapsyn, ERp75 and Bip (muscle, or muscle-like, receptors), which help proper folding of the receptors and may play a role in trafficking them to the membrane (Jeanclos et al., 2001; Huebsch and Maimone, 2003; Lansdell et al., 2005). In addition, there has been an increased interest on phosphorylation sites present in the M3-M4 linker as they may play a role in channel kinetics and trafficking (Corringer et al., 2000; Kuo et al., 2005).

CHANNEL FUNCTION

Cys-loop receptor activation can be divided into three processes: (1) neurotransmitter binding, (2) channel gating, (3) the coupling of ligand binding to channel gating. To date, there has not been a complete elucidation of the sequence of events that take place after ligand binding. This information has to be transmitted from the LBD to the channel gate lying

deep within the TMDs, over a distance of ~50Å in a matter of tens of microseconds. The identification of residues that play a role in transmitting neurotransmitter binding to channel gating is now possible as a result of combining structural information with electrophysiological, pharmacological and computational studies. All conclusions, however, are limited by the resolution of our current structural models.

The classical method for quantifying the potency of an agonist at a LGIC has been the determination of the concentration that evokes a half-maximal response (EC_{50}). Agonist efficacy is the ability of the agonist to evoke a response, which in the case of LGICs is a measure of the magnitude of the agonist-elicited macroscopic current. Both of these parameters can conveniently be measured using recombinant receptors expressed in *Xenopus* oocytes (Barnard et al., 1984; Colquhoun, 1998). Oocytes are commonly the expression system of choice as they can express high levels of the recombinant protein of interest. While interpreting the effects of mutational studies performed on Cys-loop receptors, one should not forget that this interpretation is limited due to the complex nature of receptor activation. Measurements of pharmacological parameters in these receptors are a composite of binding, gating and desensitization. Thus, at times, conclusions can be elusive and difficult to interpret.

In the following sections I will discuss the dynamic structural elements that are thought to play a role in receptor activation. My primary goal is to convey the complexity of this process and the multiple structural elements of the receptor that may be involved (Sine, 2002; Lee and Sine, 2005; Unwin, 2005; Sine and Engel, 2006). In most cases, I do not discuss specific amino acid residues but rather attempt to describe the intricate process of binding-gating coupling.

C-LOOP AND PRE-M1 REGION

One would expect that communication between the ligand binding site and the channel gate begins with dynamic changes in receptor conformation local to the binding region. Of the six classic binding loops A-F in the LBD, loop-C displays the largest movement in response to agonist binding (Hansen et al., 2005). Recently, attention has focused on the C-loop of the "principal subunit" as a possible initiator of ligand-induced conformational changes across the whole Cys-loop family of LGICs. In the apo (unbound/resting) state of the receptor, it is believed the C-loop extends radially from the receptor complex in the uncapped formation, thus creating a portal for agonist binding (figure 1-11) (Hansen et al., 2005; Unwin, 2005; Mokrab et al., 2007). Upon binding of the agonist it is thought that the C-loop moves in towards the "complementary subunit" creating a capped conformation, essentially trapping the agonist in the binding site (Hansen et al., 2005; Lee and Sine, 2005; Mukhtasimova et al., 2009). Analyses of crystal structures of

Aplysia AChBP complexed with different nicotinic agonists and antagonists have shown the degree of closure of the C-loop is dependent on the efficacy of the ligand present in the binding pocket (Hansen et al., 2005). Upon interaction with an antagonist there appears to be no C-loop closure. There was an observed outward movement of the C-loop in AChBP when the large peptide antagonist α-conotoxin ImI is present in the binding pocket, a movement that was interpreted as an "opening" of the C-loop. If the magnitude of C-loop closure displays a positive correlation with agonist efficacy, these data would suggest that agonist efficacy lies in its ability to alter the conformation of the C-loop.

One theory as to how this C-loop movement could relay the information of ligand binding to the TMDs is that the capping movement may bring residues in the C-loop into close proximity with the binding pocket. These residues may destabilize electrostatic contacts in this region, which could lead to further conformational changes in the LBD and the whole β-sandwich. In 2005, Lee and Sine proposed that after capping of the binding site in the *Torpedo* nAChR the C-loop can interact with residues on β-strand 7 (part of the Cys-loop), which straddles the M2-M3 linker to provide a link to the TMDs (Lee and Sine, 2005).

The pre-M1 region connects the β-10 strand of loop-C to the M1 domain and is therefore a direct physical link of the LBD and the TMDs.

Previous studies in several Cys-loop receptors have shown that the pre-M1 domain forms electrostatic interactions with residues in loop 2 (Lee and Sine, 2005; Mercado and Czajkowski, 2006) (figure 1-12). Loop 2 is believed to straddle the M2-M3 linker and help stabilize the TMDs in the closed position. This theory presents an alternate route as to how C-loop closure may lead to opening of the channel gate. In addition, it is suggested that upon C-loop closure the movement of the pre-M1 region could cause movement in the M1 TMD altering its interactions with the other TMDs. This motion could also play a role in the movement of the M2 and therefore in channel gating (Lee and Sine, 2005).

THE CYS-LOOP, LOOPS 2 AND 9

The ECD-TMD interface is where β-sheet secondary structure of the LBD meets α-helical secondary structure of the channel domain. This area of structural transition is an obvious site for the communication of ligand binding to channel gating and therefore has been an area of great interest. This interface is composed of loops connecting secondary structural elements, with the Cys-loop, loop 2 and loop 9 being donated from the ECD with the M2-M3 linker (Unwin, 2005). The Cys-loop, loop 2 and loop 9 are required to couple agonist binding to channel gating (Bouzat et al., 2004). Together the Cys-loop and loop 2 are suggested to stabilize the M2-M3 linker (figure 1-13) maintaining the channel gate in the closed position. Upon the binding of agonist, movement of the C-loop, β-7 and the pre-M1 region may

interrupt this interaction allowing the M2 TMD to rotate and the channel gate to open (Lee and Sine, 2005; Unwin, 2005; Sine and Engel, 2006). A recent study of the homomeric α1 GlyR suggested that there may be a positive correlation between the magnitude of conformational change in loop 2 and agonist efficacy (Pless and Lynch, 2009b, a), similar to previous work on the C-loop of AChBP (Hansen et al., 2005).

The role of loop 9 is poorly understood, due to a low level of sequence homology in this domain across the receptor family and its poorly defined structure (Unwin, 2005). However modeling and functional evidence suggest that it is involved in the gating process. It has been proposed that a positive correlation exists between agonist efficacy and loop 9 movement (Khatri et al., 2009). Performing simultaneous electrophysiology and site-directed fluorescence spectroscopy on the $GABA_AR$ and a series of ligands ranging from full efficacy to competitive antagonists showed no correlation between rearrangement of loop 9 and receptor activation (Khatri et al., 2009). This observation led the investigators to believe that, although loop 9 does not appear to play a role in receptor activation, it may be a component of the structural machinery that locks the ligand in the binding site (Khatri et al., 2009). It has also been proposed that loop 9 stabilizes the closed state of the $GABA_AR$ as mutations in this region enhance activation by GABA and produce a constitutively active leak current that is inhibited by the channel blocker picrotoxin (Williams et al., 2009).

M2-M3 LINKER

The M2-M3 linker was one of the earliest structures to be implicated in the channel gating mechanism of the Cys-loop family of LGICs (Lynch et al., 1997). Several residues in the M2-M3 linker are highly conserved and appear to play a critical role in channel gating. Earlier studies reported that the cis-trans isomerization of a highly conserved proline residue may be crucial for the coupling of ligand binding to channel gating (Lummis et al., 2005). It was suggested that the interaction of the Cys-loop and loop 2 with the M2-M3 linker prevented this isomerization. However, upon agonist binding, movement in these loops would weaken the interaction to promote this isomerization. More recent evidence has shown that although this residue is conserved in the cation-selective Cys-loop receptors it does not appear crucial for channel gating (Paulsen et al., 2009). Although a complete elucidation of which residues are crucial in each member of the Cys-loop family is still needed, it is now clear that it is an intricate structural interplay between these loops at the LBD and TMD transition zone that is responsible for the transfer of information between these two domains.

nAChRs

Like many other neurotransmitters, ACh acts at two types of ligand-activated receptors: the metabotropic muscarinic ACh receptor (mAChR) and the ionotropic nAChR. Both receptors are expressed by neuronal and non-neuronal cells throughout the body. The mAChRs are heptahelical

transmembrane proteins that couple to the activation of second messengers systems. These receptors were classically defined by their pharmacology as they are activated by muscarine, a toxin derived from the mushroom *Amanita muscaria* and antagonized by atropine, a toxin from *Atropa belladonna*, a member of the nightshade genus. Both of these compounds were characterized primarily from their activity at postganglionic parasympathetic nerve terminals. The activation of mAChRs is much slower then the nAChR, taking milliseconds to seconds for activation. Depending on the subtype present (M1-M5) and the G-protein to which they are coupled ($G_{i/o}$, G_s, G_q), activation of mAChRs can directly alter the cell concentration levels of cAMP , inositol trisphosphate, phosphorylation, phospholipase C and free Ca^{2+} (Eglen, 2005).

The other subtype of AChR is the nAChR, a member of the Cys-loop family of LGICs. These receptors are responsible for mediating fast synaptic excitatory transmission in the peripheral nervous system (PNS) (at the neuromuscular junction and at the ganglia of the autonomic nervous system) and the CNS. The peripheral neuromuscular junction nAChR is the prototypical member of the Cys-loop family of LGICs, as it was the first to be discovered and thoroughly studied. Our in-depth knowledge of this receptor can be attributed to two observations. The first being the realization that *Torpedo californica*, a fish that possesses an electric organ capable of producing an electric current strong enough to stun its prey, expresses

nAChRs at an incredibly high density (O'Brien and Gilmour, 1969; O'Brien et al., 1970). Approximately 40% of the protein from the electric organ of *Torpedo califonica* is composed of nAChRs and has provided an excellent source of starting material for purification and isolation of the receptor (Miledi et al., 1971). The second discovery was a component of the venom of the snake *Bungarus multicinctus* , α-bungarotoxin (α-BgTx) that binds to the peripheral nAChR with near irreversible affinity (Changeux et al., 1970; Raftery et al., 1971). These two findings made it possible to measure the abundance of *Torpedo* nAChR due to its interaction with radioactive labeled α-BgTx. Isolation of *Torpedo* nAChR was performed by affinity chromatography using [*N*-(ε-aminohexanoyl)-3-aminopropyl]trimethyl ammonium bromide hydrobromide covalently linked to agarose (Schmidt and Raftery, 1972) and also a cobrotoxin-Sepharose resin (Raftery, 1973; Schmidt and Raftery, 1973). Following purification of the nAChR, it was sequenced using the newly emerging reverse genetics methods of the time, thus leading to the cloning and sequencing of the genes encoding these receptors (Raftery et al., 1980; Noda et al., 1982; Noda et al., 1983).

To date, there are 17 identified homologous nAChR subunits in vertebrates (α1-10, β1-4, δ, γ and ε) that assemble into a variety of pharmacologically diverse and distinct receptor subtypes. One distinction separating the α subunits from the non-α subunits is the presence of two conserved adjacent cysteine residues which contribute to ligand binding.

These residues are homologous to cysteine residues 192 and 193 in the *Torpedo* receptor α subunit (Noda et al., 1982). In mammals the embryonic muscle type nAChR is most closely related to the *Torpedo* receptor, both forming a heteropentamer with a subunit stoichiometry of $(\alpha1)_2\beta1\gamma\delta$. In post-embryonic mammals the γ subunit is exchanged for the ε subunit, $(\alpha1)_2\beta1\varepsilon\delta$. Together the neuromuscular junction (NMJ) and the *Torpedo* nAChRs are referred to as either the muscle-type, or peripheral, nAChR. The family of neuronal nAChRs is composed of the subunits α2-10 and β2-4. These subunits can form homopentamers (α7, α8, α9, and α10) or heteropentamers composed of various combinations of α (α2-6) and β (β2-4) subunits. Some examples of heteropentameric receptors that are believed to be expressed physiologically are α4β2, α3β4 and α3α5β3. However, it has been suggested that the α5 and β3 subunits are lacking amino acid residues that are crucial to ligand binding and these subunits may therefore play a purely structural role (Corringer et al., 2000). It has been suggested that some heteropentamers may also be comprised purely of α-subunits, α7α8, α9α10 (Gotti and Clementi, 2004). The presence, or absence, of a certain subunit may affect the function, biophysics, pharmacology and localization of these receptors (Gotti and Clementi, 2004).

NEURONAL nAChRs

Neuronal nAChRs received their designation due to their origin of discovery. Neuronal nAChRs were originally cloned from neuronal-like cells,

such as the pheochromocytoma cell line PC12, or cDNA libraries derived from brain tissue. While these subunits are indeed expressed in both the CNS and PNS, their title can be somewhat misleading as there is a growing body of evidence to suggest that some of the neuronal nAChR subunits may be expressed in non-neuronal cell types throughout the body. Tissues where neuronal nAChRs are present include endothelial cells, bronchial epithelial cells, skin keratinocytes and vascular smooth muscle cells (Conti-Fine et al., 2000).

NEURONAL nAChRs AND CALCIUM REGULATION

The activation of neuronal nAChRs can lead to the influx of both Na^+ and Ca^{2+}, thus leading not only to rapid alterations in the membrane potential but also increases in the local concentration of Ca^{2+}. It is the receptor's ability to alter the local concentration of Ca^{2+} that gives it a crucial role in modulating cellular functions (Wonnacott et al., 2005). Receptor heterogeneity also plays a large role in ion selectivity as the subunit composition dictates the receptor's Ca^{2+} permeability, (Fucile, 2004). Heteromeric receptors possess a moderate Ca^{2+} permeability while homomeric $\alpha 7$ receptors possess a Ca^{2+}permeability similar to heteromeric NMDA receptors (Vernino et al., 1992; Bertrand et al., 1993).

In addition to their ability to increase local Ca^{2+} concentrations via the influx of Ca^{2+} ions, activation of neuronal nAChRs can also increase Ca^{2+} via

the activation of voltage-operated calcium channels (VOCCs), or by mobilizing the release of Ca^{2+} from intracellular stores via calcium-induced calcium release (CICR) (Dajas-Bailador and Wonnacott, 2004). Previous studies suggest that activation of heteromeric receptors promotes the activation of VOCCs, whereas homomeric α7 receptor activation induces CICR from ryanodine sensitive stores (Dickinson et al., 2007; Dickinson et al., 2008). Coupling of nAChR activation to either VOCC or CICR may generate specific Ca^{2+} signals with distinct kinetic, spatial and temporal characteristics. nAChR modulation of Ca^{2+} dependent neuronal processes can range from neurotransmitter release to gene transcription and synaptic plasticity (Dajas-Bailador and Wonnacott, 2004).

SUBCELLULAR LOCALIZATION OF NEURONAL nAChRs

The consequences of activating neuronal nAChRs are heavily dependent on their subcellular location. Evidence for their involvement in synaptic transmission in the brain is limited, suggesting their most prominent role may be in the extrasynaptic/presynaptic and somatodendritic space (Dani and Bertrand, 2007). Presynaptic neuronal nAChRs have been shown to exert a direct influence on neurotransmitter release where they can potentiate neurotransmitter release via the initiation of action potentials in a tetrodotoxin sensitive manner (Lena et al., 1993; Wonnacott, 1997). Recent evidence suggests that the presynaptic homomeric α7 receptor may be present in glutamatergic and GABAergic

synapses in the CA1 area where they augment the release of these neurotransmitters (Fabian-Fine et al., 2001).

nAChR REGULATION OF GENE EXPRESSION

As stated previously, one consequence of the activation of somatodendritic neuronal nAChRs is the increase in the concentration of intracellular Ca^{2+}. This may lead to the modulation of Ca^{2+} sensitive proteins such as kinases, phosphatases and various transcription factors (Eilers et al., 1997). One example of this process has been observed in cultured neurons and cell lines where nicotine activation of somatic α7 homomeric nAChRs results in increased levels of the transcriptional regulator phospho-cyclic AMP response element-binding protein (CREB) and the immediate early gene c-Fos (Hu et al., 2002). Previous work in mice has shown that low dose (0.4mg/kg) nicotine exposure alters gene expression in the nucleus accumbens, prefrontal cortex and other brain regions involved in the mesolimbic dopamine pathway believed to play a role in addiction (Valjent et al., 2004). Similar responses were observed after administration of other addictive drugs of abuse, but not of non-addictive drugs, leading one to believe nicotinic receptors may play a crucial role in the addictive processes (Valjent et al., 2004).

Nicotine-induced activation of CREB is coupled to an increase in the transcription level of tyrosine hydroxylase, the rate-limiting enzyme in the

synthesis of catecholamines in PC12 cells (Gueorguiev et al., 2006). Nicotine's ability to increase catecholaminergic transmission may play a role in its reinforcing properties.

$GABA_AR$s

γ-Aminobutyric acid (GABA) is the major inhibitory transmitter in the brain and 20-50% of all synapses in the CNS utilize GABA as a neurotransmitter (Bloom and Iversen, 1971). After GABA is released into the synapse and diffuses across the synaptic cleft, GABA exerts its actions via metabotropic $GABA_BR$s and ionotropic $GABA_AR$s. $GABA_BR$s are heptahelical G-protein coupled receptors, and depending on which G-protein they associate with (e.g., $G_{i/o}$, $G_{\alpha s}$), they can modulate neuronal excitability via the inhibition of voltage activated calcium channels, activation of GIRKs, the regulation of cyclic AMP, or inositol phosphate signaling (Bowery et al., 2002).

$GABA_AR$ GENES

Upon completion of the sequencing of the human genome and several other vertebrate species, 19 genes coding for $GABA_AR$ subunits have been discovered (α1-6, β1-3, γ1-3, ρ1-3, δ, ε, π, and θ) (Simon et al., 2004). Most $GABA_AR$s are heteropentamers and the properties of an individual receptor are dictated by the precise complement of subunits in the complex. Notable exceptions are the 3 ρ subunits which form homopentamers that are

expressed mainly in the retina. These subtypes display unique ligand binding characteristics that originally led them to be classified as a distinct class i.e., the $GABA_C$ receptors. However, in the latest nomenclature (Olsen and Sieghart, 2008), $GABA_C$ receptors have been included in the $GABA_A$ receptor class on the basis of their extensive structural and functional homology. Some species of birds lack the ε and θ subunits yet still maintain a total of 19 $GABA_AR$ subunit genes as they express the β4 and γ4 subunits (Simon et al., 2004). These differences in subunit genes suggests an evolutionary relationship as the θ and β subunits are closely related, as are the ε and γ subunits (Simon et al., 2004) (figure 1-14).

A majority of the genes encoding human $GABA_AR$ subunits are found in clusters on different chromosomes i.e., α1, α6, β2 and γ2 on 5q34; α2, α4, β1 and γ1 on 4p12; α5, β3 and γ3 on 15q13; α3, ε and θ on Xq28. The ρ1 and ρ2 genes are separated by 40 kbs on 6q15 and the ρ3, π and δ subunit genes are located on human chromosomes 3q12.1, 5q35.1 and 1p36.3 respectively (Simon et al., 2004). Such clustering of $GABA_AR$ subunit genes is likely to be an evolutionary tool that allows for spatial and temporal changes in expression of different $GABA_AR$ subtypes in response to varying physiological and pharmacological conditions.

$GABA_AR$ Heterogeneity

As noted above, nineteen mammalian $GABA_A$ subunits have been identified and most $GABA_A$ receptors are heteropentamers that include two, or more, different subunit isoforms in the complex. There is thus a huge potential for receptor heterogeneity (Olsen and Sieghart, 2008) but it is thought likely that only approximately 20 subunit combinations exist *in vivo* (Macdonald and Olsen, 1994). The most abundant $GABA_AR$ subunits in the CNS are $\alpha1$, $\beta2$ and $\gamma2$. Occurring in a stoichiometry of 2α, 2β and 1γ, this $\alpha1\beta2\gamma2$ containing receptor is likely to be the major postsynaptic receptor at GABAergic synapses (Macdonald and Olsen, 1994; Farrant and Nusser, 2005). Other studies that used subunit-specific antibodies have suggested that other major $GABA_ARs$ formed in the CNS are the $\alpha2\beta\gamma2$, $\alpha3\beta\gamma2$, $\alpha4\beta\gamma2$, $\alpha5\beta\gamma2$, $\alpha6\beta\gamma2$ and $\alpha4\beta\delta$ combinations (Sieghart and Sperk, 2002).

In situ hybridization and immunohistochemical studies have indicated a subunit-specific distribution throughout the brain. In addition to differences in cellular expression, a distinct subcellular distribution of some subunits has been reported (Pirker et al., 2000; Sieghart and Sperk, 2002). For example, in cerebellar granule cells, the $\alpha1$, $\alpha6$, $\beta2$, $\beta3$ and $\gamma2$ subunits are concentrated at the postsynaptic membrane, whereas there is a lower density of these subunits in the extrasynaptic membrane. In contrast, the δ subunit, which is undetectable at synaptic junctions, is abundant in the extrasynaptic membrane and somatic spines (Nusser et al., 1998a).

PHASIC AND TONIC INHIBITION

It has long been known that rapid synaptic GABA-mediated "phasic" inhibition is fundamental to information transfer in the CNS (Jones and Westbrook, 1996). However, studies from the early 1990s suggested the presence of a slow sustained "tonic" inhibitory current present in cerebellar granule cells (Kaneda et al., 1995) and hippocampal neurons (Otis et al., 1991). It is now clear that $GABA_AR$-mediated inhibition is composed of two distinct types: phasic inhibition, mediated by synaptic receptors and tonic inhibition, mediated by extrasynaptic receptors (Farrant and Nusser, 2005).

Phasic inhibition involves the rapid and precise transmission of presynaptic activity into a postsynaptic signal. A defining feature of phasic inhibition is its short duration (100-500μs) exposure to millimolar concentrations of GABA in the synapic cleft (Mody et al., 1994; Mozrzymas et al., 2003; Mozrzymas, 2004). Previous studies indicate that receptors containing the γ2 subunit in association with the α1, α2, or α3 subunit(s) are predominantly involved in mediating phasic inhibition (Farrant and Nusser, 2005). The most abundant synaptic α1β2γ2 receptor displays lower GABA affinity (EC_{50} ~20-30μM) (Maconochie et al., 1994) as well as an increased rate and extent of desensitization in comparison to receptors mediating tonic inhibiton (Haas and Macdonald, 1999; Bianchi et al., 2001) (discussed below).

In contrast to phasic inhibition, tonic inhibition involves the activation of a subset of $GABA_AR$s in a manner that is temporally and spatially dissociated from phasic synaptic events. Receptors expressed at the extrasynaptic membrane can be tonically activated by low ambient concentrations of GABA released from glial cells or "spilled over" GABA that has diffused from the synaptic cleft (Farrant and Nusser, 2005). Tonic inhibition was first demonstrated in cerebellar granule cells in 1995 by Kaneda et al. who observed that application of the $GABA_AR$ antagonists, bicuculline and SR-95531, not only blocked spontaneously occurring inhibitory post-synaptic currents, but also decreased the 'holding' current that was required to clamp the cells at a given membrane potential. The observed reduction in input conductance was associated with a reduction in current variance, consistent with reduction in the number of open $GABA_AR$s (Kaneda et al., 1995; Brickley et al., 1996; Tia et al., 1996; Wall and Usowicz, 1997). Subsequent studies identified similar phenomena in CA1 pyramidal neurons (Bai et al., 2001), granule cells of the dentate gyrus (Nusser and Mody, 2002) and in inhibitory interneurons of the hippocampus (Semyanov et al., 2003).

It has been suggested that specific $GABA_AR$ subtypes may be responsible for mediating tonic inhibition. Immunohistochemistry has indicated co-localization of the α6- and δ-subunits in the extrasynaptic area of cerebellar granule cells (Nusser et al., 1998b). In α6- and δ-subunit

knockout mice tonic conductance in cerebellar granule cells was abolished (Brickley et al., 2001). Recombinant α6βδ receptors display slow desensitization and a high sensitivity to GABA, biophysical and pharmacological properties similar to the tonic conductance observed in cerebellar granule cells (Saxena and Macdonald, 1996). These observations led to the suggestion that tonic inhibition in the cerebellum is likely to be mediated by the α6βδ $GABA_AR$.

$GABA_ARs$ containing the α4 and δ subunits have been implicated in mediating tonic inhibition in dentate granule cells, ventrobasal neurons and the dorsal lateral nucleus of the thalamus (Wisden et al., 1992; Stell et al., 2003; Chandra et al., 2006). In 2002, Peng et al. showed there was a decrease in α4 subunit surface expression in δ subunit knockout mice. Although tonic inhibition was not completely abolished in these cells, it was significantly reduced (Peng et al., 2002). In dentate granule cells and ventrobasal neurons of the thalamus of α4 subunit knockout mice there is a complete lack of tonic inhibition (Chandra et al., 2006). These studies suggest that one of the roles for α4 and δ subunit containing $GABA_ARs$ is to mediate tonic inhibition. A previous study using confocal microscopy and electrophysiology suggests that the α4βδ receptor is exclusively co-assembled and predominantly co-localized to the extrasynaptic membrane where it contributes to tonic inhibition (Jia et al., 2005). It is important to note that in these brain regions the α4 and β subunits also are found co-

localized with the γ2 subunit, a putative synaptic form (Peng et al., 2002). In 1999 Sur et al. reported that only one-third of the α4 subunits co-localize with the γ2 subunit, while the other two-thirds co-localize with the δ subunit in the hippocampus and thalamus (Sur et al., 1999). It seems reasonable to assume that tonic inhibition is mediated by $GABA_A$Rs containing the δ subunit co-assembled with either the α6, or α4, subunit.

SYNAPTIC TARGETING OF $GABA_A$Rs

The interest in tonic inhibition mediated by extrasynaptic $GABA_A$Rs has rekindled interest in receptor trafficking. The clustering of $GABA_A$Rs at the synaptic membrane is essential for efficient neurotransmission but the underlying mechanisms remain poorly understood. Much work has focused on gephyrin, a 93 kDa protein (Baer et al., 2009) that is highly expressed at inhibitory postsynaptic membranes. This protein was first found to associate with the intracellular MA helix of the glycine receptor β subunit. Gephyrin binds to both microtubules and tubulin with high affinity and it is this interaction that has been proposed to contribute to the synaptic clustering of $GABA_A$Rs (Kirsch et al., 1991; Kirsch, 1999). The interactions between gephyrin and the $GABA_A$R are complex since removal of gephyrin using either mRNA interference, or gene targeting, techniques strongly reduces $GABA_A$R clustering. However, it has also been well documented that some neurons lacking gephyrin display normal clustering (Levi et al., 2004; Yu et al., 2007).

The γ2 subunit has been implicated in studies of $GABA_AR$-gephyrin interactions. Targeted deletion of the γ2 subunit gene disrupted clustering and resulted in $GABA_ARs$ being dispersed from the post synaptic density (Luscher and Keller, 2004). To date it is still unclear whether gephyrin interacts directly with the receptor protein or whether it plays a role in trafficking of the receptors to the membrane. The search for intermediary proteins that interact with both gephyrin and $GABA_ARs$ has so far identified one candidate i.e., the $GABA_AR$-associated protein (GABARAP) which has been implicated in membrane targeting and/or recycling of $GABA_ARs$ (Alldred et al., 2005; Kanematsu et al., 2007). Clearly, dynamic changes in receptor expression are dependent on many factors including receptor synthesis, trafficking, membrane insertion, internalization, degradation, lateral diffusion and multiple intracellular signaling cascades, all of which are stringently regulated.

$GABA_AR$ PHARMACOLOGY

AGONISTS

Ligands which have a direct activating effect, i.e. they open the integral Cl^- conducting channel of the receptor are termed $GABA_AR$ agonists. The endogenous agonist for these receptors is the neurotransmitter GABA. GABA is a flexible molecule that can adopt a variety of low energy conformations allowing it to interact with a multitude of different proteins,

including receptors, enzymes and transporters. GABA is synthesized from glutamate by decarboxylation by the enzyme glutamic acid decarboxylase. The potency of GABA and other $GABA_AR$ agonists varies greatly depending on the subunit composition of the receptor. One example is found in δ subunit-containing receptors where GABA displays an approximate 20-fold greater potency at the α4β3δ receptor compared to the α4β3γ2 receptor (You and Dunn, 2007). One of the earliest exogenous $GABA_AR$ agonists identified, muscimol, is a plant toxin isolated from the mushroom *Amanita muscarina*, and is a rigid structural analogue of GABA. Muscimol proved to be a useful prototype for the development of a battery of $GABA_AR$ agonists, including dihydromuscimol, thiomuscimol, THIP (4, 5, 6, 7-tetrahydroisoxazolo[5, 4]pyridin-3-ol) (also known as gaboxadol), isoguvacine, P4S (piperidine-4-sulphonic acid), ZAPA (Z-3-[(aminoiminomethyl)thio]prop-2-enoic acid) and thio-4-PIOL (5-(4-piperidyl)-3-isothiazolol) (Krogsgaard-Larsen et al., 1975; Krogsgaard-Larsen et al., 2004). Endogenous agonists of the $GABA_AR$ include taurine, β-alanine and 14AA (imidazole-4-caetic acid) (Quinn and Harris, 1995; Tunnicliff, 1998). WIth regard to efficacy, muscimol and isoguvacine display similar properties to GABA as they act as full agonists at the synaptic α1β2γ2 $GABA_AR$. In contrast, THIP, P4S and 14AA are described as partial agonists at this receptor. At saturating concentrations, THIP, P4S and 14AA are unable to evoke macroscopic currents equal to the response evoked from saturating concentrations of full agonist. Interestingly, agonists display different levels of efficacy depending on subunit composition of the receptor.

THIP and 14AA, which are regarded as partial agonists at the $\alpha1\beta2\gamma2$ receptor, produce supramaximal currents relative to saturating concentrations of GABA at the $\alpha4\beta3\delta$ receptor. Hence, such compounds have been coined "super agonists" (Brown et al., 2002; You and Dunn, 2007).

ANTAGONISTS

Bicuculline, the first identified $GABA_AR$ antagonist is a plant alkaloid isolated from extracts of many different plants, including *Dicentra cucullaria*, *Adlumia fungosa*, *Fumariaceae* and several *Corydalis* species (Curtis et al., 1970). Further studies on this compound showed that not all GABA receptors were sensitive to its effects. This led to the classification of the two different classes of receptors, i.e, the ionotropic $GABA_AR$ and the G-protein coupled $GABA_BRs$ (Hill and Bowery, 1981). Bicuculline and the pyridazinyl GABA derivative SR-95531 (gabazine) share some structural similarities with the agonist muscimol but are described as competitive antagonists of GABA at the $GABA_AR$. These competitive antagonists interact with the GABA binding site at the β-α subunit interface forming a reversible complex with the receptor. The reversible nature of the receptor-antagonist complex is the basis for the antagonists ability to shift the concentration-effect curve of a competing agonist to the right, resulting in an apparent loss of potency for the agonist (Vestergaard et al., 2007). Recent work has focused on a number of 4-PIOL analogues that have been shown to have no agonist activity, but to act in the manner of a competitive antagonist (Frolund et al., 2005).

Picrotoxin is the prototype of a non-competitive $GABA_AR$ antagonist isolated from *Anamirta cocculus*, a plant native to Southeast Asia. Picrotoxin does not interact with either the GABA, or benzodiazepine, binding sites but interacts with the lumen of the channel pore (Inoue and Akaike, 1988). Picrotoxin's channel blocking properties are mimicked by several other $GABA_AR$ channel blockers which are believed to interact with a similar site inside the channel pore. These compounds, such as fipronil and lindane, are used as insecticides (Bloomquist, 2003; Chen et al., 2006).

ALLOSTERIC MODULATORS: THE BENZODIAZEPINES

Many of the clinically relevant drugs that exert their effects via the $GABA_AR$ act as allosteric modulators of these proteins. The high affinity binding site for classical benzodiazepines has been shown to lie in a homologous position to GABA binding sites at an adjacent subunit interface. In the abundant $\alpha1\beta2\gamma2$ receptor, the major benzodiazepine binding site lies at the interface of the α-γ subunit interface. The primary subunit ($\alpha1$) contributes binding loops A-C and the complimentary subunit ($\gamma2$) contributes loops D-F of the secondary α subunit (Ernst et al., 2003). The particular α-subunit present in the receptor has a major influence on benzodiazepine pharmacology. Receptors containing $\alpha1$, $\alpha2$, $\alpha3$ and $\alpha5$ are generally thought to be "diazepam-sensitive" while $\alpha4$- and $\alpha6$-containing receptors are often described as "diazepam-insensitive" (Heyers and

Luddens, 1998). Subunit specific benzodiazepine sensitivity has been narrowed down to a single amino acid in the N-terminal domain. Replacement of a histidine residue (His 101 in the α1 subunit) in diazepam-sensitive α subunits by an arginine (as occurs in α4 and α6) has been shown to render the receptor insensitive to diazepam modulation (Wieland et al., 1992).

The first benzodiazepine to be identified, chlordiazepoxide, was introduced in 1960, followed by diazepam in 1963 predating the identification of GABA (Tobin and Lewis, 1960; Difrancesco, 1963). A multitude of studies throughout the 70s and 80s demonstrated that benzodiazepine compounds acted as clinically relevant drugs, being used as sedatives, anticonvulsants, hypnotics, anxiolytics, muscle relaxants and amnesia-producing agents for surgery, and that these effects were a result of their ability to interact with the $GABA_AR$ (Macdonald and Barker, 1978; Gavish and Snyder, 1980). Benzodiazepines, on their own, have no effect, and do not directly activate, or inhibit, the $GABA_AR$. Subsequent electrophysiological and chloride flux experiments showed that benzodiazepines increase GABA-evoked chloride flux in a concentration dependent fashion (Obata and Yamamura, 1986; Mathers and Yoshida, 1987; Yang and Olsen, 1987). Single channel analysis showed that the classical 1,4-benzodiazepines, such as diazepam and flunitrazepam increase the frequency of channel opening in the presence of GABA (Twyman et al., 1989). Some

benzodiazepine binding site ligands, such as the structurally related β-carbolines and imidazobenzodiazepines act as negative allosteric modulators and display pro-convulsant activity. Negative allosteric modulators act by decreasing the frequency of channel opening in the presence of GABA. Other compounds such as flumazenil (Ro15-1788) and ZK93426 (ethyl-5-isopropoxy-4-methyl-beta-carboline-3-carboxylate) act as benzodiazepine site antagonists. In theory these compounds would have no effect rather than blocking the modulatory effects of other benzodiazepine site ligands (Barnard et al., 1998).

BARBITURATES

The barbiturates (such as thiopental, pentobarbital and phenobarbital) are another class of positive allosteric modulators that act at the $GABA_AR$. Although they are currently used to a lesser extent as sedatives, hypnotics, muscle relaxants and anxiolytics, they are still used clinically as anesthetics and anticonvulsants. The molecular mechanisms by which barbiturates modulate the $GABA_AR$ differ from those of the benzodiazepines. At a single channel level, barbiturates lengthen the duration of time the $GABA_AR$ ion channel spends in the open state, whereas benzodiazepines increase the frequency of channel openings (Twyman et al., 1989). In addition to being positive modulators, at high concentrations (100-800μM) barbiturate ligands can open the channel gate in the absence of GABA, suggesting the possibility the receptor may contain two independent sites at

which these ligands can interact (Twyman et al., 1989; Thompson et al., 1996). Amino acid residues thought to be responsible for direct activation by barbiturates are believed to be distinct from residues involved in receptor activation by GABA. Mutations that alter the receptor's activation in response to GABA binding (Amin and Weiss, 1993) do not affect the receptor's direct activation by barbiturates. In addition, bicuculline and SR-95531, competitive antagonists of GABA, do not affect the direct activation of the receptor by the barbiturate pentobarbitone (Thompson et al., 1996).

NEUROSTEROIDS

Another class of potent allosteric modulators of the $GABA_AR$ are the neurosteroids. Neurosteroids can originate from peripheral glands (i.e. adrenal gland, ovaries), *de novo,* or may be synthesized in neurons. Neurosteroids can effect $GABA_ARs$ at very low nanomolar physiological concentrations (Lambert et al., 2003). Early studies with pregnane steroids suggested that these molecules had little subunit specificity in regard to receptors at which they act. One interesting finding with these modulators is that although they do not display subunit-specific effects with regard to which α, β, or γ, subunits are present in the receptor, neurosteroids possess a high potency for δ-containing extrasynaptic $GABA_ARs$ (Wohlfarth et al., 2002). The activity of neurosteroids at δ-containing receptors is thought to possibly enhance their activity in the presence of endogenous agonists such as taurine, or for small ambient spill over concentrations of GABA, leading to

a longer duration of current after a synaptic event (Bianchi and Macdonald, 2003; Puia et al., 2003).

AIMS OF THE PRESENT STUDIES

The goal of the studies described in this thesis was to further our current understanding of how the structure of the members of the Cys-loop family of LGICs relates to their function. Recombinant receptors were expressed in *Xenopus* oocytes. Response to agonists were measured using two-electrode voltage-clamp techniques. To investigate the role of individual amino acids in receptor pharmacology, I performed site-directed mutagenesis on residues of interest.

In Chapter 2 I examine the binding and functional properties of the bischoline ester series of agonists exemplified by suberyldicholine using radioligand binding, thallium flux assays and recombinant receptors expressed in *Xenopus* oocytes. The specific aims of this Chapter are to compare and contrast binding and function of these agonists.

In Chapter 3, the goal of this study was an attempt to lock the C-loop in the capped position following application of agonist. Utilizing our working model of the $\alpha1\beta2\gamma2$ $GABA_AR$ (Mokrab et al., 2007) based of the 4Å resolution of the *Torpedo* nAChR (Unwin, 2005), I hypothesized that the distance separating the residues, β2V223 (loop-C) and α1V205 (loop-F) was

reduced following interaction with agonist. In an effort to lock the C-loop in the capped position, I mutated these two valine residues to cysteines. The hypothesis was that after oxidation and the application of agonist these two residues would come in close enough proximity to form a cystine bond. In addition, I attempted to alter C-loop closure via the attachment of large a chemical moiety, thereby introducing a steric hindrance effect, proposing that this may decrease the efficacy of agonist.

In Chapter 4, the goal was to compare the properties of the agonists, GABA and THIP acting on the synaptic $\alpha1\beta2\gamma2$ and extrasynaptic $\alpha4\beta3\delta$ $GABA_A$Rs. Using current structural models Dr. P-L Chau performed ligand docking studies with both agonists. It appeared that a conserved arginine residue in loop-D (Hartvig et al., 2000) may play a different role in each receptor with each agonist. In the $\alpha1\beta2\gamma2$ receptor I proposed that the residue α1R94 played a larger role in the stabilization of GABA than THIP in the binding pocket, whereas in the $\alpha4\beta3\delta$ receptor the α4R100 residue appeared to play a larger role in the stabilization of THIP than GABA. To test this hypothesis, I performed the conservative mutations α1R94K and α4R100K. These mutations decrease the volume of the amino acid side chain, therefore reducing its stabilizing effect on the agonists. The aim of this study was to determine the stabilizing effect of this residue on these agonists and what role that it plays in the agonists profile.

In conclusion, the purpose of the work undertaken in this thesis is to further our current understanding of ligand recognition in the Cys-loop family of LGICs. I have attempted to achieve this goal by either manipulating the structure of the ligand, such as in Chapter 2, or the structure of the protein itself, as in Chapters 3 and 4. A better understanding of ligand recognition and its effects at this family of receptors would be beneficial in understanding the pharmacology of these proteins, allowing their manipulation for a therapeutic goal.

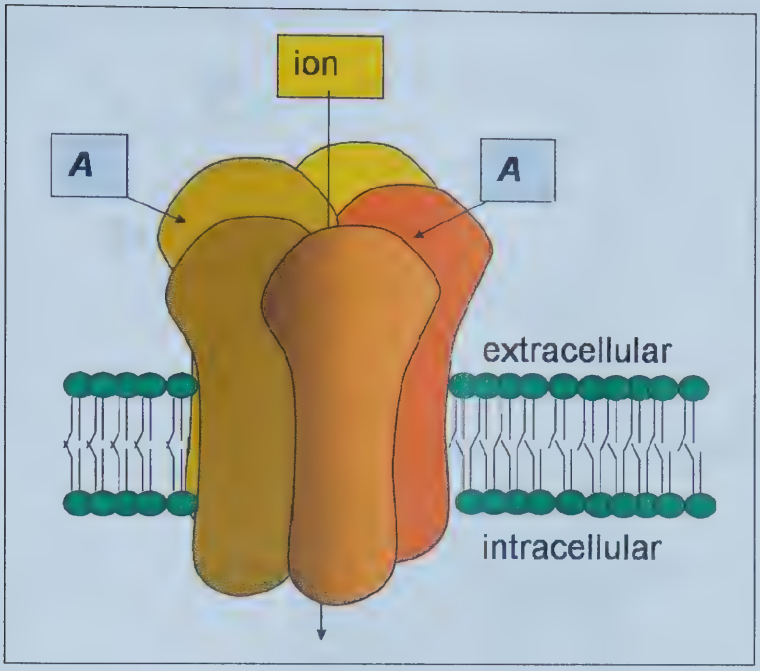

Figure 1-1: A cartoon representation of a member of the Cys-loop family of LGICs. Note the receptor's pentameric structure which transverses the membrane, and the central ion conducting channel pore. Agonist binding sites at subunit interfaces are denoted by "A". **Courtesy Dr. Susan Dunn**

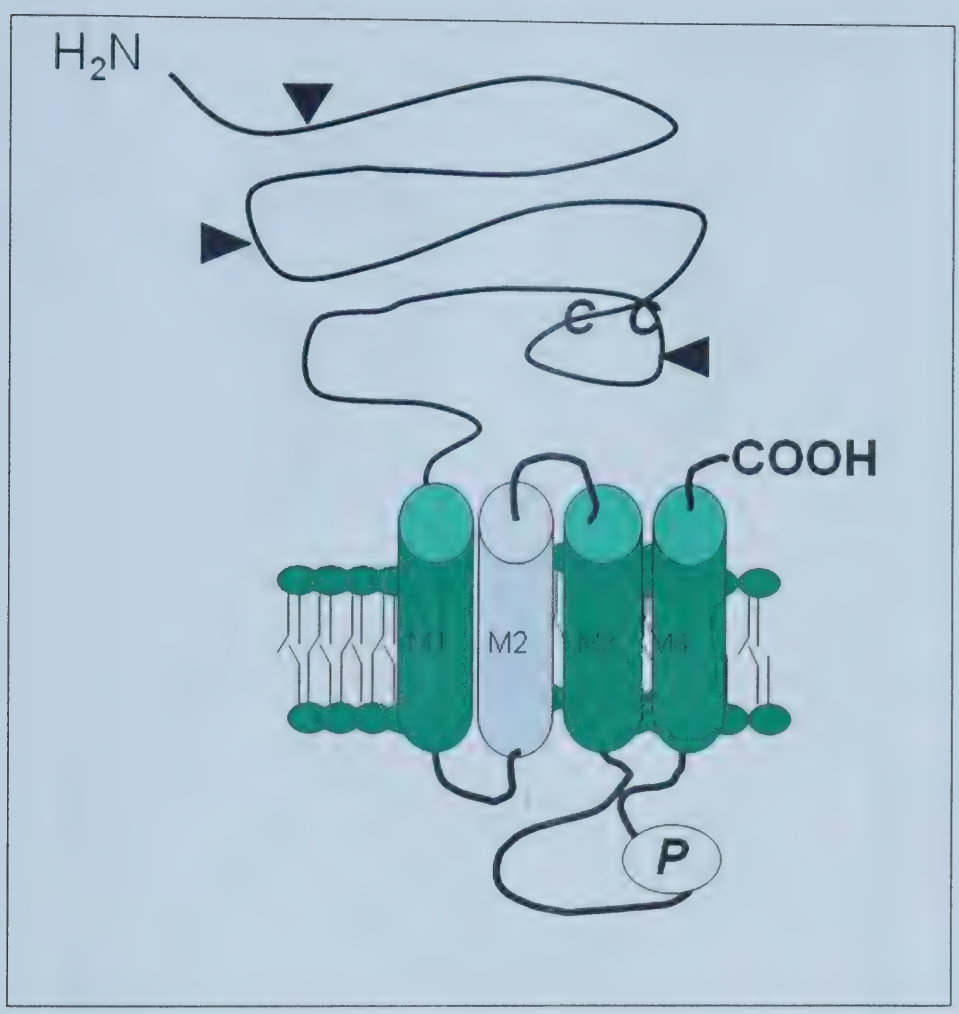

Figure 1-2: A cartoon representation of single subunit from a member of the Cys-loop family of LGICs. The subunit's long N-terminal LBD contains the characteristic Cys-loop as well as various glycosylation sites denoted by triangles. TMDs represented by cylinders, of which M2 (colored light purple), lines the ion channel pore. Also note the M3-M4 linker which contains the MA helix and is a location that can undergo phosphorylation at multiple locations. **Courtesy Dr. Susan Dunn.**

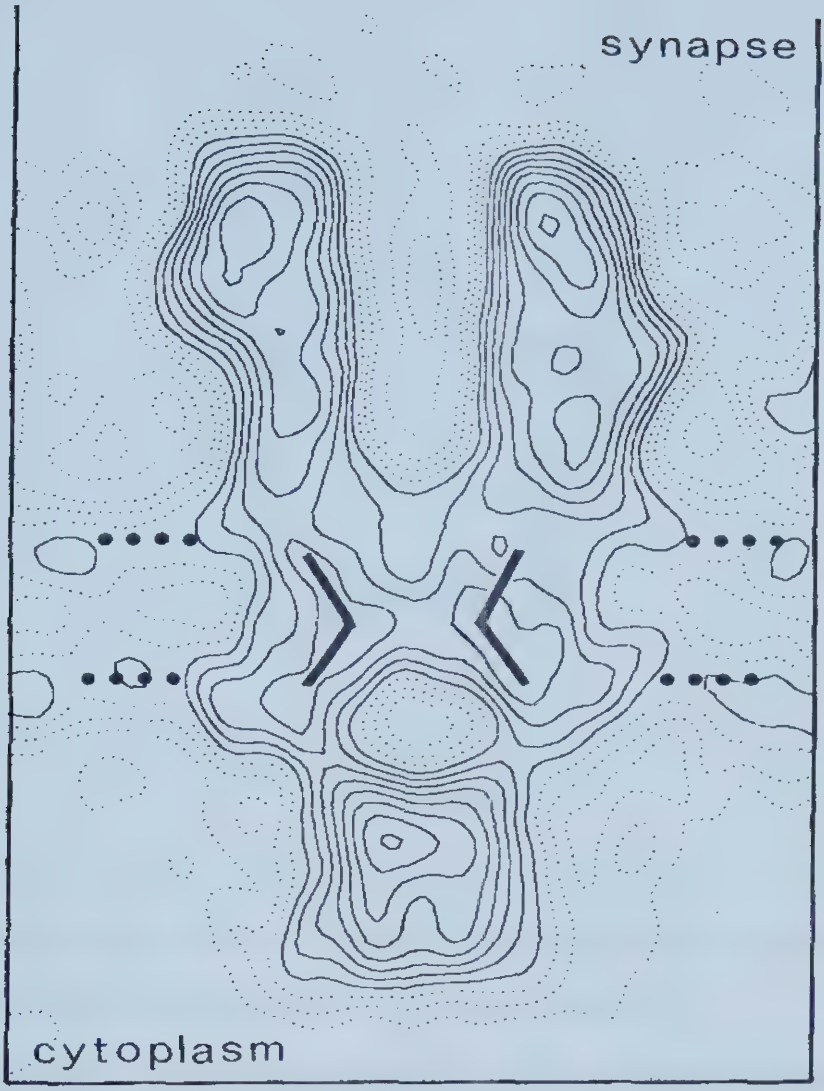

Figure 1-3: Profile view of a *Torpedo* nAChR channel associated with the membrane. Dotted lines indicate limits of the lipid bilayer which are located approximately 30Å apart. **Unwin, N. (1993)."Nicotinic acetylcholine receptor at 9 Å resolution."** J Mol Biol **229(4): 1101-24.**

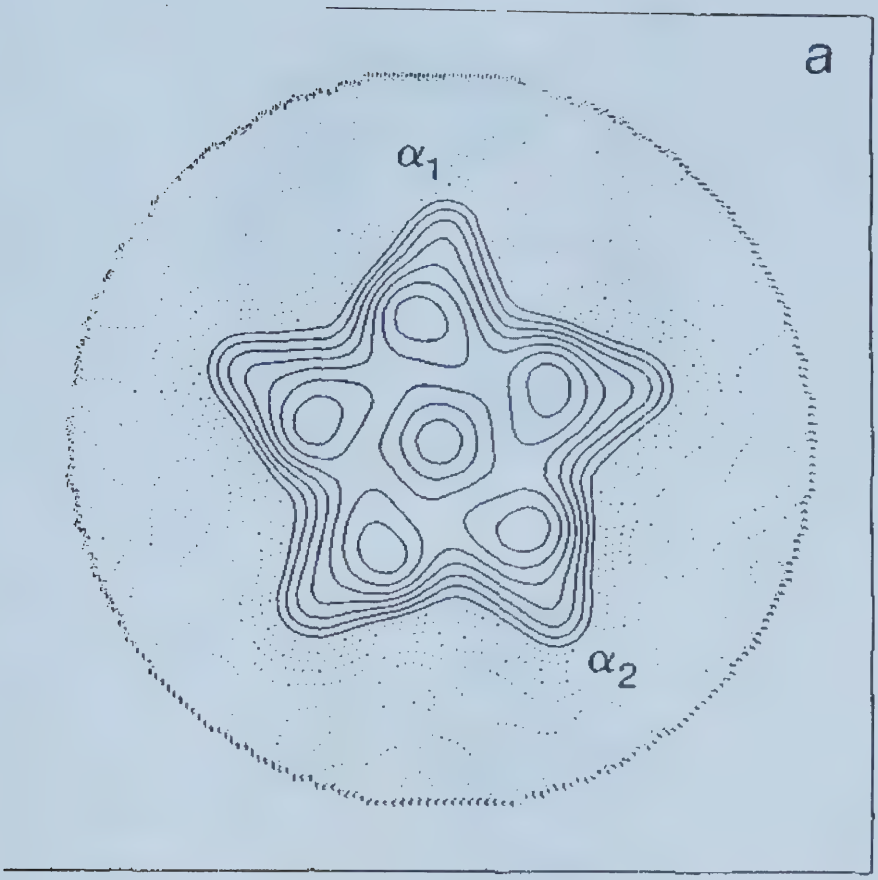

Figure 1-4: Sections normal to the pseudo-5-fold axis of a single *Torpedo* nAChR in the lipid bilayer spanning (TMD) region. **Unwin, N. (1993)."Nicotinic acetylcholine receptor at 9 Å resolution."** **J Mol Biol 229(4): 1101-24.**

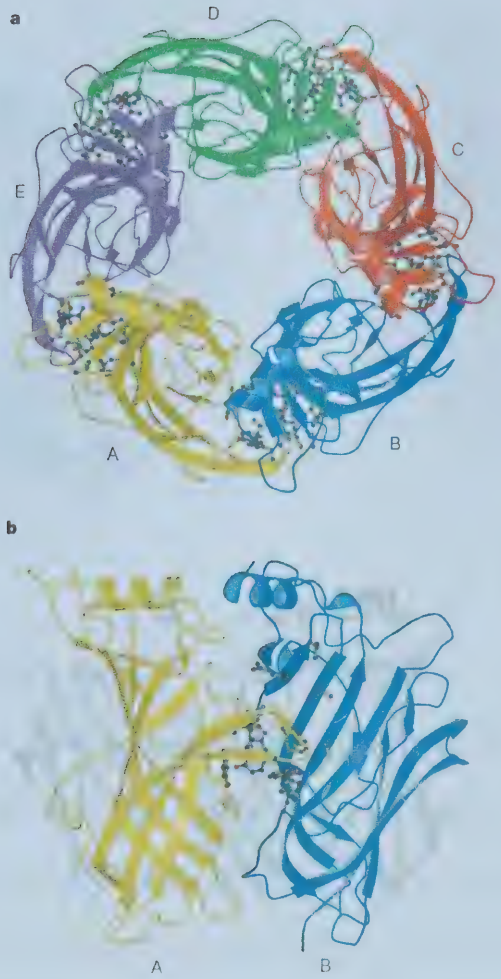

Figure 1-5: (A) A representation of the pentameric AChBP protein with each protomer in a different color. Subunits are labeled anti-clockwise, with A–B, B–C, C–D, D–E and E–A forming the plus and minus interface side, with the principal and complementary ligand-binding sites, respectively. (B) A view of the AChBP pentamer perpendicular to the five-fold axis. The ligand-binding site, at the A (yellow) and B (blue) interface. **Brejc, K., W. J. van Dijk, et al. (2001). "Crystal structure of an ACh-binding protein reveals the ligand-binding domain of nicotinic receptors." Nature 411(6835): 269-76.**

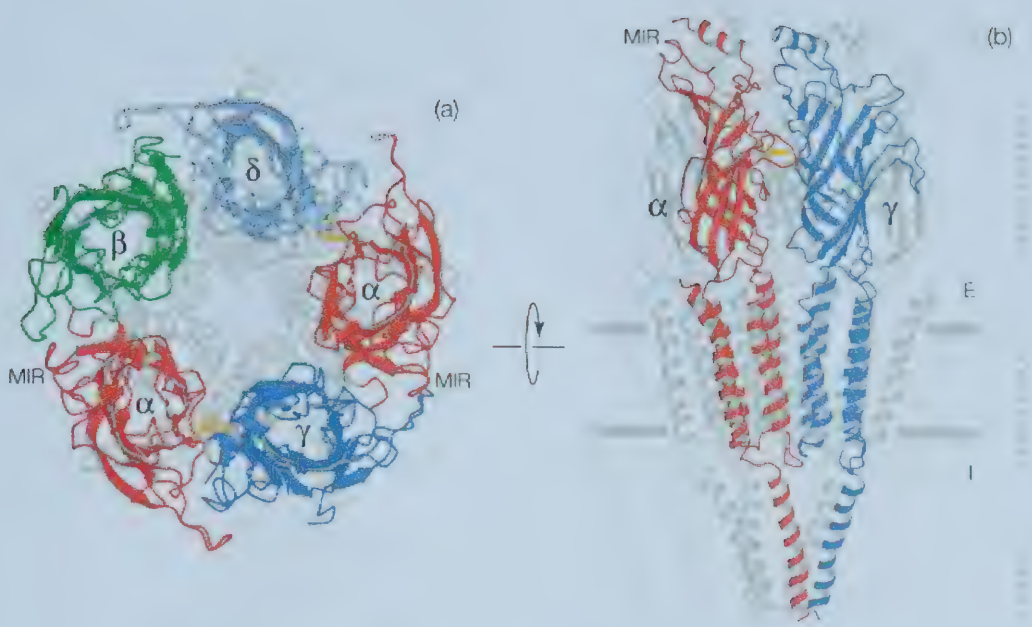

Figure 1-6: (A) Ribbon diagram of the *Torpedo* nAChR, as viewed from the synaptic cleft (B) and parallel with the membrane plane. For clarity, only the ligand-binding domain is highlighted in (A) and only the front two subunits are highlighted in (B) (α, red; β, green; γ, blue; δ, light blue). Also shown is the location of the membrane (horizontal bars; E, extracellular; I, intracellular). The dotted lines on the right denote the three main zones of subunit–subunit contacts. **Unwin, N. (2005). "Refined structure of the nicotinic acetylcholine receptor at 4 Å resolution." J Mol Biol 346(4): 967-89.**

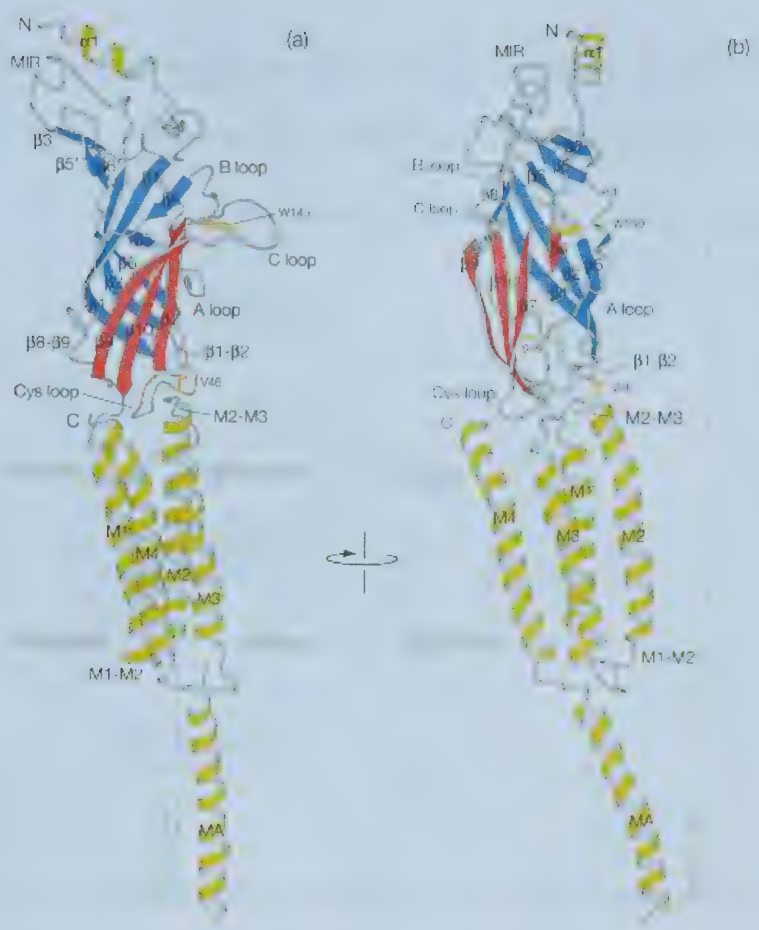

Figure 1-7: Ribbon diagram of a single α subunit viewed parallel with the membrane plane, in an orientation such that the central axis of the pentamer (vertical line) is at the back (A) and to the side (B). The α-helices are colored yellow, the β-strands comprising the β-sandwich are colored blue (inner) and red (outer). Locations of the N and C termini, αTrp149, αV46, the Cys-loop disulphide bridge and the membrane (horizontal bars) are indicated. Part of the M3–M4 loop (connecting MA to M3) is missing. **Unwin, N. (2005). "Refined structure of the nicotinic acetylcholine receptor at 4 Å resolution." J Mol Biol 346(4): 967-89.**

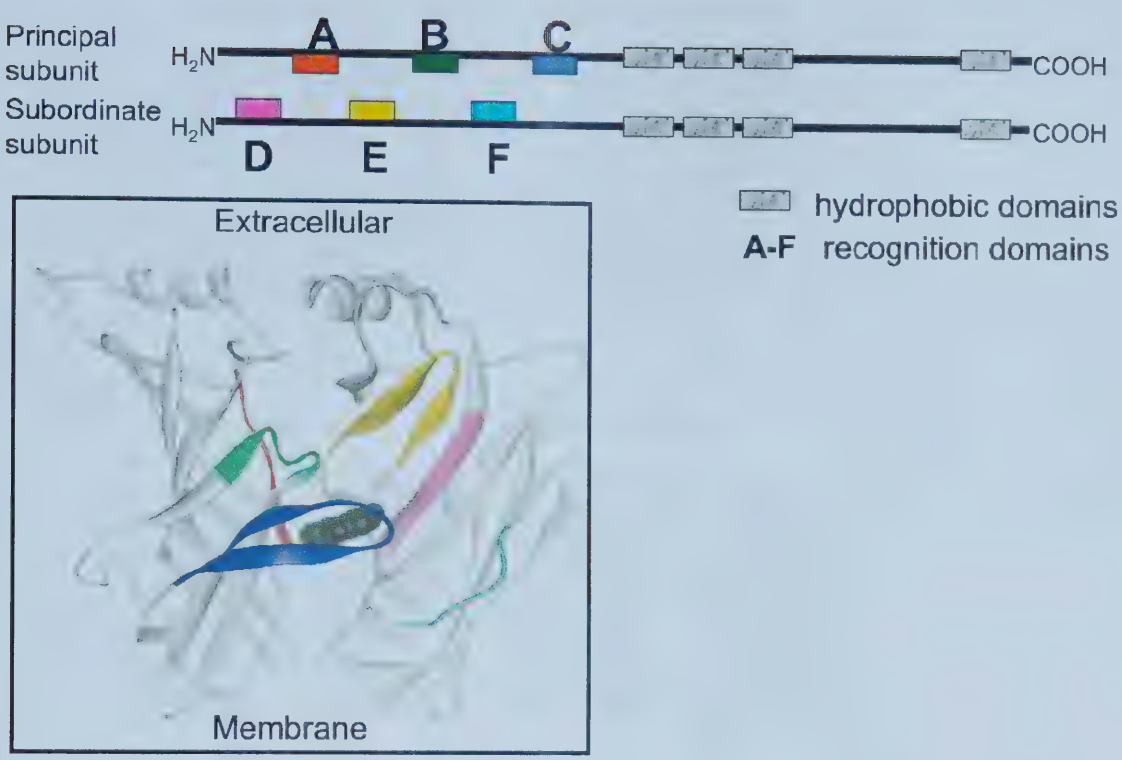

Figure 1-8: A schematic representation of the "six loop" model shows ligand binding domains lying at the interface between two subunits i.e. the principal subunit, carrying loops A-C, and the complementary subunit, contributing loops A-F. In the upper part of the figure, they are shown in sequence format while in the lower panel, the extracellular domain shows the juxtaposition of the recognition loops (using the same color coding) within the protein structure. **Courtesy Drs. Ian Martin and Susan Dunn**

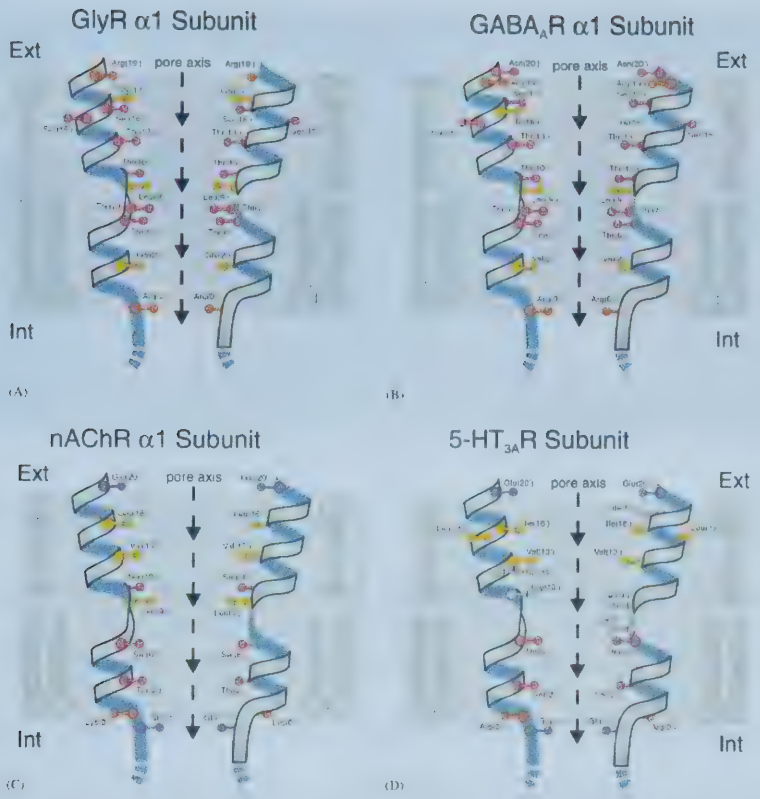

Figure 1-9: Schematic representation of the open state conformation of two M2 segments of the α1 subunits of the anion-selective GlyR (A), $GABA_AR$ (B) and the cation-selective nAChR (C) and the 5-HT3AR subunits (D). Note the tapering of the pores to a constriction at their intracellular end and the charged residues flanking the intra and extracellular mouths of the channels.

Keramidas, A., A. J. Moorhouse, et al. (2004). "Ligand-gated ion channels: mechanisms underlying ion selectivity." Prog Biophys Mol Biol 86(2): 161-204.

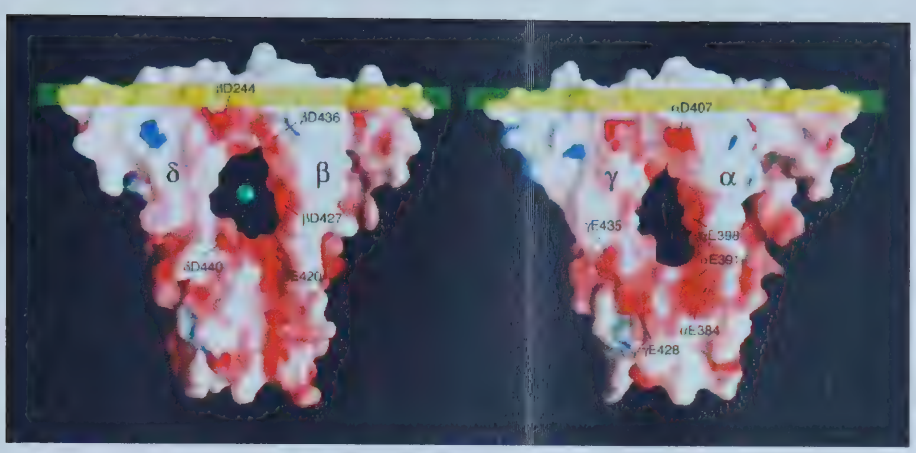

Figure 1-10: Electrostatic surface potential representations showing portals for cations between the MA helices of different subunits of the *Torpedo* nAChR. The windows formed between δ and β, and between γ and α_δ, are on the left and right, respectively. Labels identify exposed charged side chains. The location of the intracellular membrane surface is indicated (horizontal bars). The sphere in the δ–β window is the size of a potassium ion (2.7 Å diameter). Negative and positive charge in red and blue, respectively. **Unwin, N. (2005). "Refined structure of the nicotinic acetylcholine receptor at 4 Å resolution." J Mol Biol 346(4): 967-89.**

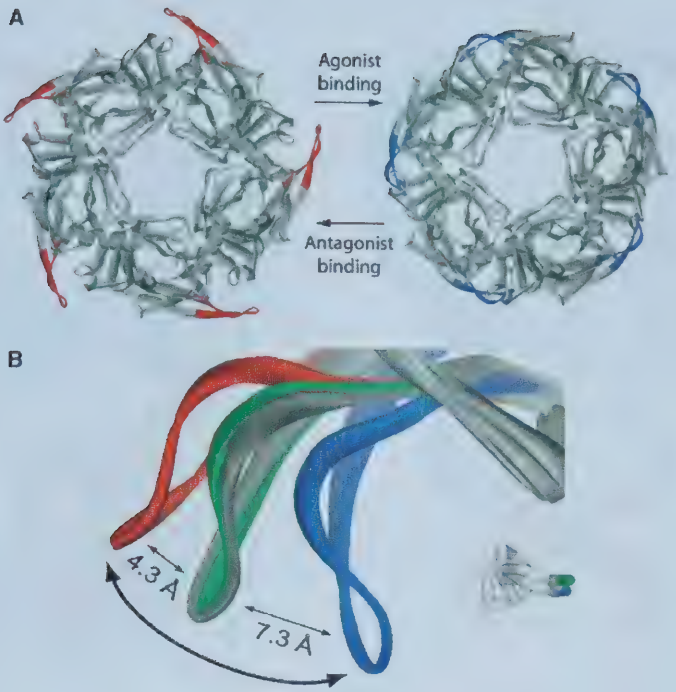

Figure 1-11: Ribbon diagram of the conformational fit mechanism and ligand selectivity. (A) Top views of the antagonist bound (red loops C) and full agonist bound AChBP pentamers (blue loops C) showing the distinctive conformations of the complexes. (B) Overlay of loop C in apo/unbound AChBP (gray), antagonist bound (red), partial agonist bound (green), and full agonist complexes (blue); full agonist molecule is shown in light gray. The curved arrow denotes opening and closure of loop C upon antagonist and agonist binding. **Hansen, S. B., G. Sulzenbacher, et al. (2005). "Structures of *Aplysia* AChBP complexes with nicotinic agonists and antagonists reveal distinctive binding interfaces and conformations." EMBO J 24(20): 3635-46.**

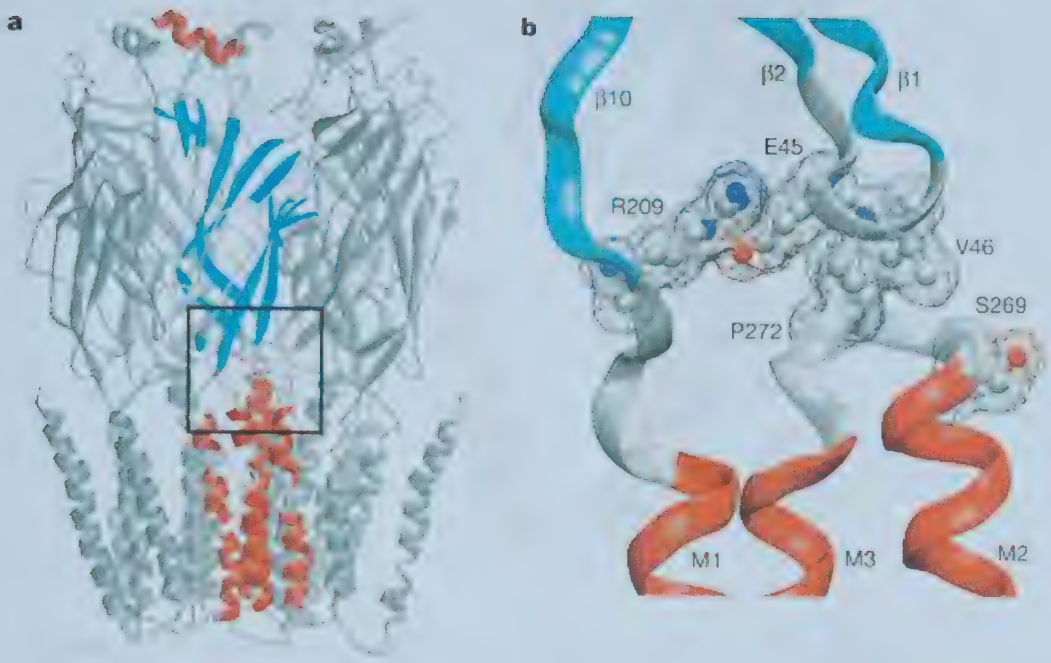

Figure 1-12: (A) Ribbon diagram showing the pentameric structure of the *Torpedo* nAChR. The secondary structures of one α subunit are highlighted (-helices, red; -sheets, cyan; loops, grey) and the region of communication between the LBDs and TMDs is located in the square. (B) Close-up view of the principal pathway in the α subunit, atoms of key residues are highlighted according to electrostatic charge (blue is positive, red is negative and grey is neutral). Van der Waals surfaces are rendered as a wire mesh. The key residues branch from β-strand 10 of the C-loop, the 1–2 linker and the linker spanning M2 and M3. The Cys-loop, 8–9 linker and M4 helix have been removed for clarity. **Lee, W. Y. and S. M. Sine (2005). "Principal pathway coupling agonist binding to channel gating in nicotinic receptors." Nature 438(7065): 243-7.**

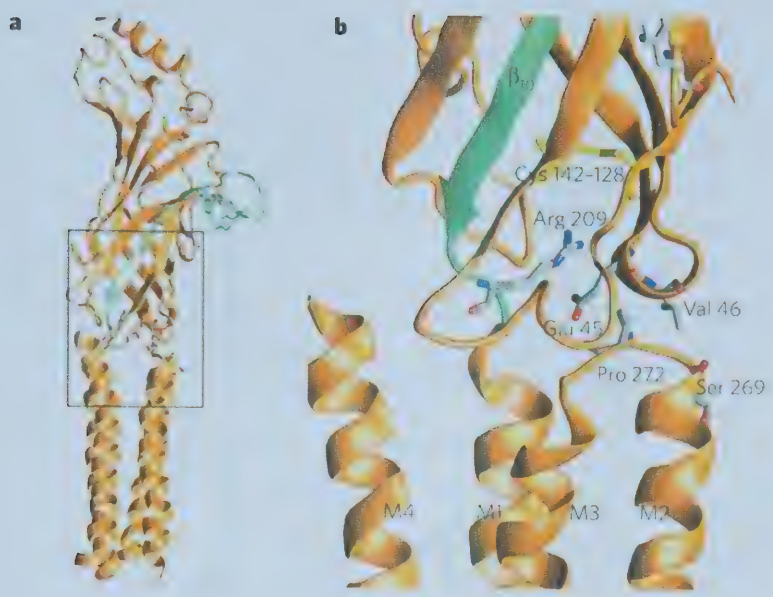

Figure 1-13: (A) Ribbon diagram representation of the side view of an α subunit from the *Torpedo* nAChR (Protein Data Bank code 2BG9), with the C-loop and β-strand 10 highlighted in green to illustrate connectivity between the binding site and the top of the ion channel domain. (B) Close-up view of the binding–channel interface with key residues of the principal pathway rendered in stick representation. The signature Cys-loop is formed by Cys 142 and Cys 128 through a disulphide bond (yellow). The loop 2 harbors Val 46 and Glu 45, and the M2–M3 linker harbors Ser 269 and Pro 272. **Sine, S. M. and A. G. Engel (2006). "Recent advances in Cys-loop receptor structure and function." Nature 440(7083): 448-55.**

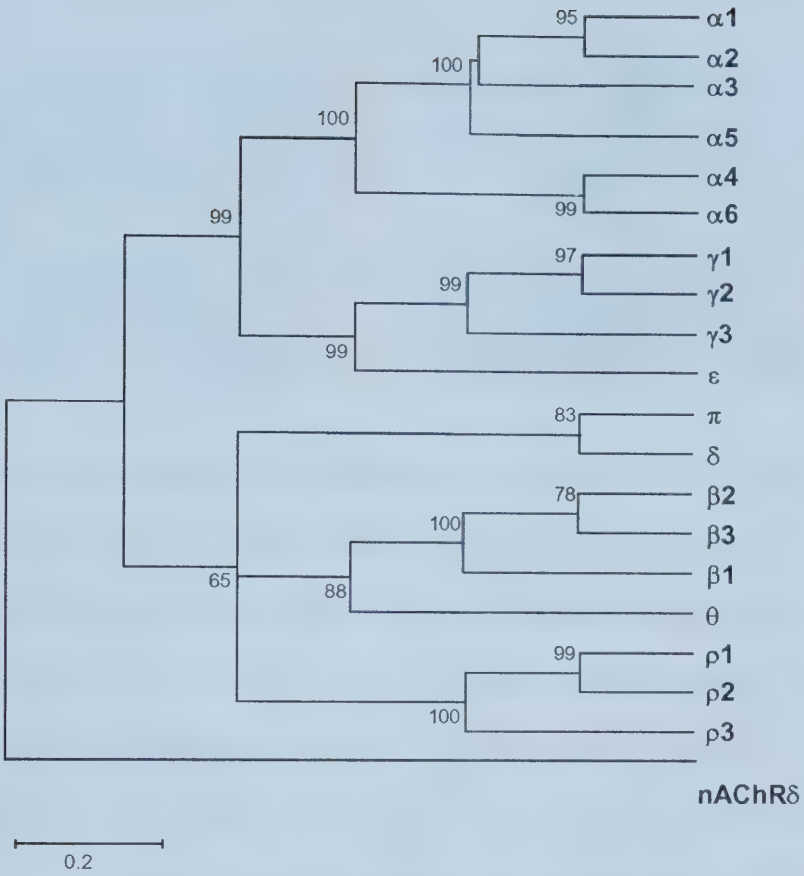

Figure 1-14: Dendrogram showing the sequence relationships of 19 human genes encoding $GABA_A$ receptor subunits. Sequences used are those of the mature protein following signal peptide removal. The nAChR δ subunit, a distantly related out-group marker was used for refinement of the plot. The length of horizontal branches connecting any two $GABA_A$ receptor subunits represents the fractional divergence in their amino acid sequence. The *scale bar* corresponds to 20% sequence divergence. Numbers at the junctions are bootstrap values for 100,000 replications. **Simon, J., H. Wakimoto, et al. (2004). "Analysis of the set of $GABA_A$ receptor genes in the human genome." J Biol Chem 279(40): 41422-35.**

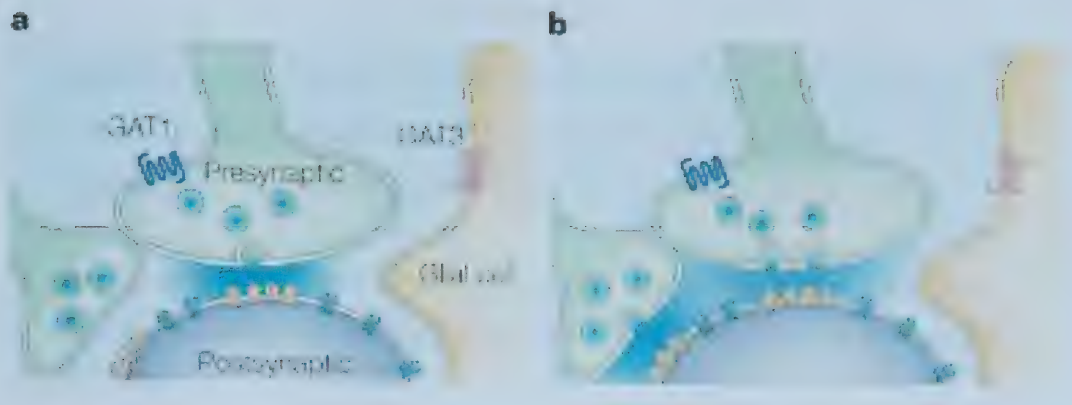

Figure 1-15: (A) The release of a single GABA containing vesicle from a presynaptic terminal activates $GABA_A$Rs clustered in the membrane immediately beneath the release site (yellow). The diffuse blue shading indicates the spread of released GABA (GAT is the GABA transporter which is responsible for its reuptake). (B) Action potential-dependent release of multiple vesicles, or evoked release, from several terminals promotes GABA "spillover", and activates both synaptic receptors and perisynaptic, or extrasynaptic, receptors (blue). A sustained low ambient concentration GABA persists despite the activity of the neuronal and glial GABA transporters (GAT1 and GAT3) tonically activates high-affinity extrasynaptic receptors. **Farrant, M. and Z. Nusser (2005). "Variations on an inhibitory theme: phasic and tonic activation of $GABA_A$ receptors." Nat Rev Neurosci 6(3): 215-29.**

REFERENCES

Alldred, M.J., Mulder-Rosi, J., Lingenfelter, S.E., Chen, G., Luscher, B., 2005. Distinct γ2 subunit domains mediate clustering and synaptic function of postsynaptic $GABA_A$ receptors and gephyrin. J Neurosci 25, 594-603.

Amin, J., Weiss, D.S., 1993. GABAA receptor needs two homologous domains of the β-subunit for activation by GABA but not by pentobarbital. Nature 366, 565-569.

Baer, K., Waldvogel, H.J., Faull, R.L., Rees, M.I., 2009. Localization of glycine receptors in the human forebrain, brainstem, and cervical spinal cord: an immunohistochemical review. Front Mol Neurosci 2, 25.

Bai, D., Zhu, G., Pennefather, P., Jackson, M.F., MacDonald, J.F., Orser, B.A., 2001. Distinct functional and pharmacological properties of tonic and quantal inhibitory postsynaptic currents mediated by γ-aminobutyric acid(A) receptors in hippocampal neurons. Mol Pharmacol 59, 814-824.

Bali, M., Akabas, M.H., 2007. The location of a closed channel gate in the $GABA_A$ receptor channel. J Gen Physiol 129, 145-159.

Barik, J., Wonnacott, S., 2009. Molecular and Cellular Mechanisms of Action of Nicotine in the CNS. In: Heidelberg, S.-V.B. (Ed.), Handbook of Experimental Pharmacology pp. 174-207.

Barnard, E.A., Beeson, D., Bilbe, G., Brown, D.A., Constanti, A., Houamed, K., Smart, T.G., 1984. A system for the translation of receptor messenger-RNA and the study of the assembly of functional receptors. J Recept Res 4, 681-704.

Barnard, E.A., Skolnick, P., Olsen, R.W., Mohler, H., Sieghart, W., Biggio, G., Braestrup, C., Bateson, A.N., Langer, S.Z., 1998. International Union of Pharmacology. XV. Subtypes of γ-aminobutyric acid A receptors: classification on the basis of subunit structure and receptor function. Pharmacol Rev 50, 291-313.

Beck, M., Brickley, K., Wilkinson, H.L., Sharma, S., Smith, M., Chazot, P.L., Pollard, S., Stephenson, F.A., 2002. Identification, molecular cloning, and characterization of a novel $GABA_A$ receptor-associated protein, GRIF-1. J Biol Chem 277, 30079-30090.

Bera, A.K., Chatav, M., Akabas, M.H., 2002. $GABA_A$ receptor M2-M3 loop secondary structure and changes in accessibility during channel gating. J Biol Chem 277, 43002-43010.

Bertrand, D., Galzi, J.L., Devillers-Thiery, A., Bertrand, S., Changeux, J.P., 1993. Mutations at two distinct sites within the channel domain M2 alter calcium permeability of neuronal α 7 nicotinic receptor. Proc Natl Acad Sci U S A 90, 6971-6975.

Bianchi, M.T., Haas, K.F., Macdonald, R.L., 2001. Structural determinants of fast desensitization and desensitization-deactivation coupling in $GABA_A$ receptors. J Neurosci 21, 1127-1136.

Bianchi, M.T., Macdonald, R.L., 2003. Neurosteroids shift partial agonist activation of $GABA_A$ receptor channels from low- to high-efficacy gating patterns. J Neurosci 23, 10934-10943.

Bloom, F.E., Iversen, L.L., 1971. Localizing [^{3}H] GABA in nerve terminals of rat cerebral cortex by electron microscopic autoradiography. Nature 229, 628-630.

Bloomquist, J.R., 2003. Chloride channels as tools for developing selective insecticides. Arch Insect Biochem Physiol 54, 145-156.

Bocquet, N., Nury, H., Baaden, M., Le Poupon, C., Changeux, J.P., Delarue, M., Corringer, P.J., 2009. X-ray structure of a pentameric ligand-gated ion channel in an apparently open conformation. Nature 457, 111-114.

Bourne, Y., Talley, T.T., Hansen, S.B., Taylor, P., Marchot, P., 2005. Crystal structure of a Cbtx-AChBP complex reveals essential interactions between snake α-neurotoxins and nicotinic receptors. EMBO J 24, 1512-1522.

Bouzat, C., Gumilar, F., Spitzmaul, G., Wang, H.L., Rayes, D., Hansen, S.B., Taylor, P., Sine, S.M., 2004. Coupling of agonist binding to channel gating in an ACh-binding protein linked to an ion channel. Nature 430, 896-900.

Bowery, N.G., Bettler, B., Froestl, W., Gallagher, J.P., Marshall, F., Raiteri, M., Bonner, T.I., Enna, S.J., 2002. International Union of Pharmacology. XXXIII. Mammalian γ-aminobutyric acid(B) receptors: structure and function. Pharmacol Rev 54, 247-264.

Brejc, K., van Dijk, W.J., Klaassen, R.V., Schuurmans, M., van Der Oost, J., Smit, A.B., Sixma, T.K., 2001. Crystal structure of an ACh-binding protein reveals the ligand-binding domain of nicotinic receptors. Nature 411, 269-276.

Brickley, S.G., Cull-Candy, S.G., Farrant, M., 1996. Development of a tonic form of synaptic inhibition in rat cerebellar granule cells resulting from persistent activation of $GABA_A$ receptors. J Physiol 497 (Pt 3), 753-759.

Brickley, S.G., Revilla, V., Cull-Candy, S.G., Wisden, W., Farrant, M., 2001. Adaptive regulation of neuronal excitability by a voltage-independent potassium conductance. Nature 409, 88-92.

Brown, N., Kerby, J., Bonnert, T.P., Whiting, P.J., Wafford, K.A., 2002. Pharmacological characterization of a novel cell line expressing human α4β3δ $GABA_A$ receptors. Br J Pharmacol 136, 965-974.

Carland, J.E., Cooper, M.A., Sugiharto, S., Jeong, H.J., Lewis, T.M., Barry, P.H., Peters, J.A., Lambert, J.J., Moorhouse, A.J., 2009. Characterization of the effects of charged residues in the intracellular loop on ion permeation in α1 glycine receptor channels. J Biol Chem 284, 2023-2030.

Celie, P.H., Kasheverov, I.E., Mordvintsev, D.Y., Hogg, R.C., van Nierop, P., van Elk, R., van Rossum-Fikkert, S.E., Zhmak, M.N., Bertrand, D., Tsetlin, V., Sixma, T.K., Smit, A.B., 2005a. Crystal structure of nicotinic acetylcholine receptor homolog AChBP in complex with an α-conotoxin PnIA variant. Nat Struct Mol Biol 12, 582-588.

Celie, P.H., Klaassen, R.V., van Rossum-Fikkert, S.E., van Elk, R., van Nierop, P., Smit, A.B., Sixma, T.K., 2005b. Crystal structure of acetylcholine-binding protein from Bulinus truncatus reveals the conserved structural scaffold and sites of variation in nicotinic acetylcholine receptors. J Biol Chem 280, 26457-26466.

Celie, P.H., van Rossum-Fikkert, S.E., van Dijk, W.J., Brejc, K., Smit, A.B., Sixma, T.K., 2004. Nicotine and carbamylcholine binding to nicotinic acetylcholine receptors as studied in AChBP crystal structures. Neuron 41, 907-914.

Chandra, D., Jia, F., Liang, J., Peng, Z., Suryanarayanan, A., Werner, D.F., Spigelman, I., Houser, C.R., Olsen, R.W., Harrison, N.L., Homanics, G.E., 2006. $GABA_A$ receptor α 4 subunits mediate extrasynaptic inhibition in thalamus and dentate gyrus and the action of gaboxadol. Proc Natl Acad Sci U S A 103, 15230-15235.

Changeux, J., Edelstein, S.J., 2001. Allosteric mechanisms in normal and pathological nicotinic acetylcholine receptors. Curr Opin Neurobiol 11, 369-377.

Changeux, J.P., Galzi, J.L., Devillers-Thiery, A., Bertrand, D., 1992. The functional architecture of the acetylcholine nicotinic receptor explored by affinity labelling and site-directed mutagenesis. Q Rev Biophys 25, 395-432.

Changeux, J.P., Kasai, M., Lee, C.Y., 1970. Use of Snake Venom Toxin to Characterize the Cholinergic Receptor Protein. Proc Natl Acad Sci U S A 67, 1241-1247.

Charych, E.I., Yu, W., Miralles, C.P., Serwanski, D.R., Li, X., Rubio, M., De Blas, A.L., 2004. The brefeldin A-inhibited GDP/GTP exchange factor 2, a protein involved in vesicular trafficking, interacts with the beta subunits of the GABA receptors. J Neurochem 90, 173-189.

Chen, L., Durkin, K.A., Casida, J.E., 2006. Structural model for γ-aminobutyric acid receptor noncompetitive antagonist binding: widely diverse structures fit the same site. Proc Natl Acad Sci U S A 103, 5185-5190.

Colquhoun, D., 1998. Binding, gating, affinity and efficacy: the interpretation of structure-activity relationships for agonists and of the effects of mutating receptors. Br J Pharmacol 125, 924-947.

Conti-Fine, B.M., Navaneetham, D., Lei, S., Maus, A.D., 2000. Neuronal nicotinic receptors in non-neuronal cells: new mediators of tobacco toxicity? Eur J Pharmacol 393, 279-294.

Corringer, P.J., Le Novere, N., Changeux, J.P., 2000. Nicotinic receptors at the amino acid level. Annu Rev Pharmacol Toxicol 40, 431-458.

Curtis, D.R., Duggan, A.W., Felix, D., Johnston, G.A., 1970. Bicuculline and central GABA receptors. Nature 228, 676-677.

Dajas-Bailador, F., Wonnacott, S., 2004. Nicotinic acetylcholine receptors and the regulation of neuronal signalling. Trends Pharmacol Sci 25, 317-324.

Dani, J.A., Bertrand, D., 2007. Nicotinic acetylcholine receptors and nicotinic cholinergic mechanisms of the central nervous system. Annu Rev Pharmacol Toxicol 47, 699-729.

Davies, P.A., Pistis, M., Hanna, M.C., Peters, J.A., Lambert, J.J., Hales, T.G., Kirkness, E.F., 1999. The 5-HT3B subunit is a major determinant of serotonin-receptor function. Nature 397, 359-363.

Dellisanti, C.D., Yao, Y., Stroud, J.C., Wang, Z.Z., Chen, L., 2007. Crystal structure of the extracellular domain of nAChR α1 bound to α-bungarotoxin at 1.94 Å resolution. Nat Neurosci 10, 953-962.

Dickinson, J.A., Hanrott, K.E., Mok, M.H., Kew, J.N., Wonnacott, S., 2007. Differential coupling of α7 and non- α 7 nicotinic acetylcholine receptors to calcium-induced calcium release and voltage-operated calcium channels in PC12 cells. J Neurochem 100, 1089-1096.

Dickinson, J.A., Kew, J.N., Wonnacott, S., 2008. Presynaptic α 7- and β 2-containing nicotinic acetylcholine receptors modulate excitatory amino acid release from rat prefrontal cortex nerve terminals via distinct cellular mechanisms. Mol Pharmacol 74, 348-359.

Difrancesco, A., 1963. Diazepam, a new tranquilizer. Am J Psychiatry 119, 989-990.

Eglen, R.M., 2005. Muscarinic receptor subtype pharmacology and physiology. Prog Med Chem 43, 105-136.

Eilers, H., Schaeffer, E., Bickler, P.E., Forsayeth, J.R., 1997. Functional deactivation of the major neuronal nicotinic receptor caused by nicotine and a protein kinase C-dependent mechanism. Mol Pharmacol 52, 1105-1112.

Ernst, M., Brauchart, D., Boresch, S., Sieghart, W., 2003. Comparative modeling of $GABA_A$ receptors: limits, insights, future developments. Neuroscience 119, 933-943.

Fabian-Fine, R., Skehel, P., Errington, M.L., Davies, H.A., Sher, E., Stewart, M.G., Fine, A., 2001. Ultrastructural distribution of the α 7 nicotinic acetylcholine receptor subunit in rat hippocampus. J Neurosci 21, 7993-8003.

Farrant, M., Nusser, Z., 2005. Variations on an inhibitory theme: phasic and tonic activation of $GABA_A$ receptors. Nat Rev Neurosci 6, 215-229.

Finer-Moore, J., Stroud, R.M., 1984. Amphipathic analysis and possible formation of the ion channel in an acetylcholine receptor. Proc Natl Acad Sci U S A 81, 155-159.

Frolund, B., Jensen, L.S., Guandalini, L., Canillo, C., Vestergaard, H.T., Kristiansen, U., Nielsen, B., Stensbol, T.B., Madsen, C., Krogsgaard-Larsen, P., Liljefors, T., 2005. Potent 4-aryl- or 4-arylalkyl-substituted 3-isoxazolol $GABA_A$ antagonists: synthesis, pharmacology, and molecular modeling. J Med Chem 48, 427-439.

Fucile, S., 2004. Ca2+ permeability of nicotinic acetylcholine receptors. Cell Calcium 35, 1-8.

Galzi, J.L., Revah, F., Bessis, A., Changeux, J.P., 1991. Functional architecture of the nicotinic acetylcholine receptor: from electric organ to brain. Annu Rev Pharmacol Toxicol 31, 37-72.

Gavish, M., Snyder, S.H., 1980. Soluble benzodiazepine receptors: GABAergic regulation. Life Sci 26, 579-582.

Gotti, C., Clementi, F., 2004. Neuronal nicotinic receptors: from structure to pathology. Prog Neurobiol 74, 363-396.

Grutter, T., Changeux, J.P., 2001. Nicotinic receptors in wonderland. Trends Biochem Sci 26, 459-463.

Gueorguiev, V.D., Cheng, S.Y., Sabban, E.L., 2006. Prolonged activation of cAMP-response element-binding protein and ATF-2 needed for nicotine-triggered elevation of tyrosine hydroxylase gene transcription in PC12 cells. J Biol Chem 281, 10188-10195.

Haas, K.F., Macdonald, R.L., 1999. $GABA_A$ receptor subunit γ2 and δ subtypes confer unique kinetic properties on recombinant $GABA_A$ receptor currents in mouse fibroblasts. J Physiol 514 (Pt 1), 27-45.

Hales, T.G., Dunlop, J.I., Deeb, T.Z., Carland, J.E., Kelley, S.P., Lambert, J.J., Peters, J.A., 2006. Common determinants of single channel conductance within the large cytoplasmic loop of 5-hydroxytryptamine type 3 and α4β2 nicotinic acetylcholine receptors. J Biol Chem 281, 8062-8071.

Hansen, S.B., Sulzenbacher, G., Huxford, T., Marchot, P., Taylor, P., Bourne, Y., 2005. Structures of Aplysia AChBP complexes with nicotinic agonists and antagonists reveal distinctive binding interfaces and conformations. EMBO J 24, 3635-3646.

Hartvig, L., Lukensmejer, B., Liljefors, T., Dekermendjian, K., 2000. Two conserved arginines in the extracellular N-terminal domain of the $GABA_A$ receptor α5 subunit are crucial for receptor function. J Neurochem 75, 1746-1753.

Heyers, W., Luddens, H., 1998. The diversity of $GABA_A$ receptors. Pharmacological and electrophysiological properties of $GABA_A$ channel subtypes. Mol Neurobiol 18, 35-86.

Hilf, R.J., Dutzler, R., 2008. X-ray structure of a prokaryotic pentameric ligand-gated ion channel. Nature 452, 375-379.

Hilf, R.J., Dutzler, R., 2009a. A prokaryotic perspective on pentameric ligand-gated ion channel structure. Curr Opin Struct Biol.

Hilf, R.J., Dutzler, R., 2009b. Structure of a potentially open state of a proton-activated pentameric ligand-gated ion channel. Nature 457, 115-118.

Hill, D.R., Bowery, N.G., 1981. 3H-baclofen and [^{3}H] GABA bind to bicuculline-insensitive $GABA_B$ sites in rat brain. Nature 290, 149-152.

Hu, M., Liu, Q.S., Chang, K.T., Berg, D.K., 2002. Nicotinic regulation of CREB activation in hippocampal neurons by glutamatergic and nonglutamatergic pathways. Mol Cell Neurosci 21, 616-625.

Huebsch, K.A., Maimone, M.M., 2003. Rapsyn-mediated clustering of acetylcholine receptor subunits requires the major cytoplasmic loop of the receptor subunits. J Neurobiol 54, 486-501.

Imoto, K., Busch, C., Sakmann, B., Mishina, M., Konno, T., Nakai, J., Bujo, H., Mori, Y., Fukuda, K., Numa, S., 1988. Rings of negatively charged amino acids

determine the acetylcholine receptor channel conductance. Nature 335, 645-648.

Inoue, M., Akaike, N., 1988. Blockade of γ-aminobutyric acid-gated chloride current in frog sensory neurons by picrotoxin. Neurosci Res 5, 380-394.

Jansen, M., Bali, M., Akabas, M.H., 2008. Modular design of Cys-loop ligand-gated ion channels: functional 5-HT_3 and GABA ρ1 receptors lacking the large cytoplasmic M3M4 loop. J Gen Physiol 131, 137-146.

Jeanclos, E.M., Lin, L., Treuil, M.W., Rao, J., DeCoster, M.A., Anand, R., 2001. The chaperone protein 14-3-3eta interacts with the nicotinic acetylcholine receptor α 4 subunit. Evidence for a dynamic role in subunit stabilization. J Biol Chem 276, 28281-28290.

Jia, F., Pignataro, L., Schofield, C.M., Yue, M., Harrison, N.L., Goldstein, P.A., 2005. An extrasynaptic $GABA_A$ receptor mediates tonic inhibition in thalamic VB neurons. J Neurophysiol 94, 4491-4501.

Jones, A.K., Sattelle, D.B., 2008. The cys-loop ligand-gated ion channel gene superfamily of the nematode, Caenorhabditis elegans. Invert Neurosci 8, 41-47.

Jones, M.V., Westbrook, G.L., 1996. The impact of receptor desensitization on fast synaptic transmission. Trends Neurosci 19, 96-101.

Kalamida, D., Poulas, K., Avramopoulou, V., Fostieri, E., Lagoumintzis, G., Lazaridis, K., Sideri, A., Zouridakis, M., Tzartos, S.J., 2007. Muscle and neuronal nicotinic acetylcholine receptors. Structure, function and pathogenicity. FEBS J 274, 3799-3845.

Kaneda, M., Farrant, M., Cull-Candy, S.G., 1995. Whole-cell and single-channel currents activated by GABA and glycine in granule cells of the rat cerebellum. J Physiol 485 (Pt 2), 419-435.

Kanematsu, T., Mizokami, A., Watanabe, K., Hirata, M., 2007. Regulation of $GABA_A$ -receptor surface expression with special reference to the involvement of GABARAP ($GABA_A$ receptor-associated protein) and PRIP (phospholipase C-related, but catalytically inactive protein). J Pharmacol Sci 104, 285-292.

Karlin, A., 2002. Emerging structure of the nicotinic acetylcholine receptors. Nat Rev Neurosci 3, 102-114.

Kelley, S.P., Dunlop, J.I., Kirkness, E.F., Lambert, J.J., Peters, J.A., 2003. A cytoplasmic region determines single-channel conductance in $5\text{-}HT_3$ receptors. Nature 424, 321-324.

Keramidas, A., Moorhouse, A.J., Schofield, P.R., Barry, P.H., 2004. Ligand-gated ion channels: mechanisms underlying ion selectivity. Prog Biophys Mol Biol 86, 161-204.

Khatri, A., Sedelnikova, A., Weiss, D.S., 2009. Structural rearrangements in loop F of the GABA receptor signal ligand binding, not channel activation. Biophys J 96, 45-55.

Kirsch, J., 1999. Assembly of signaling machinery at the postsynaptic membrane. Curr Opin Neurobiol 9, 329-335.

Kirsch, J., Langosch, D., Prior, P., Littauer, U.Z., Schmitt, B., Betz, H., 1991. The 93-kDa glycine receptor-associated protein binds to tubulin. J Biol Chem 266, 22242-22245.

Kittler, J.T., Delmas, P., Jovanovic, J.N., Brown, D.A., Smart, T.G., Moss, S.J., 2000. Constitutive endocytosis of $GABA_A$ receptors by an association with the adaptin AP2 complex modulates inhibitory synaptic currents in hippocampal neurons. J Neurosci 20, 7972-7977.

Korpi, E.R., Grunder, G., Luddens, H., 2002. Drug interactions at $GABA_A$ receptors. Prog Neurobiol 67, 113-159.

Krogsgaard-Larsen, P., Frolund, B., Liljefors, T., Ebert, B., 2004. $GABA_A$ agonists and partial agonists: THIP (Gaboxadol) as a non-opioid analgesic and a novel type of hypnotic. Biochem Pharmacol 68, 1573-1580.

Krogsgaard-Larsen, P., Johnston, G.A., Curtis, D.R., Game, C.J., McCulloch, R.M., 1975. Structure and biological activity of a series of conformationally restricted analogues of GABA. J Neurochem 25, 803-809.

Kuo, Y.P., Xu, L., Eaton, J.B., Zhao, L., Wu, J., Lukas, R.J., 2005. Roles for nicotinic acetylcholine receptor subunit large cytoplasmic loop sequences in receptor expression and function. J Pharmacol Exp Ther 314, 455-466.

Lambert, J.J., Belelli, D., Peden, D.R., Vardy, A.W., Peters, J.A., 2003. Neurosteroid modulation of $GABA_A$ receptors. Prog Neurobiol 71, 67-80.

Lansdell, S.J., Gee, V.J., Harkness, P.C., Doward, A.I., Baker, E.R., Gibb, A.J., Millar, N.S., 2005. RIC-3 enhances functional expression of multiple nicotinic acetylcholine receptor subtypes in mammalian cells. Mol Pharmacol 68, 1431-1438.

Le Novere, N., Corringer, P.J., Changeux, J.P., 2002. The diversity of subunit composition in nAChRs: evolutionary origins, physiologic and pharmacologic consequences. J Neurobiol 53, 447-456.

Lee, W.Y., Sine, S.M., 2005. Principal pathway coupling agonist binding to channel gating in nicotinic receptors. Nature 438, 243-247.

Lena, C., Changeux, J.P., Mulle, C., 1993. Evidence for "preterminal" nicotinic receptors on GABAergic axons in the rat interpeduncular nucleus. J Neurosci 13, 2680-2688.

Lester, H.A., 1992. The permeation pathway of neurotransmitter-gated ion channels. Annu Rev Biophys Biomol Struct 21, 267-292.

Levi, S., Logan, S.M., Tovar, K.R., Craig, A.M., 2004. Gephyrin is critical for glycine receptor clustering but not for the formation of functional GABAergic synapses in hippocampal neurons. J Neurosci 24, 207-217.

Lindstrom, J., 1997. Nicotinic acetylcholine receptors in health and disease. Mol Neurobiol 15, 193-222.

Lummis, S.C., Beene, D.L., Lee, L.W., Lester, H.A., Broadhurst, R.W., Dougherty, D.A., 2005. Cis-trans isomerization at a proline opens the pore of a neurotransmitter-gated ion channel. Nature 438, 248-252.

Luscher, B., Keller, C.A., 2004. Regulation of $GABA_A$ receptor trafficking, channel activity, and functional plasticity of inhibitory synapses. Pharmacol Ther 102, 195-221.

Lynch, J.W., Rajendra, S., Pierce, K.D., Handford, C.A., Barry, P.H., Schofield, P.R., 1997. Identification of intracellular and extracellular domains mediating signal transduction in the inhibitory glycine receptor chloride channel. EMBO J 16, 110-120.

Macdonald, R.L., Barker, J.L., 1978. Specific antagonism of GABA-mediated postsynaptic inhibition in cultured mammalian spinal cord neurons: a common mode of convulsant action. Neurology 28, 325-330.

Macdonald, R.L., Olsen, R.W., 1994. $GABA_A$ receptor channels. Annu Rev Neurosci 17, 569-602.

Maconochie, D.J., Zempel, J.M., Steinbach, J.H., 1994. How quickly can $GABA_A$ receptors open? Neuron 12, 61-71.

Mathers, D.A., Yoshida, H., 1987. The benzodiazepine triazolam: direct and GABA depressant effects on cultured mouse spinal cord neurons. Eur J Pharmacol 139, 53-60.

Mercado, J., Czajkowski, C., 2006. Charged residues in the α1 and β2 pre-M1 regions involved in $GABA_A$ receptor activation. J Neurosci 26, 2031-2040.

Miledi, R., Molinoff, P., Potter, L.T., 1971. Isolation of the cholinergic receptor protein of *Torpedo* electric tissue. Nature 229, 554-557.

Miller, C., 1989. Genetic manipulation of ion channels: a new approach to structure and mechanism. Neuron 2, 1195-1205.

Miyazawa, A., Fujiyoshi, Y., Stowell, M., Unwin, N., 1999. Nicotinic acetylcholine receptor at 4.6 Å resolution: transverse tunnels in the channel wall. J Mol Biol 288, 765-786.

Miyazawa, A., Fujiyoshi, Y., Unwin, N., 2003. Structure and gating mechanism of the acetylcholine receptor pore. Nature 423, 949-955.

Mody, I., De Koninck, Y., Otis, T.S., Soltesz, I., 1994. Bridging the cleft at GABA synapses in the brain. Trends Neurosci 17, 517-525.

Mokrab, Y., Bavro, V.N., Mizuguchi, K., Todorov, N.P., Martin, I.L., Dunn, S.M., Chan, S.L., Chau, P.L., 2007. Exploring ligand recognition and ion flow in comparative models of the human GABA type A receptor. J Mol Graph Model 26, 760-774.

Mozrzymas, J.W., 2004. Dynamism of $GABA_A$ receptor activation shapes the "personality" of inhibitory synapses. Neuropharmacology 47, 945-960.

Mozrzymas, J.W., Barberis, A., Mercik, K., Zarnowska, E.D., 2003. Binding sites, singly bound states, and conformation coupling shape GABA-evoked currents. J Neurophysiol 89, 871-883.

Mukhtasimova, N., Lee, W.Y., Wang, H.L., Sine, S.M., 2009. Detection and trapping of intermediate states priming nicotinic receptor channel opening. Nature 459, 451-454.

Noda, M., Takahashi, H., Tanabe, T., Toyosato, M., Furutani, Y., Hirose, T., Asai, M., Inayama, S., Miyata, T., Numa, S., 1982. Primary structure of α-subunit precursor of *Torpedo* californica acetylcholine receptor deduced from cDNA sequence. Nature 299, 793-797.

Noda, M., Takahashi, H., Tanabe, T., Toyosato, M., Kikyotani, S., Hirose, T., Asai, M., Takashima, H., Inayama, S., Miyata, T., Numa, S., 1983. Primary structures of β- and δ-subunit precursors of *Torpedo californica* acetylcholine receptor deduced from cDNA sequences. Nature 301, 251-255.

Nusser, Z., Hajos, N., Somogyi, P., Mody, I., 1998a. Increased number of synaptic $GABA_A$ receptors underlies potentiation at hippocampal inhibitory synapses. Nature 395, 172-177.

Nusser, Z., Mody, I., 2002. Selective modulation of tonic and phasic inhibitions in dentate gyrus granule cells. J Neurophysiol 87, 2624-2628.

Nusser, Z., Sieghart, W., Somogyi, P., 1998b. Segregation of different $GABA_A$ receptors to synaptic and extrasynaptic membranes of cerebellar granule cells. J Neurosci 18, 1693-1703.

O'Brien, R.D., Gilmour, L.P., 1969. A Muscarone-Binding MAterial in Electroplax and its Relation to the Acetylcholine Receptor I. Centrifugal Assay. Proc Natl Acad Sci U S A 63, 496-503.

O'Brien, R.D., Gilmour, L.P., Edefrawi, M.E., 1970. A Muscarone-Binding Material in Electroplax and its Relation to the Acetylcholine Receptor II. Dialysis Assay. Proc Natl Acad Sci U S A 65, 438-445.

Obata, T., Yamamura, H.I., 1986. The effect of benzodiazepines and β-carbolines on GABA-stimulated chloride influx by membrane vesicles from the rat cerebral cortex. Biochem Biophys Res Commun 141, 1-6.

Olsen, R.W., Sieghart, W., 2008. International Union of Pharmacology. LXX. Subtypes of γ-aminobutyric acid(A) receptors: classification on the basis of subunit composition, pharmacology, and function. Update. Pharmacol Rev 60, 243-260.

Otis, T.S., Staley, K.J., Mody, I., 1991. Perpetual inhibitory activity in mammalian brain slices generated by spontaneous GABA release. Brain Res 545, 142-150.

Paulsen, I.M., Martin, I.L., Dunn, S.M., 2009. Isomerization of the proline in the M2-M3 linker is not required for activation of the human $5\text{-}HT_3A$ receptor. J Neurochem 110, 870-878.

Peng, Z., Hauer, B., Mihalek, R.M., Homanics, G.E., Sieghart, W., Olsen, R.W., Houser, C.R., 2002. $GABA_A$ receptor changes in δ subunit-deficient mice:

altered expression of α4 and γ2 subunits in the forebrain. J Comp Neurol 446, 179-197.

Pirker, S., Schwarzer, C., Wieselthaler, A., Sieghart, W., Sperk, G., 2000. $GABA_A$ receptors: immunocytochemical distribution of 13 subunits in the adult rat brain. Neuroscience 101, 815-850.

Pless, S.A., Lynch, J.W., 2009a. Ligand-specific conformational changes in the α1 glycine receptor ligand-binding domain. J Biol Chem 284, 15847-15856.

Pless, S.A., Lynch, J.W., 2009b. Magnitude of a conformational change in the glycine receptor β1-β2 loop is correlated with agonist efficacy. J Biol Chem 284, 27370-27376.

Puia, G., Mienville, J.M., Matsumoto, K., Takahata, H., Watanabe, H., Costa, E., Guidotti, A., 2003. On the putative physiological role of allopregnanolone on $GABA_A$ receptor function. Neuropharmacology 44, 49-55.

Quinn, M.R., Harris, C.L., 1995. Taurine allosterically inhibits binding of [^{35}S]-t-butylbicyclophosphorothionate (TBPS) to rat brain synaptic membranes. Neuropharmacology 34, 1607-1613.

Raftery, M.A., 1973. Isolation of Acetylcholine Receptor-α-Bungarotoxin Complexes from *Torpedo californica* Electroplax. Arch Biochem Biophys 154, 270-276.

Raftery, M.A., Hunkapiller, M.W., Strader, C.D., Hood, L.E., 1980. Acetylcholine receptor: complex of homologous subunits. Science 208, 1454-1456.

Raftery, M.A., Schmidt, J., Clark, D.G., Wolcott, R.G., 1971. Demonstration of a specific α-bungarotoxin binding component in Electrophorous electricus electroplax membranes. Biochem Biophys Res Commun 45, 1622-1629.

Ringstad, N., Abe, N., Horvitz, H.R., 2009. Ligand-gated chloride channels are receptors for biogenic amines in C. elegans. Science 325, 96-100.

Saxena, N.C., Macdonald, R.L., 1996. Properties of putative cerebellar gamma-aminobutyric acid A receptor isoforms. Mol Pharmacol 49, 567-579.

Schmidt, J., Raftery, M.A., 1972. Use of Affinity Chromatography for Acetylcholine Receptor Purification. Biochem Biophys Res Commun 49, 572-578.

Schmidt, J., Raftery, M.A., 1973. Purification of Acetylcholine Receptors from *Torpedo californica* Electroplax by Affinity Chomatography. Biochemistry 12, 852-856.

Schonbrun, J., Wedemeyer, W.J., Baker, D., 2002. Protein structure prediction in 2002. Curr Opin Struct Biol 12, 348-354.

Semyanov, A., Walker, M.C., Kullmann, D.M., 2003. GABA uptake regulates cortical excitability via cell type-specific tonic inhibition. Nat Neurosci 6, 484-490.

Sieghart, W., Sperk, G., 2002. Subunit composition, distribution and function of $GABA_A$ receptor subtypes. Curr Top Med Chem 2, 795-816.

Simon, J., Wakimoto, H., Fujita, N., Lalande, M., Barnard, E.A., 2004. Analysis of the set of $GABA_A$ receptor genes in the human genome. J Biol Chem 279, 41422-41435.

Sine, S.M., 2002. The nicotinic receptor ligand binding domain. J Neurobiol 53, 431-446.

Sine, S.M., Engel, A.G., 2006. Recent advances in Cys-loop receptor structure and function. Nature 440, 448-455.

Stell, B.M., Brickley, S.G., Tang, C.Y., Farrant, M., Mody, I., 2003. Neuroactive steroids reduce neuronal excitability by selectively enhancing tonic inhibition mediated by δ subunit-containing $GABA_A$ receptors. Proc Natl Acad Sci U S A 100, 14439-14444.

Stroud, R.M., McCarthy, M.P., Shuster, M., 1990. Nicotinic acetylcholine receptor superfamily of ligand-gated ion channels. Biochemistry 29, 11009-11023.

Sur, C., Farrar, S.J., Kerby, J., Whiting, P.J., Atack, J.R., McKernan, R.M., 1999. Preferential coassembly of α4 and δ subunits of the γ-aminobutyric acid A receptor in rat thalamus. Mol Pharmacol 56, 110-115.

Thompson, S.A., Whiting, P.J., Wafford, K.A., 1996. Barbiturate interactions at the human $GABA_A$ receptor: dependence on receptor subunit combination. Br J Pharmacol 117, 521-527.

Tia, S., Wang, J.F., Kotchabhakdi, N., Vicini, S., 1996. Developmental changes of inhibitory synaptic currents in cerebellar granule neurons: role of $GABA_A$ receptor α 6 subunit. J Neurosci 16, 3630-3640.

Tobin, J.M., Lewis, N.D., 1960. New psychotherapeutic agent, chlordiazepoxide. Use in treatment of anxiety states and related symptoms. JAMA 174, 1242-1249.

Tunnicliff, G., 1998. Pharmacology and function of imidazole 4-acetic acid in brain. Gen Pharmacol 31, 503-509.

Twyman, R.E., Rogers, C.J., Macdonald, R.L., 1989. Differential regulation of γ-aminobutyric acid receptor channels by diazepam and phenobarbital. Ann Neurol 25, 213-220.

Ulens, C., Hogg, R.C., Celie, P.H., Bertrand, D., Tsetlin, V., Smit, A.B., Sixma, T.K., 2006. Structural determinants of selective α-conotoxin binding to a nicotinic acetylcholine receptor homolog AChBP. Proc Natl Acad Sci U S A 103, 3615-3620.

Unwin, N., 1993. Nicotinic acetylcholine receptor at 9 Å resolution. J Mol Biol 229, 1101-1124.

Unwin, N., 1995. Acetylcholine receptor channel imaged in the open state. Nature 373, 37-43.

Unwin, N., 2005. Refined structure of the nicotinic acetylcholine receptor at 4Å resolution. J Mol Biol 346, 967-989.

Unwin, N., Miyazawa, A., Li, J., Fujiyoshi, Y., 2002. Activation of the nicotinic acetylcholine receptor involves a switch in conformation of the α subunits. J Mol Biol 319, 1165-1176.

Valjent, E., Pages, C., Herve, D., Girault, J.A., Caboche, J., 2004. Addictive and non-addictive drugs induce distinct and specific patterns of ERK activation in mouse brain. Eur J Neurosci 19, 1826-1836.

Vernino, S., Amador, M., Luetje, C.W., Patrick, J., Dani, J.A., 1992. Calcium modulation and high calcium permeability of neuronal nicotinic acetylcholine receptors. Neuron 8, 127-134.

Vestergaard, H.T., Cannillo, C., Frolund, B., Kristiansen, U., 2007. Differences in kinetics of structurally related competitive $GABA_A$ receptor antagonists. Neuropharmacology 52, 873-882.

Wall, M.J., Usowicz, M.M., 1997. Development of action potential-dependent and independent spontaneous $GABA_A$ receptor-mediated currents in granule cells of postnatal rat cerebellum. Eur J Neurosci 9, 533-548.

Wieland, H.A., Luddens, H., Seeburg, P.H., 1992. A single histidine in $GABA_A$ receptors is essential for benzodiazepine agonist binding. J Biol Chem 267, 1426-1429.

Williams, C.A., Bell, S.V., Jenkins, A., 2009. A residue in loop 9 of the β2 subunit stabilizes the closed state of the $GABA_A$ receptor. J Biol Chem.

Wisden, W., Laurie, D.J., Monyer, H., Seeburg, P.H., 1992. The distribution of 13 $GABA_A$ receptor subunit mRNAs in the rat brain. I. Telencephalon, diencephalon, mesencephalon. J Neurosci 12, 1040-1062.

Wohlfarth, K.M., Bianchi, M.T., Macdonald, R.L., 2002. Enhanced neurosteroid potentiation of ternary $GABA_A$ receptors containing the δ subunit. J Neurosci 22, 1541-1549.

Wonnacott, S., 1997. Presynaptic nicotinic ACh receptors. Trends Neurosci 20, 92-98.

Wonnacott, S., Sidhpura, N., Balfour, D.J., 2005. Nicotine: from molecular mechanisms to behaviour. Curr Opin Pharmacol 5, 53-59.

Yang, J.S., Olsen, R.W., 1987. γ-Aminobutyric acid receptor-regulated 36Cl-flux in mouse cortical slices. J Pharmacol Exp Ther 241, 677-685.

You, H., Dunn, S.M., 2007. Identification of a domain in the δ subunit (S238-V264) of the α4β3δ $GABA_A$ receptor that confers high agonist sensitivity. J Neurochem 103, 1092-1101.

Yu, W., Jiang, M., Miralles, C.P., Li, R.W., Chen, G., de Blas, A.L., 2007. Gephyrin clustering is required for the stability of GABAergic synapses. Mol Cell Neurosci 36, 484-500.

CHAPTER 2[1]

Chain Length Dependence of Interactions of Bisquaternary Ligands with the *Torpedo* nAChR

---

[1] A version of this chapter has been published: Carter, CR, Cao, L, Kawai, H, Smith, PA, Dryden, WF, Raftery, MA and Dunn, SM. (2007). *Biochem. Pharmacol.* **73**, 417-426.

Radioligand binding experiments done by L Cao and thallium flux assays performed by H Kawai

INTRODUCTION

The peripheral (muscle-type) nicotinic acetylcholine receptor (nAChR) is the prototype of the "Cys-loop" family of ligand-gated ion channels (LGICs). This family includes the neuronal nAChRs, 5-hydroxytryptamine type 3 ($5\text{-}HT_3$), γ-aminobutyric acid type A ($GABA_A$) and glycine receptors. The best characterized member of the family is the nAChR from *Torpedo* electric organ. This large complex transmembrane protein is a pentamer of homologous subunits $(\alpha 1)_2\beta\gamma\delta$ that assemble pseudosymmetrically to form a central cation-selective ion channel (Raftery et al., 1980; Noda et al., 1983; Unwin, 2005). There is considerable biochemical and mutational evidence to demonstrate that a high affinity binding site for agonists and competitive antagonists lies at each of the α-γ and α-δ subunit interfaces where they are formed by at least six (A-F) non-contiguous "loops" of amino acids (Arias, 2000; Corringer et al., 2000; Karlin, 2002). The α subunit is suggested to contribute loops A-C while the neighboring subunits contribute loops D-F. The non-equivalence of the interfaces confers distinct recognition properties for some agonists and competitive antagonists (Blount and Merlie, 1989; Pedersen and Cohen, 1990; Hann et al., 1994; Sine et al., 1995; Prince and Sine, 1998).

The requirements for neurotransmitter activation of members of this LGIC family appear to be less rigorous than those of enzyme-substrate interactions that have precise stereochemical requirements for catalysis. Although the neurotransmitter binding sites within the nAChR display selectivity, they are also sufficiently spacious and flexible to accommodate ligands with a diverse range of chemical structures. Ligands that interact with these sites show a spectrum of activities ranging from antagonists to full agonists. Well characterized ligands include the large antagonist α-neurotoxins, complex alkaloids such as d-tubocurarine and small monoquaternary agonists such as acetylcholine (ACh) and phenyltrimethylammonium. While a great deal of evidence on the location of these sites has accumulated over the last several decades, direct evidence remains lacking since the nAChR (like the other members of this LGIC family) has thus far proved intransigent to crystallization. However, the reported crystal structure of a snail acetylcholine binding protein (AChBP) that is homologous to the extracellular domains of the LGIC family has proved to be a useful template on which to model binding domains (Brejc et al., 2001). Since the structure of the AChBP strongly supports earlier notions of binding site architecture and the location of binding "loops" at the subunit-subunit interfaces, this has rejuvenated interest in structure-function relationships of the LGICs.

In this study, I focus on the binding and functional properties of the bischoline ester series exemplified by suberyldicholine (SbCh; figure 2-1). The unusual effects of bisquaternary cholinergic antagonists acting at the neuromuscular junction and the strong correlation between the interonium distance of the compound and its ability to block neuromuscular transmission has long been recognized (Paton and Zaimis, 1952). As discussed in an early treatise by Michaelson and Zeimal (1973), results obtained with bisquaternary ligands have given considerable insights into the nature of cholinergic binding sites and provided early evidence to suggest that multiple subsites may exist within each neurotransmitter binding domain(s). Differences in the binding of SbCh and ACh to the *Torpedo* nAChR have been reported previously (Dunn and Raftery, 1997a, b). Based on studies of the kinetics of dissociation and association of these ligands, a model was proposed in which each of the two high affinity sites on the nAChR is composed of two subsites (sites A and B; see figure 2-2) that are allosterically coupled. It was suggested that, although the two subsites are mutually exclusive for ACh under equilibrium conditions, the large bisquaternary SbCh may be able to physically bridge these subsites. A preliminary study of the kinetics of association of this series of bischoline esters placed physical constraints on the potential distance between these sites (Dunn and Raftery, 1997b). Ligands of the size of pimelyldicholine (one methylene group shorter than SbCh) and longer displayed SbCh-like kinetics whereas shorter bisquaternary ligands displayed ACh-like characteristics.

The interonium distance of the extended conformation of pimelyldicholine is approximately 17.3Å (figure 2-1) suggesting that, under the conditions of these experiments, the putative subsites may be separated by approximately this distance (see also figure 2-2).

In the present report, the interactions of bischoline esters with the *Torpedo* nAChR have been examined using both native membrane-bound receptors and *Torpedo* recombinant nAChRs expressed in *Xenopus* oocytes. It is shown that the apparent affinities of these ligands, measured in both binding and functional studies, are correlated with their interonium distance. However, the maximum responses induced by the bischoline esters are significantly less than the maximum response elicited by ACh i.e., all bisquaternary ligands examined are partial agonists. The results shed further light on multiple binding domains within the nAChR structure and how their occupancy may be related to receptor function.

MATERIALS AND METHODS

Materials

ACh, SbCh and succinyldicholine were from Sigma Chemical Company. The other bischoline esters were synthesized from their corresponding acid chlorides (obtained from Aldrich Chemical Company) by Matt Kula in the

laboratory of Dr. W. Dryden using established procedures (Dunn and Raftery, 1997a). [^{3}H]ACh and [^{125}I]α-bungarotoxin (α-BTx) were from DuPont Canada (Mississauga, ON). [^{3}H]SbCh was synthesized as previously described (Dunn and Raftery, 1997b). 8-Amino-1,3,6-naphthalene trisulfonic acid (ANTS) was from either Chem Service Inc. (West Chester, PA), or Molecular Probes Inc. (Eugene, OR) and 1,3,6,8-pyrenetetrasulfonic acid (PTSA) was from Molecular Probes. Restriction enzymes and cRNA transcript preparation materials were from Invitrogen (Burlington, ON), New England Biolabs (Pickering, ON), or Promega (Madison, WI). The γ subunit cDNA clone (in the SP64-based plasmid, pMXT) of the *Torpedo* nAChR was kindly provided by Dr. J.B. Cohen (Harvard Medical School, Boston, MA), while the δ subunit (in the SP65 plasmid) and the α and β subunits (in the SP64 plasmid) cDNA clones were generous gifts from Dr. H.A. Lester (California Institute of Technology, Pasadena, CA).

Preparation of nAChR-Enriched Membrane Fragments

Membrane fragments enriched in nAChR were prepared from frozen *Torpedo californica* electric organ (Pacific Biomarine, Venice, CA, or Aquatic Research Consultants, San Pedro, CA) as described previously (Elliott et al., 1980). Membrane preparations were stored at -85°C before use. Protein concentrations were determined using the BioRad (Mississauga, ON) assay

and the concentration of receptor sites for [^{125}I]-α-BgTx was measured by the DEAE-disc assay (Schmidt and Raftery, 1973). As indicated in the text, for some experiments, nAChR-enriched membranes were first alkali-extracted at pH 11 to remove peripheral membrane proteins (Elliott et al., 1979; Neubig et al., 1979).

Equilibrium Binding of [^{3}H]ACh and [^{3}H]SbCh to Membrane-Bound nAChR

Measurements of [^{3}H]ACh and [^{3}H]SbCh binding were carried out using centrifugation assays (Dunn and Raftery, 1997a). Prior to binding assays, acetylcholinesterase activity in concentrated non-alkali extracted membrane fragments (approximately 5 mg protein/ml) was inhibited by the addition of a 1/200 volume of a 0.3 M stock solution of diethyl-p-nitrophenyl phosphate (DNPP, Sigma) prepared in isopropanol. After 3 minutes at room temperature, the membranes were diluted by about 10-fold in *Torpedo* Ringer's solution (20 mM Hepes-Na^+, 250 mM NaCl, 5 mM KCl, 4 mM $CaCl_2$, 2 mM $MgCl_2$, 0.02% NaN_3, pH7.4) and stored on ice until use. Aliquots of DNPP-treated membranes were added to various concentrations of [^{3}H]ACh or [^{3}H]SbCh in *Torpedo* Ringer's solution to give a final protein concentration of 0.1 mg/ml in a final volume of 0.5 ml. After incubation for 45 min at room temperature, duplicate 50 μl aliquots were removed for estimation of the

total added radioligand concentration. The remaining samples were centrifuged at 12,000 g for 15 min at 4°C, after which duplicate 50 µl aliquots of the supernatant were removed for determination of the free radioligand concentration. The amount of bound radioligand was calculated by subtracting free from total ligand concentration. Non-specific binding was determined from parallel measurements of binding in the presence of excess unlabeled ligand (1 mM Ach or 1 mM SbCh). Equilibrium binding experiments were performed in replicates of three or greater.

Competition Assays

Displacement experiments were carried out using a centrifugation procedure similar to that described above. Aliquots of DNPP-treated *Torpedo* membranes (final concentration of 0.1 mg/ml) were incubated with either 0.2 µM [^{3}H]ACh, or [^{3}H]SbCh, and increasing concentrations of unlabelled ligand (0 - 1 mM) for 30 min at room temperature before quantification of the concentrations of bound and free radioligand as above.

Thallium (1) Flux Assays

Stopped-flow measurements of agonist-induced Tl^+ flux using alkali-extracted *Torpedo* membrane preparations were carried out using a

fluorescence assay modified from that of Moore and Raftery (Moore and Raftery, 1980) after loading of the membrane vesicles with either of the membrane-inpermeant fluorescent probes, ANTS or PTSA (Kawai et al., 1999). The kinetics of Tl^+ influx were measured using an Applied Photophysics (Leatherhead, UK) SF.17MV Microvolume instrument and appropriate wavelengths for each dye. Briefly, a suspension of fluorophore-loaded vesicles (in 10 mM nitrilotriethanol, 35 mM $NaNO_3$, pH 7.4) was mixed rapidly with an equal volume of a solution of agonist (in 10 mM nitrilotriethanol, 35 mM $TlNO_3$, pH 7.4) at 25 °C and the kinetics of the fluorescence quench resulting from Tl^+ influx were monitored using an Archimedes computer and Applied Photophysics software.

In Vitro Transcription

Plasmid cDNAs encoding the *Torpedo* nAChR subunits were linearized by digestion with *Xba*I (γ and δ subunits), *Eco*RI (α subunit) or *Fsp*I (β subunit). *In vitro* transcription of cRNA was performed using methods previously described (Goldin and Sumikawa, 1992). Briefly, the linearized cDNA templates (5μg) were transcribed *in vitro* by SP6 RNA polymerase (Promega) in the presence of RNA capping analogue (New England Biolabs) and ribonucleotide triphosphates (NTP mix, Invitrogen). RNA transcripts were then extracted using a 25:24:1 (v/v) phenol:chloroform:isoamyl alcohol

mixture. Final cRNA pellets were resuspended in diethylpyrocarbonate-treated water to a final concentration of 1 μg/μl and aliquots were stored at −80°C until use.

Expression in *Xenopus* Oocytes and Electrophysiology

Isolated, follicle-free oocytes from *Xenopus laevis* were microinjected with a total of 50 ng of subunit cRNAs in the ratio of 2α:1β:1γ:1δ (ratio by weight). Oocytes were incubated in ND96 buffer (5 mM HEPES, 96 mM NaCl, 1.8 mM $CaCl_2$, 2 mM KCl, 1 mM $MgCl_2$, pH 7.6) supplemented with 50 μg/ml gentamicin at 14°C for at least 48 hours prior to recording. Currents elicited by bath application of agonist were measured using standard two-electrode voltage clamp techniques and a GeneClamp500 amplifier (Axon Instruments, Foster City, CA) at a holding potential of -60 mV. Electrodes were filled with 3 M KCl and only electrodes with resistances of 0.5-1.5 MΩ were used. The recording chamber was continuously perfused (at a rate of ~5 ml/min) with low calcium ND96 buffer (as above but with the $CaCl_2$ concentration reduced to 0.1 mM) supplemented with 1 μM atropine. Atropine was included in the perfusion buffer to block the activation of endogenous muscarinic receptors present on the surface of the oocytes (Barnard et al., 1982) and the Ca^{2+} concentration was reduced to decrease the rate of receptor desensitization (Miledi, 1980). Agonist-evoked responses were measured by applying drug

(via the perfusion system) for 10-20 seconds unless otherwise indicated. Drugs were washed out for 12-min between applications to ensure complete recovery from desensitization.

Data Analysis

Binding data were analyzed using GraphPad Prism (San Diego, CA) software. Saturation binding data (after correction for non-specific binding) were fit by a simple binding isotherm:

$$[RL] = \frac{[R_0][L]}{K_D + [L]}$$

where [RL], [R_0] and [L] are the concentrations of occupied receptor, available receptor sites and free radioligand concentration, respectively.

Displacement of radiolabelled ligand by unlabelled ligands was fitted by a simple competition curve:

$$[RL] = [RL]_{min} + \frac{[RL]_{max} - [RL]_{min}}{1 + 10^{(\log[X] - \log IC_{50})}}$$

where [RL] is bound radioligand, $[RL]_{min}$ and $[RL]_{max}$ are the minimum and maximum amount of bound radioligand measured, [X] is the total concentration of competing ligand and IC_{50} is the concentration of the unlabelled ligand that causes 50% displacement.

Apparent K_I values were calculated using the Cheng-Prusoff equation (Cheng and Prusoff, 1973):

$$K_I = \frac{IC_{50}}{1+[L]/K_D}$$

where K_D is the equilibrium dissociation constant for the radioligand used in the assay and other parameters are as defined above.

The kinetic traces for thallium (1) flux were fitted using Applied Photophysics software and a modified Stern-Volmer equation (Moore and Raftery, 1980):

$$F(t) = \frac{A_1}{1+KT_\infty(1-e^{-k_{app}t})} + k_0 t + A_0$$

where F(t) is the fluorescence intensity at time t, A_1 is the amplitude of the specific agonist-induced fluorescence quench, K is the Stern-Volmer constant for quenching of the fluorophore by Tl^+ (96 M^{-1} for ANTS or 201 M^{-1} for PTSA), T_∞ is the final concentration of Tl^+, k_{app} is the apparent rate constant of Tl^+ flux, k_0 is the rate of Tl^+ leak through the membrane and A_0 is the baseline fluorescence intensity.

The concentration dependence of the rate of agonist-induced Tl^+ flux was fit using GraphPad software and the sigmoidal equation:

$$k_{app} = k_{min} + \frac{[k_{max} - k_{min}]}{1+10^{(\log[X]-\log EC_{50})^{nH}}}$$

where k_{app} is the apparent rate constant at each concentration of ligand, [X], k_{min} and k_{max} are the minimum and maximum rates respectively and n_H is the apparent Hill coefficient.

The peak amplitudes of agonist-induced current responses of recombinant receptors expressed in *Xenopus* oocytes were analyzed using Axoscope 8 software. Concentration-effect curves were analyzed using GraphPad Prism software and the following equation:

$$I = \frac{I_{max}[L]^{n_H}}{EC_{50} + [L]^{n_H}}$$

where I is the measured agonist-evoked current, [L] is the agonist concentration, EC_{50} is the agonist concentration that evokes half the maximal current (I_{max}) and n_H is the apparent Hill coefficient. All values are reported as the mean ± SEM.

RESULTS

Binding of [^{3}H]ACh and [^{3}H]SbCh to *Torpedo* Membrane Preparations

In agreement with previous results in which alkali-extracted *Torpedo* membranes were used (Dunn and Raftery, 1997a), the binding of both radioligands was to an apparently homogeneous population of high affinity sites (figure 2-3A). In replicate experiments (n = 5 to 8), the estimated

dissociation constant (K_D) for [^{3}H]SbCh and [^{3}H]ACh binding were 14.9 ± 2.5 nM and 11.4 ± 1.9 nM respectively and binding was to an equivalent number of sites (approximately 0.4 nmol/mg protein). Thus these ligands display very similar binding characteristics under equilibrium conditions.

Apparent Affinities of the Bischoline Esters Measured in Competition Assays

In competition studies, ACh and SbCh appear to interact with the membrane-bound *Torpedo* receptor in a simple competitive manner. Unlabelled SbCh competed for all bound [^{3}H]ACh with an estimated K_I of 3.9 ± 1.4 nM (n = 3) and unlabelled ACh caused complete inhibition of [^{3}H]SbCh binding with a K_I of 17.1 ± 1.0 nM (n = 3). These results are in reasonable agreement with the direct binding assays shown in figure 2-3A. Similar competition assays have been carried out to study the inhibition of either [^{3}H]ACh or [^{3}H]SbCh binding by the bischoline esters shown in figure 2-1. Representative inhibition curves are shown in figure 2-3B. In no case was there any evidence for binding site heterogeneity and a simple competitive equation adequately described all of the data. Figure 2-4 illustrates the estimated K_I values for all of the ligands as a function of their chain length i.e., number of methylene groups (n). Parameters obtained from data fitting are summarized in Table 2-1. These data show a clear chain length dependence

on equilibrium binding apparent affinity. The short chain derivatives (oxalyl, malonyl and succinyl; where n = 0 - 2 respectively; see figure 2-1) display relatively low apparent affinity (with K_Is about 10-fold higher than the K_D for ACh binding) but larger ligands ($n \geq 6$) i.e. suberyldicholine and longer, were of higher apparent affinity comparable to that of ACh. The intermediate length members of the series displayed intermediate apparent affinity.

The Effects of ACh and SbCh on Activation of *Torpedo* nAChR Expressed in *Xenopus* Oocytes

Figure 2-5A shows representative concentration-effect curves for agonist-mediated flux responses of the native membrane-bound *Torpedo* receptor measured using stopped-flow fluorescence techniques. Replicate experiments ($n > 6$) gave EC_{50} values of 3.4 ± 1.0 μM and 83 ± 16 μM for SbCh and ACh, respectively, showing that SbCh is approximately 24-fold more potent than ACh. However, SbCh is only a partial agonist of the *Torpedo* nAChR. In Tl^+ flux assays, SbCh consistently elicited only about 30% of the maximum rate of the response induced by ACh. Due to inherent difficulties in accurately determining the maximum flux rates using this approach, this provides only an approximation of the relative efficacies of these agonists (see below). For the recombinant receptor expressed in *Xenopus* oocytes (figure 2-5B), the potencies of SbCh and ACh were within a factor of two of

the native receptor with measured EC_{50} values of 3.4 ± 0.4 μM and 46 ± 9 μM, respectively. SbCh is also a partial agonist in this system and, as shown in the inset in Fig. 2-5B, the maximum current that this ligand elicits is only about 46% of the maximum ACh response.

Potency of Bischoline Esters

The functional responses of this series of bischoline compounds were measured using both receptor-enriched membranes from *Torpedo* electric organ (using the Tl^+ flux method) and the recombinant receptor expressed in *Xenopus* oocytes (using two-electrode voltage clamp techniques). The measured EC_{50} values for the functional responses are shown as a function of chain length in figure 2-6A (see also Table 2-1). As was seen in the binding assays (figure 2-4) there is a clear chain length dependence with the potency of the ligand increasing with the number of methylene groups present. In these experiments, it should be noted that accurate analyses of the activation of the *Torpedo* receptor by the shortest and longest members of this series is complicated by the low amplitude of responses induced by these ligands (see below).

In general, the results obtained using the two systems (*Torpedo* membranes versus recombinant receptors) were in good agreement suggesting that the oocyte expression system faithfully reproduces the

properties of the native nAChR. There were, however, some unexpected results. Using *Torpedo* membranes, the binding of the shortest bischoline ester, oxalyldicholine (n = 0) was robust, as revealed by its ability to compete for all [^{3}H]ACh and [^{3}H]SbCh binding sites. In Tl^+ flux assays, it elicited a response that was close to that of carbamylcholine (data not shown) allowing estimates of its EC_{50} for channel activation (see Table 2-1). In contrast, oxalyldicholine elicited barely detectable currents in the recombinant receptor. Succinylcholine (n = 2) had very low efficacy in both systems. In the recombinant receptor, the induced currents were too small to be analyzed accurately but a small Tl^+ flux response (less than 5% of that induced by carbamylcholine) has allowed approximation of the activation parameters for this ligand (Table 2-1).

Efficacies of the Bischoline Ligands

Determination of efficacy i.e., the magnitude of the response that can be elicited by a particular ligand, requires that the maximum response to a full agonist can be measured reliably. In this respect, the Tl^+ flux assay suffers from the disadvantage that the maximum rates of flux must be measured. Although ACh is likely to be a full agonist of the *Torpedo* nAChR, the rate of its maximum Tl^+ flux response may exceed the resolution of stopped-flow instruments (see Moore and Raftery, 1980; also figure 2-5A) and depends

also on both membrane vesicle integrity and the number of receptors per vesicle. I have, therefore, used the oocyte expression system to provide more reliable estimates of the efficacies of different members of the bischoline series. The advantage of this system is that the maximum responses to multiple ligands can be measured in the same oocyte, thus obviating problems arising from variations in levels of receptor expression. The results in figure 2-6 demonstrate that none of the bischoline esters had an efficacy equal to that of ACh. Furthermore, there is clear trend in the chain-length dependency of the response, i.e., bischoline derivates in which $n \leq 3$ are poor partial agonists as are those in which $n > 7$. Qualitatively similar results (except in the case of oxalyldicholine as noted above) have been observed in Tl^+ flux assays and the poor efficacies of the longer chain length derivatives have precluded accurate estimates of their activation parameters.

DISCUSSION

There is a wealth of experimental data to suggest that, under equilibrium conditions, the *Torpedo* nAChR carries two high affinity sites for agonists/competitive antagonists and that these sites lie at the interfaces between the α-γ and α-δ subunits (Arias, 2000; Corringer et al., 2000; Karlin, 2002). However, an inevitable complication in studying structure-function relationships of the nAChR is that the receptor, like most of the ligands with

which it interacts, is inherently flexible. Since both the protein and ligand can adapt to changes in its environment, the receptor-agonist complex can adopt multiple conformations, some of which may exist only transiently, in the pathways leading to receptor activation and/or desensitization.

In early whole animal experiments of the neuromuscular blocking activities of a series of polymethylenebis(trimethylammonium) compounds, two maxima were observed for compounds having a bisonium bridge of 10, or 16-18, methylene groups, whereas in the corresponding bis(triethylammonium) series, only the second maximum was observed, see (Paton and Zaimis, 1952; Michaelson and Zeimal, 1973). Direct studies of the interaction of a series of 1,n-bis(3-aminopyridinio)-alkane fluorescent derivatives with the *Torpedo* nAChR later revealed that compounds with 12-16 methylene groups were of significantly higher affinity than their shorter, or longer, analogues (Bode et al., 1979). In their extended conformations, the latter compounds have estimated interonium distances of 16.8 – 21.4Å , approximating the size of pimelyl- (n=5) to sebacyldicholine (n = 8) used in the present study (Figure 2-1). This clear chain length dependence suggests that separate binding domains contribute to the recognition of the two quaternary groups of these ligands.

Other studies using photoisomerizable bisquaternary ligands (Wassermann and Erlanger, 1981) have provided insights as to the involvement of these putative subsites in receptor activation. In the *Electrophorus* nAChR, cis-3,3'-bis[α-(trimethylammonium)methyl] azobenzene dibromide (Bis-Q) is an antagonist, whereas the trans-isomer is a potent agonist (Nerbonne et al., 1983; Delcour and Hess, 1986). These isomers cannot occupy the same physical space within the receptor binding site(s). Using an alkylating monoquaternary analogue (*trans*-3-(α-bromomethyl)-3'-[α-(trimethylammonium)methyl]azobenzene), which was likely to have been tethered to residues C192/193 of the α subunit (Lester et al., 1980), it was shown that receptor activation occurred only when the ligand was photolyzed to its trans-conformation. In the trans-isomer, the quaternary ammonium group lies approximately 14Å away from the tethering site, suggesting that a site involved in activation lies approximately this distance from Cys192/193. Unlike the eel receptor, in the *Torpedo* nAChR, both Bis-Q isomers act as antagonists (Nerbonne et al., 1983; also unpublished results) suggesting that there are species differences in the distance between the putative subsites.

The present study has investigated the interaction of bischoline esters with the *Torpedo* nAChR under two sets of conditions i.e., rapid ion conductance responses measured soon after exposure of the resting

(activatable) receptor to ligand, and radiolabelled binding studies carried out under equilibrium conditions. The equilibrium binding of [^{3}H]ACh and [^{3}H]SbCh to the membrane-bound *Torpedo* nAChR suggests that each ligand binds to an apparently homogeneous population of sites with similarly high apparent affinity. Inhibition of the binding of these radioligands by all of the bischoline ester compounds examined was consistent with a simple competitive model. Thus, such equilibrium binding studies did not reveal the complexity of receptor-ligand interactions that was observed previously in kinetic studies (Dunn and Raftery, 1997b, a). After saturation of all of the high affinity sites on the *Torpedo* receptor with radiolabelled ACh or SbCh, it wass shown that the rate of dissociation of [^{3}H]ACh (but not that of [^{3}H]SbCh) was significantly accelerated upon dilution into buffer containing micromolar concentrations of unlabelled cholinergic ligands. Detailed examination of this phenomenon led to the suggestion that each of the high affinity sites (designated as site A) is associated with a secondary subsite (site B) to which it is allosterically coupled. It suggested that these two subsites may be "crosslinked" by the large bisquaternary ligand, SbCh. In fluorescence studies of agonist association, evidence for transient occupancy of two subsites for ACh, but not for SbCh was obtained (Dunn and Raftery, 1997b). As noted in the Introduction, the shortest ligand to display SbCh-like association kinetics was pimelyldicholine (n=5). In the present study, adipyldicholine (n = 4) displayed similar equilibrium binding properties to pimelyldicholine (Table 2-1). These results can be rationalized by considering the differences in the

timescales of the two sets of experiments. The fluorescence studies monitor initial binding events whereas radioligand binding studies reflect the equilibrium state. As noted above, the receptor and/or ligand may adopt different conformations during the approach to equilibrium. Thus the distance between the putative subsites is unlikely to be identical in each conformation of the complex.

Here, I have extended studies of the bischoline series to include detailed characterization of functional responses. Overall, the potencies of these ligands follows a similar trend to their equilibrium apparent binding affinities. Although the shorter bischolines (n = 0 to 2) bound with approximately 10-fold lower affinity, their EC_{50} values were similar to those of ACh measured in both Tl^+ flux studies ($EC_{50} \sim 80$ μM) and in *Xenopus* oocytes ($EC_{50} \sim 46$ μM). In contrast, although the longer chain bischoline derivatives ($n \geq 6$) bind to the *Torpedo* nAChR with similar equilibrium apparent affinity to ACh, they have 10-50-fold higher potency in functional studies. A simple explanation for the higher potency of these longer bisquaternary ligands is that additional binding energy can be obtained from their ability to occupy pairs of binding sites simultaneously. Quantitative analysis of such a model is complicated by the changing conformational/affinity states of the receptor upon agonist exposure. While it is tempting to implicate the well characterized sites (sites A) for ACh in

both the "crosslinking" event and its functional consequences, there are a number of confounding issues. Numerous studies have shown that these sites do not have intrinsically high affinity in the resting state of the receptor, rather they reach their high affinity state only seconds to minutes after formation of the initial complex [reviewed in McLane et al., 1996]. Thus, the measured apparent affinity of the equilibrium complex cannot readily be equated with the concentration-dependencies of responses that occur under pre-equilibrium conditions. A more fundamental problem in relating occupancy of sites A with receptor activation is that it has been shown that their prior saturation with agonist does not inhibit channel activation upon subsequent exposure to higher agonist concentrations (Dunn and Raftery, 2000). Thus these sites A cannot be directly involved in either channel activation, or receptor desensitization. Based on circumstantial evidence i.e, an approximate correspondence between the estimated affinities of sites B and the measured concentration dependences of both activation and desensitization, it was tentatively suggested that occupancy of site B may play a role in the desensitization processes (Dunn and Raftery, 2000), although there was no clear evidence for direct involvement in channel activation.

In a recent study, a residue in the *Torpedo* receptor that may be involved in formation of the secondary subsite for SbCh and possibly other

bisquaternary ligands was identified (Kapur et al., 2006). Mutation of tryptophan-86 of the α-subunit to a phenylalanine had a large deleterious effect on the EC_{50} for activation by SbCh (approximately 200-fold) but only a minimal effect on the concentration-dependence of ACh activation. Photoaffinity labeling studies had previously implicated this residue as a site for recognition of cholinergic ligands (Galzi et al., 1990) but, based on the AChBP crystal structure (Brejc et al., 2001), it was later predicted to lie approximately 18Å from residues that are clustered to form the high affinity binding site (Karlin, 2002). These results are consistent with those of the present study that suggests the presence of binding domains that are separated by approximately this distance.

The above discussion has thus far considered only subsites A and B in receptor responses. However, evidence has previously been provided for the existence of distinct low affinity sites on the nAChR [see (Dunn and Raftery, 1993)]. These sites were revealed by monitoring of agonist-induced fluorescence changes of the probe, 4-[*N*-[(2-iodoacetoxy)ethyl]-*N*-methylamino]-7-nitrobenz-2-oxa-1,3-diazole (IANBD), that had been covalently incorporated into the receptor protein. An excellent correlation between the concentration dependence of low affinity binding revealed by this fluorophore and the concentrations of agonist-induced flux responses suggested that these sites are important for channel activation. Taken

together with the present data, we suggest that multiple agonist binding sites exist and that there is a dynamic interplay between binding to these sites and the observed responses. At the neuromuscular junction, the high concentrations of ACh that occur during evoked release suggest that all available binding sites will be rapidly occupied in the early stages of synaptic transmission.

In comparison to ACh, all of the bisonium compounds studied here were, at best, partial agonists of the *Torpedo* nAChR. In some cases, such as the effects of succinylcholine on the recombinant receptor, the responses were too small to be accurately quantified. It is becoming increasingly clear [see e.g. (Hansen et al., 2005)] that the receptor determinants for ligand recognition are likely to be diverse and that specific interactions of structurally disparate ligands with different subsets of amino acids may dictate agonist/antagonist activity. Subtle differences in receptor structure e.g. between the *Electrophorus* and *Torpedo* receptors (see above) may also play significant roles in dictating the functional consequences of ligand binding.

In conclusion, we have studied the binding of bisquaternary ligands with the native and recombinant *Torpedo* receptor. Longer chain agonists

such as suberyldicholine (n = 6) bind with high apparent affinity to this receptor and are also the most potent in functional studies. However, none of the bisonium compounds examined possessed efficacy equal to the natural ligand, ACh. We suggest that the ability of some bis-quaternary compounds to crosslink pairs of subsites within the nAChR is important for their binding and functional properties.

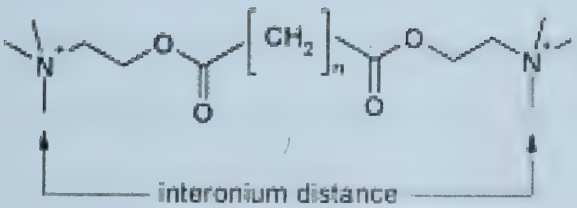

Bis-choline	n	distance (Å)
oxalyl	0	11.2
malonyl	1	12.2
succinyl	2	13.3
glutaryl	3	14.7
adipyl	4	16.0
pimelyl	5	17.3
suberyl	6	18.7
azelyl	7	20.0
sebacyl	8	21.3
dodecanyl	10	24.0

Figure 2-1: The structure of the bischoline analogues. The interonium distances of the extended ligand conformations were estimated using WebLab Viewer Lite (Accelrys, San Diego, CA).

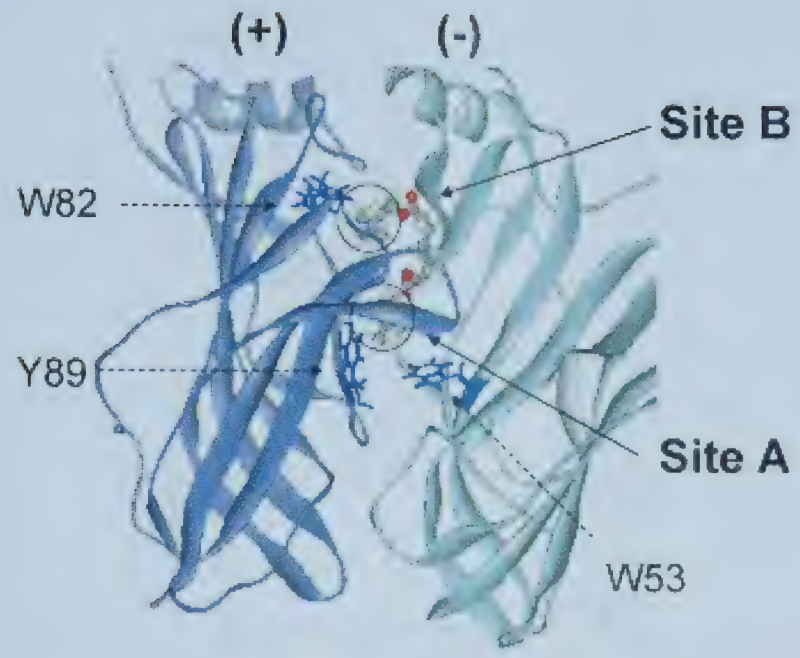

Figure 2-2: A model illustrating how SbCh may crosslink two subsites in the nAChR. The figure shows a side view of a subunit interface of the AChBP, a homologue of the extracellular domain of the LGIC family. SbCh is depicted as binding to the well characterized high affinity site (site A) which includes residues Y89, lying in loop A of the principal (+) subunit and W53 lying in loop D of the subordinate (−)-subunit. The conformation of SbCh shown is one of many that this large, flexible ligand can adopt. Although the location of site B remains speculative, here we depict this site as including W82 of the principal subunit. This residue lies in the homologous position to W86 in the *Torpedo* nAChR α subunit, a residue that has recently been shown to be important for activation of the *Torpedo* receptor by SbCh, but not by ACh (Kapur et al., 2006).

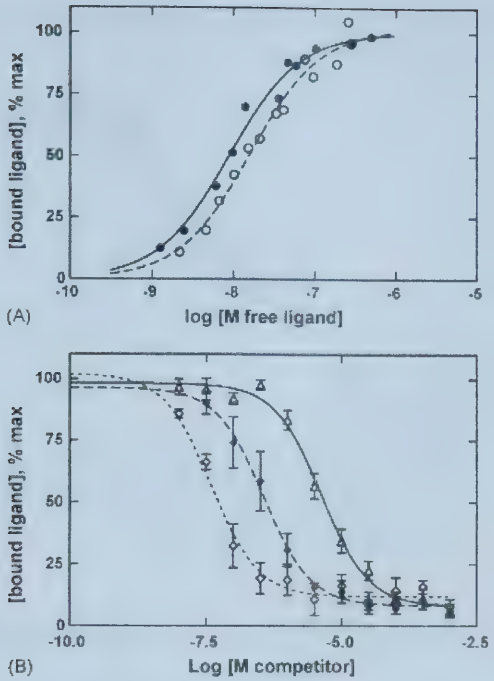

Figure 2-3: (A) Representative data for the equilibrium binding of [^{3}H]ACh (●) and [^{3}H]SbCh (○) to nAChR-enriched membrane fractions. The lines represent the best-fit curves to a simple non-cooperative binding model with estimated K_D values of 8.8 nM for ACh and 15.9 nM for SbCh. In replicate experiments, the binding of each ligand was to an approximately equal number of sites with similar affinities for the two agonists (see text for parameters). (B) Representative data for competition for [^{3}H]ACh by azelyl (◇), malonyl (△) and adipyldicholine (♦). All bischolines appear to inhibit the binding of the radioligand in a simple competitive manner and best-fit parameters for these and other bischolines in the series are shown in Table 2-1.

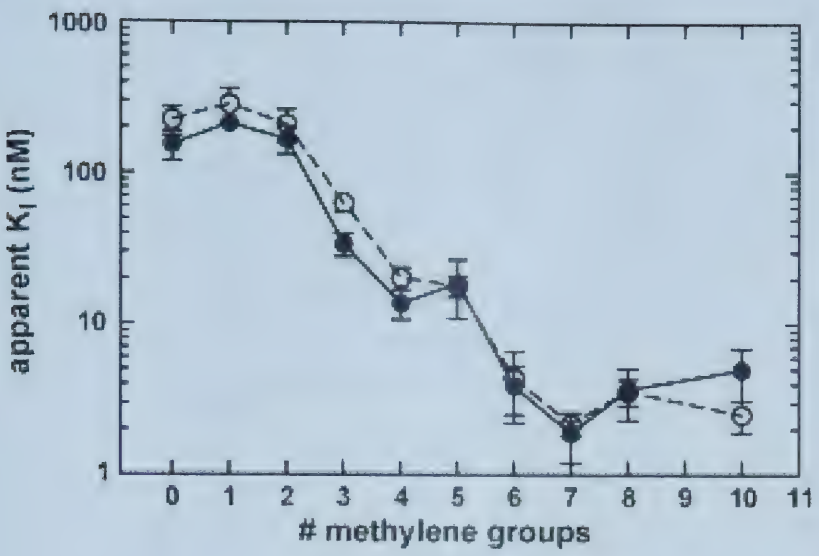

Figure 2-4: The relative apparent affinities of bischoline analogues for the membrane-bound *Torpedo* nAChR measured in competitive binding assays. The concentration dependencies of inhibition of [^{3}H]ACh (●), or [^{3}H]SbCh (○), binding by bischoline ligands were used to estimate K_I values. The data represent the mean ± S.E.M. of 3–8 independent experiments and the best fit parameters from curve fitting are summarized in Table 2-1.

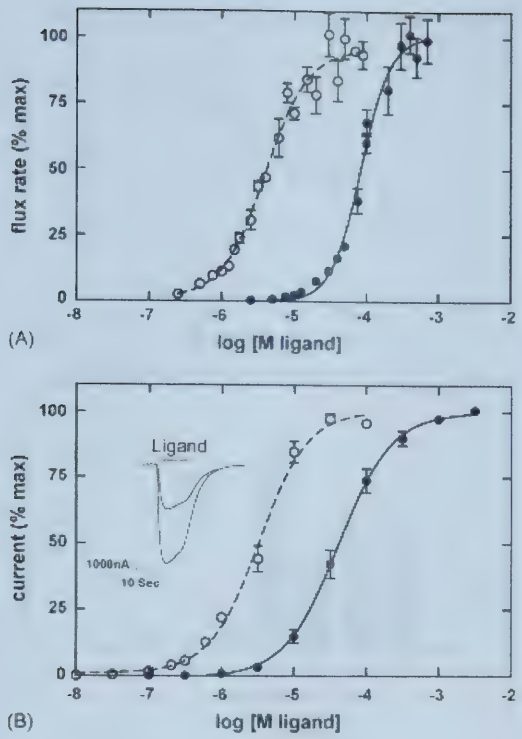

Figure 2-5: Functional responses mediated by ACh and SbCh. (A) Representative concentration-effect curves for activation of the native *Torpedo* nAChR by ACh (●) and SbCh (○) measured in Tl^+ flux assays. In each case, the measured rate was normalized to the maximum rate of flux evoked by the same ligand. Data fitting as described in the text gave an EC_{50} value of 3.9 μM and n_H of 1.8 for SbCh. Corresponding values for ACh were 84.8 μM and 2.1, respectively. In the case of ACh, the flux rates at high concentrations exceeded the time resolution of the stopped-flow technique and this required partial inactivation of the receptor by pre-treatment with 1–3 μM histrionicotoxin. Flux rates under these conditions were normalized using the factor by which histrionicotoxin slowed the flux rate at 30 μM ACh (see Moore and Raftery, 1980, for details) . (B) Concentration-effect curves for activation of the recombinant nAChR by ACh (●) and SbCh (○). The data shown are normalized to the measured I_{max} value for each agonist and represent the mean ± S.E.M. from at least three independent experiments. Curve fitting analysis as described in the text gave EC_{50} values of 3.4 ± 0.4 μM for SbCh and 46.5 ± 9.4 μM for Ach. The inset illustrates the partial agonist activity of SbCh in the recombinant receptor and show representative traces for activation by E_{max} concentrations of ACh (1 mM, lower trace) and SbCh (100 μM, upper trace). In three independent experiments, in which full concentration-effect curves were analyzed, the maximum current evoked by SbCh reached only 45.2% of that elicited by ACh (see also figure 2-6B).

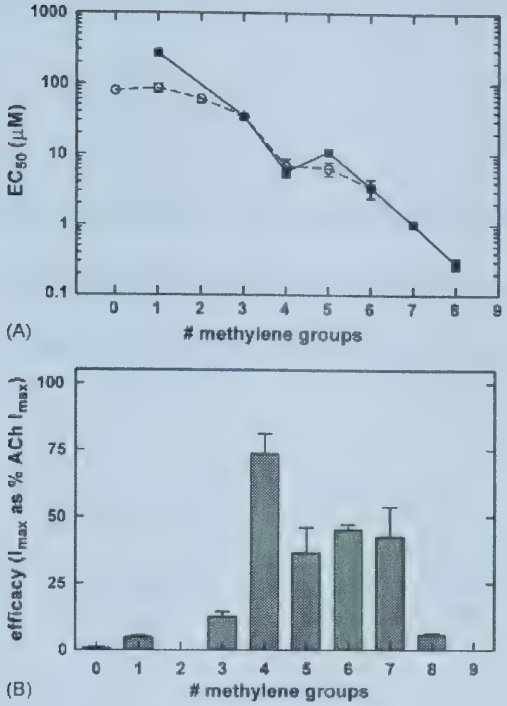

Figure 2-6: Potencies and efficacies of the bischoline analogues measured in functional studies. (A) EC_{50} values obtained from voltage-clamp analysis of recombinant receptors expressed in *Xenopus* oocytes (■) are in good agreement with estimates obtained from fluorescence assays of Tl^+ flux responses of native nAChRs in *Torpedo* membrane vesicles (○). (B) Relative efficacies of bischoline-induced current responses of *Torpedo* recombinant nAChRs. The data represent the mean ± S.E.M. of the maximum response for each ligand (obtained from full-concentration-effect curves) compared to the maximum response elicited by a saturating concentration of ACh.

Table 2-1: Summary of binding and functional data for the effects of bischoline esters using nAChR in native *Torpedo* membrane vesicles or *Torpedo* recombinant nAChRs expressed in Xenopus oocytes.

Bischoline ester (*n*)	*Torpedo* membranes			*Xenopus* oocytes		
	[^{3}H]ACh displacement, K_I (nM)	[^{3}H]SbCh displacement, K_I (nM)	Tl^+ flux, EC_{50} (μM)	Current, EC_{50} (μM)	n_H	Efficacy, I_{max}/I_{max}^{ACh} (%)
Oxalyl (0)	154 ± 34	225 ± 48	79.3 ± 9.9	>1000	–	0.8 ± 0.6
Malonyl (1)	213 ± 23	284 ± 78	85.9 ± 12.6	270 ± 25	2.28 ± 0.18	4.8 ± 0.5
Succinyl (2)	167 ± 35	209 ± 53	61.1 ± 8.4	–	–	–
Glutaryl (3)	33.7 ± 5.9	63.2 ± 8.2	34.2 ± 2.1	34.3 ± 0.3	1.36 ± 0.09	12.6 ± 1.9
Adipyl (4)	13.7 ± 1.4	20.2 ± 3.4	6.8 ± 1.7	5.7 ± 1.0	1.28 ± 0.13	73.6 ± 7.5
Pimelyl (5)	18.7 ± 7.8	17.9 ± 2.8	6.4 ± 1.4	10.8 ± 1.3	1.16 ± 0.07	36.6 ± 9.4
Suberyl (6)	3.9 ± 1.4	4.4 ± 2.2	3.4 ± 1.0	3.42 ± 0.35	1.47 ± 0.26	45.3 ± 1.9
Azelyl (7)	1.9 ± 0.7	2.2 ± 0.4	n.d.	1.03 ± 0.06	1.07 ± 0.08	42.6 ± 11.3
Sebacyl (8)	5.0 ± 1.9	3.6 ± 0.7	n.d.	0.28 ± 0.05	2.91 ± 0.27	5.4 ± 0.8

d.: not determined; –: parameters could not be obtained due to the low amplitude of the current.

REFERENCES

Arias, H.R., 2000. Localization of agonist and competitive antagonist binding sites on nicotinic acetylcholine receptors. Neurochem Int 36, 595-645.

Barnard, E.A., Miledi, R., Sumikawa, K., 1982. Translation of exogenous messenger RNA coding for nicotinic acetylcholine receptors produces functional receptors in Xenopus oocytes. Proc R Soc Lond B Biol Sci 215, 241-246.

Blount, P., Merlie, J.P., 1989. Molecular basis of the two nonequivalent ligand binding sites of the muscle nicotinic acetylcholine receptor. Neuron 3, 349-357.

Bode, J., Moody, T., Schimerlik, M., Raftery, M.A., 1979. Uses of fluorescent cholinergic ligands in *Torpedo californica* acetylcholine receptor. Biochemistry 18, 1855-1861.

Brejc, K., van Dijk, W.J., Klaassen, R.V., Schuurmans, M., van Der Oost, J., Smit, A.B., Sixma, T.K., 2001. Crystal structure of an ACh-binding protein reveals the ligand-binding domain of nicotinic receptors. Nature 411, 269-276.

Cheng, Y., Prusoff, W.H., 1973. Relationship between the inhibition constant (K_I) and the concentration of inhibitor which causes 50 % inhibition (IC_{50}) of an enzymatic reaction. Biochem Pharmacol 22, 3099-3108.

Corringer, P.J., Le Novere, N., Changeux, J.P., 2000. Nicotinic receptors at the amino acid level. Annu Rev Pharmacol Toxicol 40, 431-458.

Delcour, A.H., Hess, G.P., 1986. Chemical kinetic measurements of the effect of trans- and cis-3,3'-Bis[(trimethylammonio)methyl]azobenzene bromide on

acetylcholine receptor mediated ion translocation in *Electrophorus* electricus and Torpedo californica. Biochemistry 25, 1793-1798.

Dunn, S.M., Raftery, M.A., 1993. Cholinergic binding sites on the pentameric acetylcholine receptor of *Torpedo californica*. Biochemistry 32, 8608-8615.

Dunn, S.M., Raftery, M.A., 1997a. Agonist binding to the *Torpedo* acetylcholine receptor. 1. Complexities revealed by dissociation kinetics. Biochemistry 36, 3846-3853.

Dunn, S.M., Raftery, M.A., 1997b. Agonist binding to the *Torpedo* acetylcholine receptor. 2. Complexities revealed by association kinetics. Biochemistry 36, 3854-3863.

Dunn, S.M., Raftery, M.A., 2000. Roles of agonist-binding sites in nicotinic acetylcholine receptor function. Biochem Biophys Res Commun 279, 358-362.

Elliott, J., Blanchard, S.G., Wu, W., Miller, J., Strader, C.D., Hartig, P., Moore, H.P., Racs, J., Raftery, M.A., 1980. Purification of *Torpedo californica* post-synaptic membranes and fractionation of their constituent proteins. Biochem J 185, 667-677.

Elliott, J., Dunn, S.M., Blanchard, S.G., Raftery, M.A., 1979. Specific binding of perhydrohistrionicotoxin to *Torpedo* acetylcholine receptor. Proc Natl Acad Sci U S A 76, 2576-2579.

Galzi, J.L., Revah, F., Black, D., Goeldner, M., Hirth, C., Changeux, J.P., 1990. Identification of a novel amino acid α-tyrosine 93 within the cholinergic ligands-binding sites of the acetylcholine receptor by photoaffinity labeling.

Additional evidence for a three-loop model of the cholinergic ligands-binding sites. J Biol Chem 265, 10430-10437.

Goldin, A.L., Sumikawa, K., 1992. Preparation of RNA for injection into *Xenopus oocytes*. Methods Enzymol 207, 279-297.

Hann, R.M., Pagan, O.R., Eterovic, V.A., 1994. The α-conotoxins GI and MI distinguish between the nicotinic acetylcholine receptor agonist sites while SI does not. Biochemistry 33, 14058-14063.

Hansen, S.B., Sulzenbacher, G., Huxford, T., Marchot, P., Taylor, P., Bourne, Y., 2005. Structures of *Aplysia* AChBP complexes with nicotinic agonists and antagonists reveal distinctive binding interfaces and conformations. EMBO J 24, 3635-3646.

Kapur, A., Davies, M., Dryden, W.F., Dunn, S.M.J., 2006. Tryptophan 86 of the α Subunit in the Torpedo Nicotinic Acetylcholine Receptor Is Important for Channel Activation by the Bisquaternary Ligand Suberyldicholines. Biochemistry 45, 10337-10343.

Karlin, A., 2002. Emerging structure of the nicotinic acetylcholine receptors. Nat Rev Neurosci 3, 102-114.

Kawai, H., Carlson, B.J., Okita, D.K., Raftery, M.A., 1999. Eserine and other tertiary amine interactions with *Torpedo* acetylcholine receptor postsynaptic membrane vesicles. Biochemistry 38, 134-141.

Lester, H.A., Krouse, M.E., Nass, M.M., Wassermann, N.H., Erlanger, B.F., 1980. A covalently bound photoisomerizable agonist: comparison with reversibly bound agonists at *Electrophorus* electroplaques. J Gen Physiol 75, 207-232.

McLane, K., Dunn, S., Manfredi, A., Conti-Tronconi, B., Raftery, M., 1996. The nicotinic acetylcholine receptor as a model for a superfamily of ligand-gated ion channel proteins. . Academic Press, Inc, San Diego.

Michaelson, M.J., Zeimal, E.V., 1973. Acetylcholine: An Approach to the Molecular Mechanisms of Action. Pergamon Press, Oxford.

Miledi, R., 1980. Intracellular calcium and desensitization of acetylcholine receptors. Proc R Soc Lond B Biol Sci 209, 447-452.

Moore, H.P., Raftery, M.A., 1980. Direct spectroscopic studies of cation translocation by *Torpedo* acetylcholine receptor on a time scale of physiological relevance. Proc Natl Acad Sci U S A 77, 4509-4513.

Nerbonne, J.M., Sheridan, R.E., Chabala, L.D., Lester, H.A., 1983. cis-3,3'-Bis-[α-(trimethylammonium)methyl]azobenzene (cis-Bis-Q). Purification and properties at acetylcholine receptors of *Electrophorus* electroplaques. Mol Pharmacol 23, 344-349.

Neubig, R.R., Krodel, E.K., Boyd, N.D., Cohen, J.B., 1979. Acetylcholine and local anesthetic binding to *Torpedo* nicotinic postsynaptic membranes after removal of nonreceptor peptides. Proc Natl Acad Sci U S A 76, 690-694.

Noda, M., Takahashi, H., Tanabe, T., Toyosato, M., Kikyotani, S., Furutani, Y., Hirose, T., Takashima, H., Inayama, S., Miyata, T., Numa, S., 1983. Structural homology of *Torpedo californica* acetylcholine receptor subunits. Nature 302, 528-532.

Paton, W.D., Zaimis, E., 1952. The methonium. Pharmacol Rev 4, 219-253.

Pedersen, S.E., Cohen, J.B., 1990. d-Tubocurarine binding sites are located at α-γand α-δ subunit interfaces of the nicotinic acetylcholine receptor. Proc Natl Acad Sci U S A 87, 2785-2789.

Prince, R.J., Sine, S.M., 1998. Epibatidine binds with unique site and state selectivity to muscle nicotinic acetylcholine receptors. J Biol Chem 273, 7843-7849.

Raftery, M.A., Hunkapiller, M.W., Strader, C.D., Hood, L.E., 1980. Acetylcholine receptor: complex of homologous subunits. Science 208, 1454-1456.

Schmidt, J., Raftery, M.A., 1973. A simple assay for the study of solubilized acetylcholine receptors. Anal Biochem 52, 349-354.

Sine, S.M., Kreienkamp, H.J., Bren, N., Maeda, R., Taylor, P., 1995. Molecular dissection of subunit interfaces in the acetylcholine receptor: identification of determinants of α-conotoxin M1 selectivity. Neuron 15, 205-211.

Unwin, N., 2005. Refined structure of the nicotinic acetylcholine receptor at 4Å resolution. J Mol Biol 346, 967-989.

Wassermann, N.H., Erlanger, B.F., 1981. Agents related to a potent activator of the acetylcholine receptor of *Electrophorus* electricus. Chem Biol Interact 36, 251-258.

CHAPTER 3

C-Loop Trapping

Introduction

Throughout the nervous system, synaptic transmission relies on the rapid responses of synaptic receptors, specifically the ligand-gated ion channels (LGICs). Following the release of transmitter from the presynaptic terminal, free transmitter in the synaptic cleft interacts with receptors in the postsynaptic membrane. Postsynaptic receptors must transduce their association with transmitter in the ligand binding domain (LBD) into the subsequent opening of the receptors integral ion channel, located nearly 50 Å away (Unwin, 2005; Sine and Engel, 2006). In the central nervous system (CNS), the primary mediator of fast synaptic inhibitory neurotransmission is the γ-aminobutyric acid type-A receptor ($GABA_AR$), a chloride-selective member of the Cys-loop family of LGICs. The $GABA_AR$ is comprised of five homologous subunits arranged in a pseudo-symmetrical rosette conformation around a central ion conducting pore. Each subunit contains a large extracellular ligand binding domain (LBD) composed of ten β-sheets, four transmembrane domain (TMD) α-helices, of which the TM2 of each subunit forms the channel pore and a cytoplasmic domain composed of a partially defined α-helix (Unwin, 2005). To date there have been 19 subunits cloned i.e. α1-6, β1-3, γ1-3, δ, ε, π, θ and ρ1-3. It is now thought most $GABA_ARs$ are composed of α, β and γ subunits in a ratio of 2:2:1 respectively, while the most abundantly expressed receptor throughout the CNS is the α1β2γ2 subtype (Olsen and Tobin, 1990; Simon et al., 2004).

GABA binding sites are proposed to be located at the β-α subunit-subunit interfaces and are thought to be composed of at least six binding loops (A-F), with loops A, B and C being located on the "principal" subunit (β) and loops D, E and F on the "complementary " (α) subunit. Of these loops, loop C on the principal subunit appears to play a critical dynamic role in initiating the transmission of the ligand binding event from the LBD to the channel gate (Chang and Weiss, 2002; Wang et al., 2009). In the apo/unbound state of the receptor, the C-loop is thought to project away from the subunit interface in the uncapped position facilitating the access of ligand to the binding pocket (Hansen et al., 2005). Recently it has been suggested that the C-loop may act as an induced fit sensor in which, upon agonist binding, closes over the binding site, essentially trapping the agonist (Hansen et al., 2005). It has been speculated that this capping motion promotes a conformational change that leads to an activated pre-open state of the receptor (Lape et al., 2008). Thus, C-loop capping may initiate the conformational change from the LBD to the TMDs, thus relieving constraints that maintain the channel gate in the closed position (Sine and Engel, 2006; Lee et al., 2009; Mukhtasimova et al., 2009; Wang et al., 2009).

Binding loop-F of the complementary subunit is suggested to be located at the bottom of the binding cleft near the membrane (figure 3-1) (Mokrab et al., 2007). Previous studies have proposed that loop-F is a key transduction element that links ligand binding to channel gating (Newell and

Czajkowski, 2003; Kash et al., 2004; Thompson et al., 2006). In 2009, Khatri et al. investigated agonist-induced changes in the fluorescence of probes that were covalently attached to cysteine residues introduced into the F-loop of the ρ1 $GABA_AR$ subunit , while performing simultaneous electrophysiology (Khatri et al., 2009). Based on their data and agonist docking simulations into a structural model of the GABA binding site, the authors proposed that loop F is not involved in channel opening, but may be a component of the structural machinery that locks ligand into the agonist-binding site (Khatri et al., 2009). Although the role that the F-loop plays in ligand recognition and channel activation is controversial, it is suggested that it does move towards the binding cleft upon receptor association with agonist (Mokrab et al., 2007).

Structural insights into the dynamic processes involved in ligand recognition have been provided by the X-ray crystal structures of acetylcholine binding proteins (AChBPs) which contain LBDs that are homologous to those of the Cys-loop receptors (Brejc et al., 2001; Celie et al., 2004; Bourne et al., 2005; Celie et al., 2005a; Celie et al., 2005b; Hansen et al., 2005; Ulens et al., 2006; Dutertre et al., 2007). Unwin (2005) resolved the structure of the nAChR to a resolution of 4 Å giving a structural insight into a complete receptor that includes the TMDs of the Cys-loop family. Combining the above structural information with computer modeling programs, it has now become possible to generate molecular models of other members of the Cys-loop family of receptors. These models assist in the elucidation of

residues located within functionally crucial domains. The role that individual amino acids play in receptor function can then be explored using site-directed mutagenesis and electrophysiology.

In a current model of the α1β2γ2 $GABA_AR$ (Mokrab et al., 2007), a change in positioning of loops C and F upon GABA binding was proposed. It was suggested that the C-loop residue β2V223 and the loop-F residue α1V205 are located approximately 19.5 Å away from each other in the apo/unbound resting state of the receptor. Upon GABA binding, this distance was predicted to decrease by 12.6 Å to 6.9 Å. To investigate this hypothesis I introduced point mutations at each of these positions i.e., β2V223C and α1V205C. I hypothesized, following the oxidation of the cysteine residues by Cu:Phenanthroline (Cu:Phen) and exposure to the agonist, GABA, the receptor may become locked in the capped conformation via cystine bond formation. Locking of the C-loop in the capped position should alter the response to subsequent GABA exposure. Trapping of the C-loop in the capped position might be reversed by reduction of the cystine bond via the application of dithiothreitol (DTT), restoring the receptor back to the resting/activatable state. Although these residues were predicted to come into close enough proximity in the model of Morab et al. (2007) to achieve this result, I was unsuccessful. In an attempt to correct for any minor errors in distance calculations of our model, I increased the distance over which these residues could be covalently linked by utilizing a bisthiol linking agent,

DPDPB (1, 4-di[3'-(2'pyridyldithio)-propionamido] butane) that contains a spacer arm of 19.9 Å. DPDPB incorporation between the two cysteine residues may affect loops movement and thus, the current magnitude evoked from the application of GABA. However, the addition of DPDPB did not produce the effect I had anticipated based on the modeling data. Failure to prove my original hypothesis may have been due to inaccuracies in the model employed. In that model the side chains of the cysteine residues appear to be oriented in such a manner that their terminal thiol groups faced each other. To investigate this I hypothesized that attaching a chemical moiety may produce a steric hindrance effect, altering subsequent loop closure. However, the alkylating agents, iodoacetamide and DTNB (5, 5'-dithiobis(2-nitrobenzoic acid) had no effect on the activation parameters of the receptor, suggesting that my initial hypothesis as to loop movement, residue location or side chain orientation may be incorrect. Though my data did not support my original hypothesis, the introduced mutations did have an effect on the potency of GABA, suggesting these residues play a role in the recognition of GABA in the binding site.

MATERIALS AND METHODS

Materials

GABA, DPDPB, iodoacetamide, phenanthroline, dithiothreitol (DTT) and DTNB were obtained from Sigma (Sigma-Aldrich Canada Ltd, Oakville, ON)

Comparative Modeling

A structural model for the human $\alpha1\beta2\gamma2$ $GABA_A$ receptor was generated as described in Mokrab et al 2007. Briefly amino acid sequences were taken from UniProt (Wu et al., 2006) and a multiple alignment of these sequences, together with structural homologues collected by BLAST (Altschul et al., 1990), was generated with MAFFT (Katoh et al., 2005). A structure-based alignment of all five chains of the nAChR using the atomic coordinates from *Torpedo marmorata*, 2BG9 (protein database number) (Unwin, 2005) was then used to generate a sequence-structure alignment with this $GABA_A$ receptor subtype using FUGUE (Shi et al., 2001).

In 2BG9 (Unwin, 2005), the intracellular regions between helices M3 and M4 are disordered and, with the exception of the MA helices, no atomic coordinates are available. Sequence alignment with the above $GABA_A$ receptor subunits showed them to be poorly conserved with those of the nAChR in this region and, as a consequence, these segments of the sequence,

together with the short variable N-terminal segments, were excised prior to model building. A 'two-gap' alignment was adopted for this region following the discussion of Ernst et al. (2005). Only one template structure was used for each subunit of the $GABA_A$ receptor; the basis of the following subunit equivalences being the accepted position of the agonist recognition sites within these two receptors:

nAChR	$GABA_A$ receptor
α (2BG9 chain A)	β2
β (2BG9 chain B)	γ2
δ (2BG9 chain C)	α1
α ((2BG9 chain D)	β2
γ (2BG9 chain E)	α1

The target template pairs were extracted from the sequence structure alignment and concatenated to create a single alignment corresponding to the entire receptor. This was used as input to MODELLER (Sali and Blundell, 1993; Fiser et al., 2000) together with all five chains of the 2BG9 Protein Data Base entry as the template.

Mutagenesis

Site directed mutagenesis was performed as described previously (Derry et al., 2004). Briefly, the QuickChange protocol (Stratagene, La Jolla, CA) was used to introduce specific substitutions into the rat wild-type β2 and α1 cDNA sequences. The individual subunit cDNA sequences had been previously subcloned into pcDNA3.1(+) (Invitrogen, San Diego, CA) and these

plasmids were used as templates in separate PCR-mediated mutagenesis protocols. The presence of mutations were then verified by restriction endonuclease digestion and double-stranded cDNA sequencing.

In Vitro Transcription

Plasmid cDNAs encoding the wild-type and mutant $GABA_AR$ subunits were linearized by digestion with *Xba*I (α1 and γ2 subunit)and BamHI (β2 subunit). *In vitro* transcription of cRNA was performed using methods previously described (Goldin, 1992). Briefly, the linearized cDNA templates (5μg) were transcribed *in vitro* using T7 RNA polymerase (Invitrogen) in the presence of RNA capping analogue (New England Biolabs) and ribonucleotide triphosphates (NTP mix, Invitrogen). RNA transcripts were then extracted using a 25:24:1 (v/v) phenol:chloroform:isoamyl alcohol mixture. Final cRNA pellets were resuspended in diethylpyrocarbonate-treated water to a final concentration of 1 μg/μl and aliquots were stored at –80°C until use.

Expression in *Xenopus* Oocytes and Electrophysiology

Isolated follicle-free oocytes from *Xenopus laevis* were microinjected with a total of 50ng of wild-type and mutant subunit cRNAs in the ratio of 2β:2α:1γ (ratio by weight) . Oocytes were incubated in ND96 buffer (5 mM HEPES, 96 mM NaCl, 1.8 mM $CaCl_2$, 2 mM KCl, 1 mM $MgCl_2$, pH 7.6) supplemented with 50 μg/ml gentamicin at 14°C for at least 48 hours prior

to recording. Currents elicited by bath application of agonist were measured using standard two-electrode voltage clamp techniques and a GeneClamp500 amplifier (Axon Instruments, Foster City, CA) at a holding potential of -60 mV. Electrodes were filled with 3 M KCl and only electrodes with resistances of 0.5-1.5 MΩ were used. The recording chamber was continuously perfused (at a rate of ~5 ml/min) with frog Ringer's solution (110mM NaCl, 2mM KCl, 1.8mMCaCl2, 5mM HEPES, pH 7.4). Agonist-evoked responses were measured by applying drug (via a gravity flow perfusion system) for 10-20 seconds unless otherwise indicated. Drugs were washed out for 12-min between applications to ensure complete recovery from desensitization. Oocytes were only used for experiments when current responses were stable (±5%) between successive applications of agonist. All compounds were dissolved in perfusion buffer except DPDPB which also contained 0.1% DMSO in the solution.

C-Loop Trapping and Alkylating Experiments

C-loop trapping experiments were done as described below: After stabilization with EC_{50} concentrations of GABA (48μM) oocytes were challenged with an EC_{50} concentration of GABA in the presence of Cu:Phen in a 1:4 ratio (100μM:400μM) for 2 mins. After 7 minutes of washout, oocytes were again challenged with EC_{50} GABA. After GABA challenge, oocytes were superfused with 10mM DTT, followed by washout for 10 minutes upon which time the oocyte's stability was again determined by application of an EC_{50}

concentration of GABA (figure 3-2). A similar protocol was followed for the DPDPB cross-linking experiments, DPDPB (50μM) was added with the EC_{50} concentration of GABA in the presence of Cu:Phen in a 1:4 ratio (100μM:400μM) for 2 mins. Iodoacetamide/DTNB experiments were performed as follows: following stabilization with EC_{50} concentrations of GABA (48μM), oocytes were superfused with either iodoacetamide (1mM), or DTNB (50μM) for 5 minutes followed by a 10min washout period to allow complete recovery from desensitization. Oocytes were subsequently challenged with EC_{50} concentrations of GABA (figure 3-3). Three replicate experiments were performed for each C-loop trapping and steric hindrance protocol.

Data and statistical analysis

To determine potencies of GABA activation at each $GABA_AA$ receptor subtype expressed, concentration effect data were fit by a three-parameter logistic equation using Prism 3.0 (GraphPad, San Diego, CA):

$$I=(I_{max} X [L]^n) / (EC^n_{50} + [L]^n)$$

where I is the measured agonist-evoked current, $[L]$ is the agonist concentration, EC_{50} is the agonist concentration that elicits the half maximal current (I_{max}) and n is the Hill coefficient. All values of EC_{50} are reported as

+/- SEM. C-loop trapping and steric hindrance data was analyzed by the unpaired t-test.

RESULTS

Structural Modeling

For a review of the model of the α1β2γ2 $GABA_AR$ employed in this study see the foregoing Materials and Methods section. Based on that model, in the apo/unbound state of the receptor the C-loop residue β2V223 is separated from the F-loop residue α1V205 by a distance of approximately 19.5 Å (figure 3-4). Upon GABA binding, it is hypothesized that the C-loop may move in a capping motion towards the adjacent α subunit while the F-loop on the α subunit would displaced away from the membrane, towards the N-terminus of the receptor. These movements may bring the C-loop residue β2V223 to within 6.9 Å of the F-loop residue α1V205, decreasing their separation by 12.6 Å. Figure 4-13 shows location of the two residues in sequence alignment format.

Potency of GABA on Wild-Type and Mutant Receptors

GABA concentration-effect curves were constructed for wild-type and mutant receptors. The EC_{50} value for GABA at the wild-type α1β2γ2 receptor was 48.4±0.2 μM, which is comparable to that in the literature (~30-50 μM) (Baumann et al., 2002; Sieghart and Sperk, 2002) (figure 3-5). GABA appeared to be approximately 5-fold more potent at the single mutant

receptor α1V205Cβ2γ2 with an EC_{50} of 9.5±0.8 μM (figure 3-6). A similar observation was made in the single mutant receptor α1β2V223Cγ2 where GABA potency increased approximately 6-fold in the mutant displaying an EC_{50} of 8.0±1.3 μM (figure 3-7). Interestingly, in the double mutant receptor, α1V205Cβ2V223Cγ2, the shift in GABA potency was less than that observed for either of the single mutant receptors with an EC_{50} of 15.7±0.7 μM i.e., an approximate 3-fold increase in potency compared to the wild-type receptor (figure 3-8). Figure 3-9 is a compilation displaying the potency of GABA at all of the receptors investigated. Figure 3-10 displays representative current traces of wild-type and mutant receptors to 100 μM GABA challenge.

C-Loop Trapping/Steric Hindrance Experiments

Oxidation of wild-type and mutant receptors by the application of Cu:Phen in a 1:4 ratio (100μM:400μM) in the presence of EC_{50} GABA for 2 mins (see figure 3-2) had had no effect on subsequent EC_{50} GABA response ($P>0.05$)(see figure 3-11A). The exposure to DPDPB also did not affect subsequent GABA EC_{50} challenges ($P>0.05$)((see figure 3-11B).

The exposure to iodoacetamide (1mM) also had no statistically significant effect on subsequent EC_{50} GABA response ($P>0.05$)((see figure 3-12A). However, exposure to the alkylating agent DTNB (50μM) for 5 minutes to wild-type and mutant receptors had a statistically significant increase ($P<0.001$***) on currents elicited by EC_{50} GABA challenges, rather than a

decrease as I had predicted from the modeling data (see figure 3-12B). This increase in current following exposure to DTNB was only 5% and may only be statistically significant due to the low replicate number of experiments.

DISCUSSION

Recent advances in determining the structure of the Cys-loop family of LGICs have proven to be useful tools in elucidating the local rearrangements that occur in the binding upon ligand binding (see introduction). Sequence alignments of an unresolved protein with a homologue of crystallized, or resolved, structure can provide an estimate of the molecular architecture of the un-resolved protein, providing that significant similarities between sequences and folding patterns exist. Aligning the primary amino acid sequence of the $\alpha1\beta2\gamma2$ $GABA_AR$ with the 4 Å resolution structure of the *Torpedo* nAChR (Unwin, 2005) has provided us with an *in silico* model of the $\alpha1\beta2\gamma2$ $GABA_AR$ (Mokrab et al., 2007).

For the purpose of this study I focused on the distance separating two valine residues, $\beta2V223$ of the C-loop of the primary subunit and $\alpha1V205$ of the F-loop of the complimentary subunit. According to the model of Mokrab et al. (2007), upon GABA binding the distance between these residues is reduced. Based on this model, it may be possible to form a cystine bond if cysteine residues were introduced at these locations. Locking of the C-F loops may be observed as a failure of subsequent applications of GABA to

elicit a response. I also attempted to increase the distance of bond formation locking the C-loop in place by using the bisthiol linker DPDPB which contains a spacer arm of 19.9 Å, allowing a possible linkage between residues to be over 20 Å long and impairing loop movement. If DPDPB successfully covalently linked these two residues it may alter the mobility of the two binding loops, altering receptor function. However, no changes in the magnitude of current evoked in response to EC_{50} GABA exposure were observed. I was also unsuccessful at altering loop movement via the addition of the alkylating agent iodoacetamide and the introduction of a possible steric hindrance affect. Though there appeared to be a statistically significant increase in current following DTNB exposure, this may be due to the low replicate number of these experiments, as the increase was only 5%.

In 2009, Mukhtasimova et al. reported that they were successful in locking the C-loop in the capped position in the peripheral muscle nAChR. The adult peripheral muscle nAChR does not contain the γ subunit; rather its role is fulfilled by the ε subunit. ACh binding sites in the adult peripheral muscle nAChR occur at the α-δ and α-ε subunit interfaces where the role of the principal subunit is fulfilled by α-subunits, while the δ and ε subunits comprise the complementary subunits. One property distinguishing nAChR α subunits from the non-α subunits is the presence of two conserved adjacent cysteine C-loop residues, Cys192 and Cys193 (Noda et al., 1982). The authors introduced the mutation αC193S generating a single free cysteine residue at

the tip of the C-loop, αCys192. In addition, they introduced cysteine residues into binding loop-E of the complementary subunits i.e., δL121C and εL119C (Miller and Smart, 2010; Mukhtasimova et al., 2009). The authors suggest that these cysteine residues in Loops C and E come into close enough proximity upon interaction with agonist that they may form a disufide bond, locking the C-loop in the capped position. In addition, a conserved residue comprising a portion of the hydrophobic gate in TMD2, Leu9', was mutated in the β and δ subunits (βL262S and δL265S) to produce increased spontaneous channel openings. In this study the authors investigated spontaneous channel openings at the single channel level. They propose that spontaneous channel opening, due to disruption of the channel gate via mutations introduced in TMD2, will be transmitted in a retrograde fashion to the LBD causing the C-loops to adopt the capped conformation similar to the agonist bound state. The authors then monitored open channel events, in the absence of agonist, before and after applying the oxidizing agent H_2O_2. Prior to oxidation, channels activate in episodes of predominately brief openings. However, following oxidation channels activate in a quick succession of long duration openings, suggesting a covalent reaction locking the C-loop in the capped conformation. These functional consequences of oxidation were reversible as application of the reducing agent DTT restored brief channel openings.

Peripheral muscle and *Torpedo* nAChRs share a high degree of sequence homology (Corringer et al., 2000; Brejc et al., 2001). In addition, the *Torpedo* nAChR it is the only member of the Cys-loop receptor family to be resolved to a 4 Å resolution (Unwin, 2005). These two factors may allow for a better estimation of residue location and orientation in the work done by Mukhtasimova et al. (2009). Though the current model of the α1β2γ2 $GABA_AR$ was constructed via homology modeling using the *Torpedo* nAChR as a template, these two proteins share only approximately 15-18% sequence homology (Corringer et al., 2000; Brejc et al., 2001; Simon et al., 2004). It should be noted that sequence alignments become increasingly difficult once the sequence identity falls to a value less than 30%, termed the proverbial "twilight zone" of homology modeling (Rost, 1999). As sequence similarity decreases, alignments contain an increasingly large number of gaps and alignment errors, regardless of alignment method used. Evidence suggests as sequence homology falls below 30% a rapid decrease is observed in conservation of side-chain packing. Therefore, although the overall fold of the protein may be conserved the pattern of side-chain interactions may be lost (Russell and Barton, 1994; Chung and Subbiah, 1996). My experimental data suggests that in the model of the α1β2γ2 $GABA_AR$ generated by Mokrab et al. (2009), estimates of dynamic protein movement, residue location, or side chain orientation, may be incorrect. In addition, alteration in the exposure time to Cu:Phen, DPDPB, Iodoacetamide and DTNB may provide different results, as there is no evidence the oxidation/reduction reactions have taken

place. My negative results may be explained by insufficient oxidation/reduction of the introduced cysteine residues.

Though my data do not indicate that I was able to trap the C-loop in the capped position, or to alter the loops movement by attaching an alkylating agent, I did make some interesting observations. Each mutant receptor displayed an increase in potency for GABA, compared to wild-type. These data indicates the addition of a cysteine residue in these loops may help stabilize GABA in the binding pocket to some extent.

In conclusion, I was unable to alter receptor function by covalently linking introduced cysteine residues on binding loops C and F. I suggest this may be due to the lack of a high-resolution receptor structure and a low level of sequence homology between the $\alpha1\beta2\gamma2$ $GABA_AR$ and related proteins of resolved structure (Brejc et al., 2001; Unwin, 2005). However, the addition of cysteine residues to loops C and F did increase the potency of GABA at the mutant receptors, suggesting that these residues may be involved the receptors interaction with the agonist.

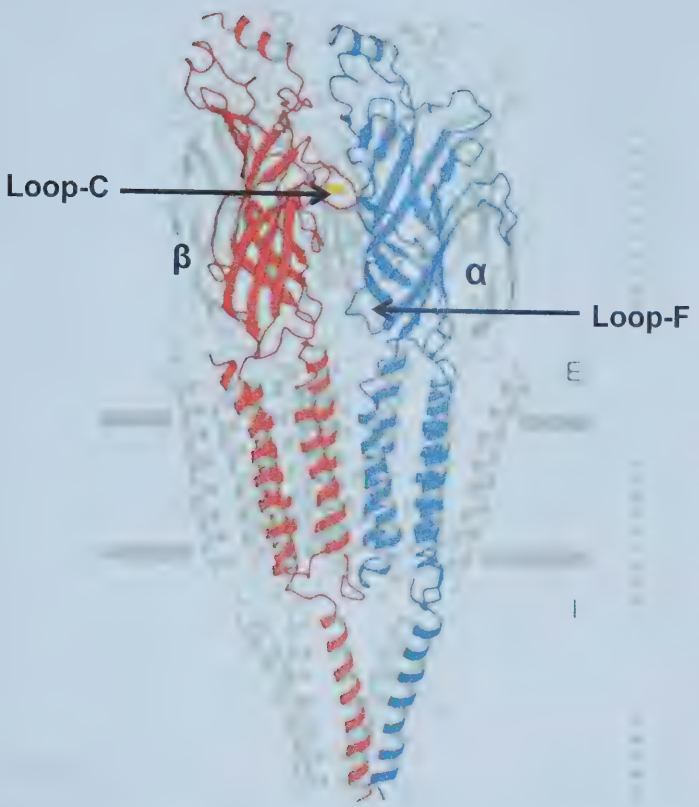

Figure 3-1: Ribbon diagram of the α1β2γ2 receptor (adapted from a model of the *Torpedo* nAChR), as viewed parallel with the membrane plane. The primary β subunit (red) and the complementary α subunit (blue) form a GABA binding site at the subunit interface. Note the F-loops is located in close proximity to the membrane while the C-loop is located ~30 Å above the membrane. Horizontal bars; E, extracellular; I, intracellular. The dotted lines on the right denote the three main zones of subunit–subunit contacts. Adapted from **Unwin, N. (2005). "Refined structure of the nicotinic acetylcholine receptor at 4Å resolution." J Mol Biol 346(4): 967-89.**

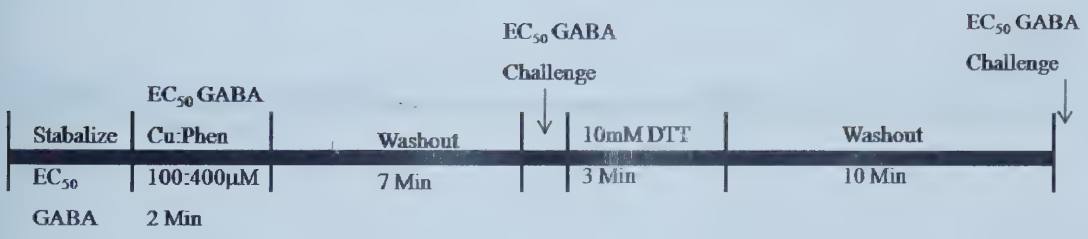

Figure 3-2: Experimental protocol for C-loop trapping experiments. Oocytes were considered to be stable after 3 successive applications of agonist at EC_{50} concentration eliciting currents within ±5%. Following stabilization, oocytes were challenged with an EC_{50} concentration of GABA in the presence of Cu:Phen in a 1:4 ratio (100µM:400µM) for 2 mins. After 7 minutes of washout, oocytes were again challenged with EC_{50} GABA. After GABA challenge, oocytes were superfused with 10mM DTT, followed by washout for 10 minutes upon which time the oocyte's stability was again determined by application of an EC_{50} concentration of GABA.

Figure 3-3: Experimental protocol for steric hinderence experiments. Oocytes were considered to be stable after 3 successive applications of agonist at EC_{50} concentration eliciting currents within ±5%. Following stabilization eggs were superfused for five minutes with either iodoacetamide (1mM) or DTNB (50µM) for 5 minutes, following this oocytes were given a 10min washout period after which they were again challenged with EC_{50} doses of GABA

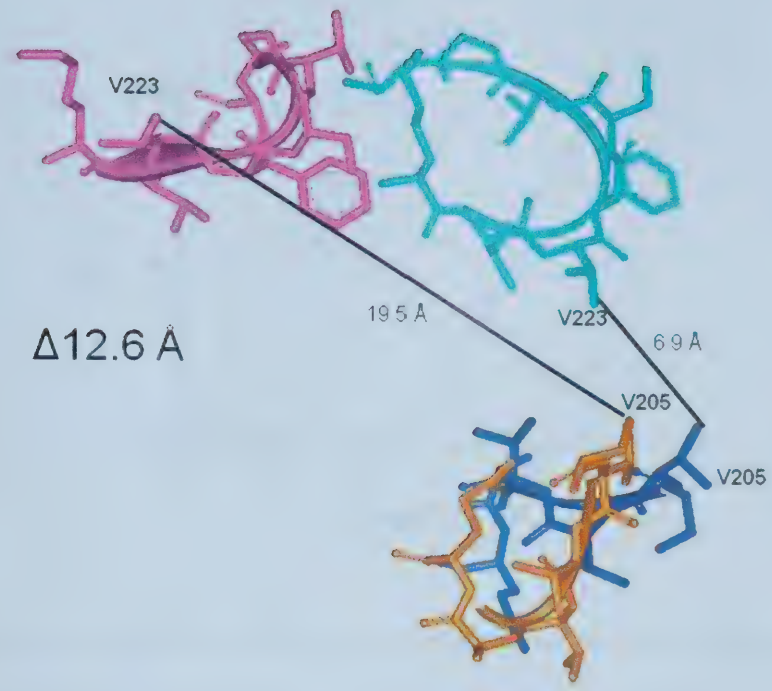

Figure 3-4: Molecular stick figure model of the C-loop (β2 subunit) and the F-loop (α1 subunit). In the apo/unbound position the C-loop (purple) residue V223 and F-loop (orange) residue V205 are positioned 19.5 Å apart. Upon agonist binding, C-loop closure and other allosteric movements the C-loop (aqua) and the F-loop (blue) Val residues close this gap by 12.6 Å, coming within 6.9 Å of each other.

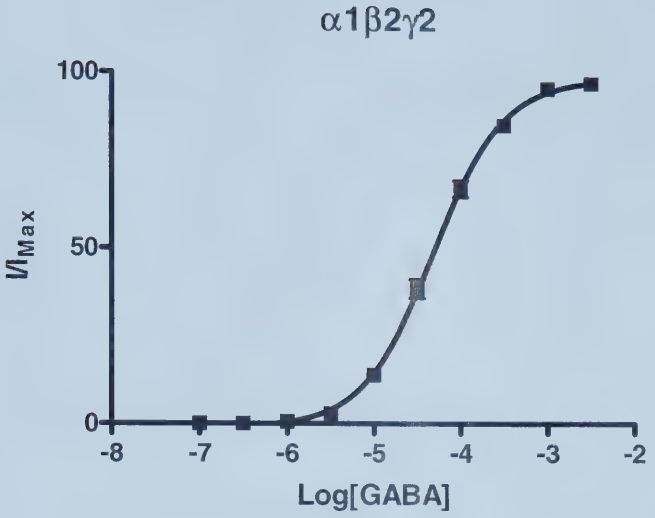

Figure 3-5: Concentration-effect curve of GABA on the wild-type α1β2γ2 $GABA_AR$ (black). The EC_{50} concentration of GABA is 48.4±0.2 μM.

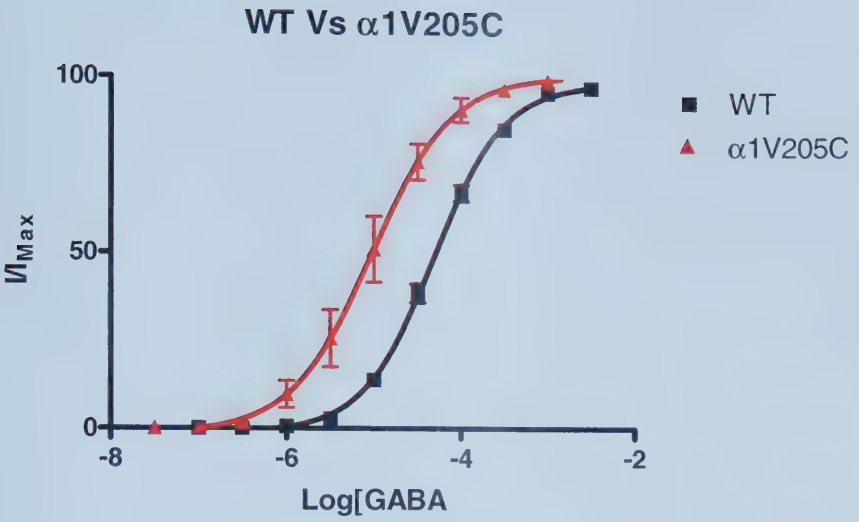

Figure 3-6: Concentration-effect curves comparing the potency of GABA at the wild-type α1β2γ2 (black) and the mutant α1V205Cβ2γ2 $GABA_A$Rs (red). The EC_{50} concentration of GABA at these receptors was 48.4±0.2 μM and 9.5±0.8 μM, respectively. GABA displays an approximate 5-fold increase in potency at the mutant receptor.

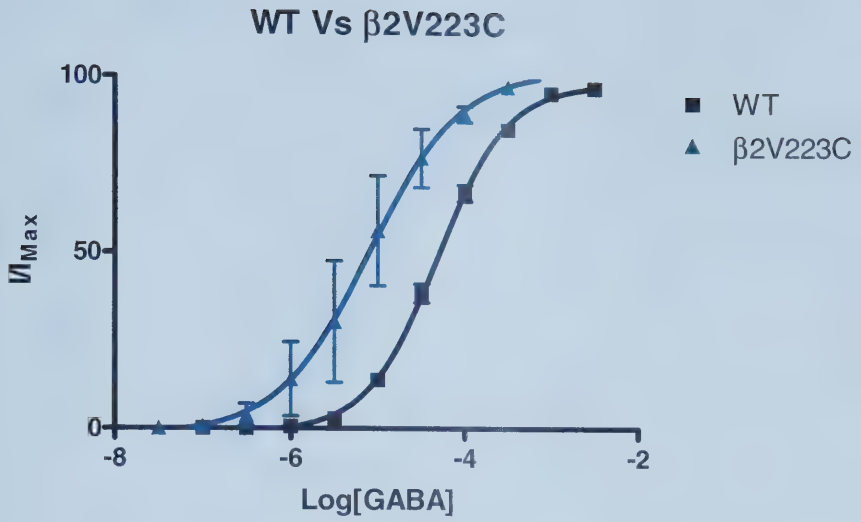

Figure 3-7: Concentration-effect curves comparing the potency of GABA at the wild-type α1β2γ2 (black) and the mutant α1β2V223Cγ2 $GABA_A$Rs (blue). The EC_{50} concentration of GABA at these receptors was 48.4±0.2 μM and 8.0±1.3 μM respectively. GABA displays an approximate 6-fold increase in potency at the mutant receptor.

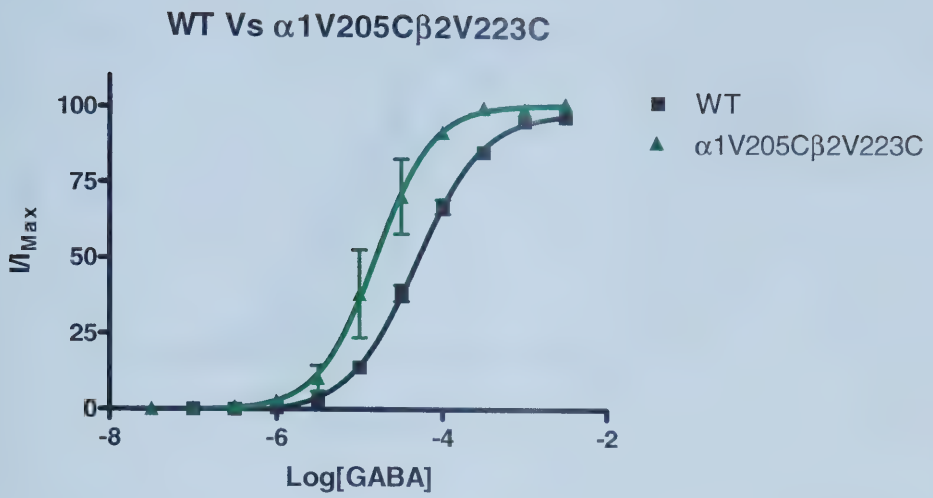

Figure 3-8: Concentration-effect curves comparing the potency of GABA at the wild-type α1β2γ2 (black) and the double mutant α1V205Cβ2V223Cγ2GABA$_A$Rs (green). The EC_{50} concentration of GABA at these receptors was48.4±0.24 μM and 15.7±0.7 μM respectively. GABA displays an approximate3-fold increase in potency at the double mutant receptor.

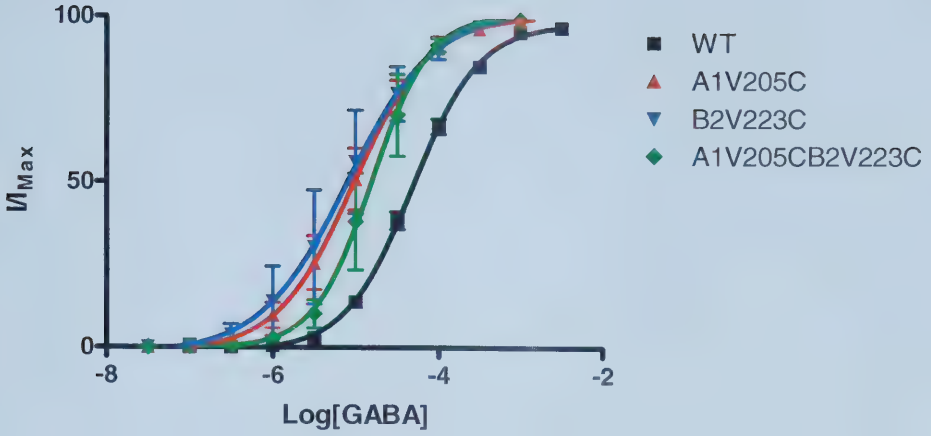

Figure 3-9: Compilation of concentration-effect curves of comparing the potency of GABA at the wild-type α1β2γ2 (black), the mutant α1V205Cβ2γ2 (red), the mutant α1β2V223Cγ2 (blue) and the double mutant α1V205Cβ2V223Cγ2 $GABA_ARs$ (green). The respective $EC_{50}s$ for the receptors were 48.4±0.2 μM, 9.5±0.8 μM, 8.0±1.3 μM and 15.7±0.7 μM.

Figure 3-10: Representative current traces following 100 μM GABA challenge. (A) Wild-type α1β2γ2, (B) mutant α1V205Cβ2γ2, (C) α1β2V223Cγ2 and (D) α1V205Cβ2V223Cγ2.

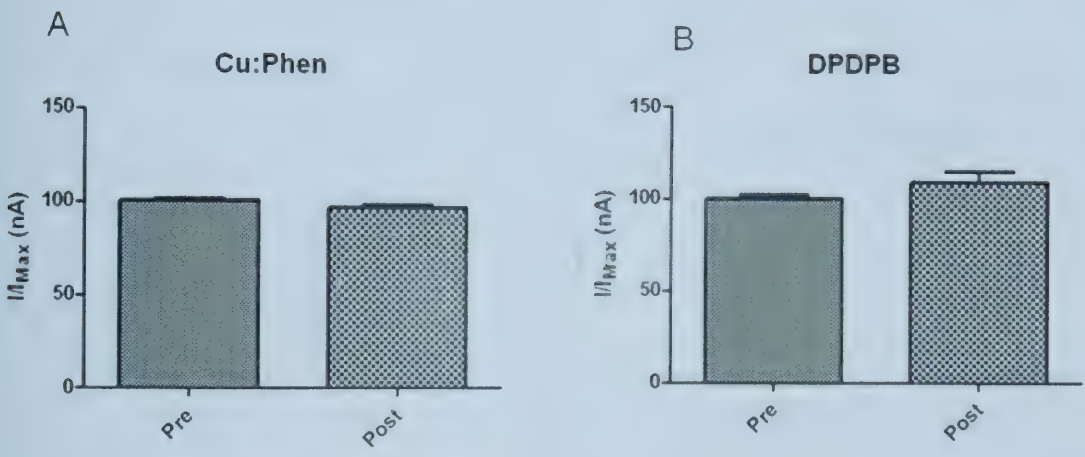

Figure 3-11: Bar graphs representing normalized current following the perfusion of (A) Cu:Phen or (B) DPDPB. Oocytes were challenged with EC_{50} GABA pre- and post-perfusion with either compound. Neither Cu:Phen or DPDPB produced a statistically significant change in current amplitude.

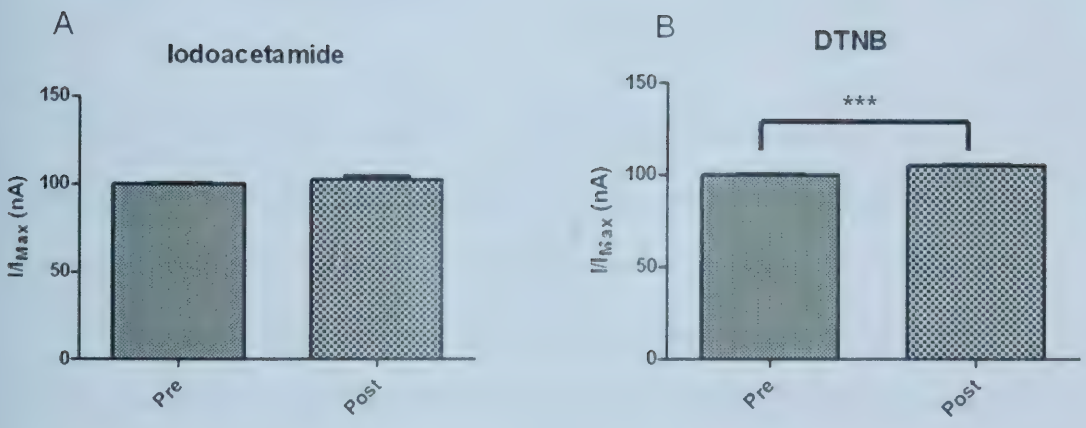

Figure 3-12: Bar graphs representing normalized current following the perfusion of (A) iodoacetamide or (B) DTNB. Oocytes were challenged with EC_{50} GABA pre- and post-perfusion with either compound. Iodoacetamide failed to produce a statistically significant change in current amplitude. However, DTNB caused a statistically significant ($P<0.001^{***}$) 5% increase in current amplitude.

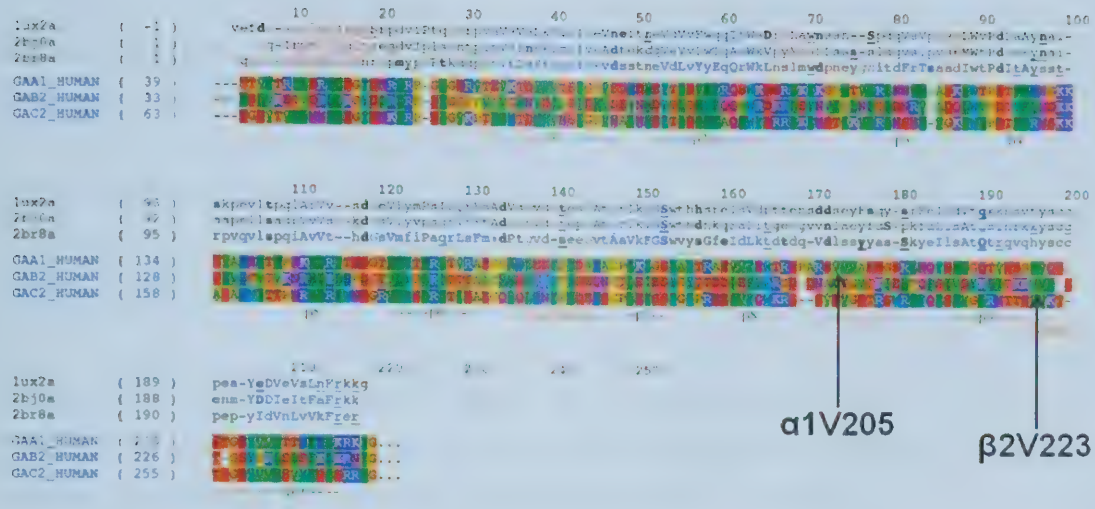

Figure 4-13: Multiple sequence alignment between the structures of acetylcholine binding proteins (AChBP) from *Lymnaea stagnalis*, *Bulinus truncates*, *Aplysia californica* and the amino acid sequence of the α1, β2 and γ2 subunits of the human $GABA_AR$. Arrows indicate the locations of F-loop residue α1V205 (ARSVVVA) and C-loop residue β2V223 (TKKVVF-), mutated valine residues are underlined. Adapted from **Mokrab, Y et al. (2007). Exploring ligand recognition and ion flow in comparative models of the human GABA type A receptor. J Mol Graph Model 26, 760-774.**

REFERENCES

Altschul, S.F., Gish, W., Miller, W., Myers, E.W., Lipman, D.J., 1990. Basic local alignment search tool. J Mol Biol 215, 403-410.

Baumann, S.W., Baur, R., Sigel, E., 2002. Forced subunit assembly in α1β2γ2 $GABA_A$ receptors. Insight into the absolute arrangement. J Biol Chem 277, 46020-46025.

Bourne, Y., Talley, T.T., Hansen, S.B., Taylor, P., Marchot, P., 2005. Crystal structure of a Cbtx-AChBP complex reveals essential interactions between snake α-neurotoxins and nicotinic receptors. EMBO J 24, 1512-1522.

Brejc, K., van Dijk, W.J., Klaassen, R.V., Schuurmans, M., van Der Oost, J., Smit, A.B., Sixma, T.K., 2001. Crystal structure of an ACh-binding protein reveals the ligand-binding domain of nicotinic receptors. Nature 411, 269-276.

Celie, P.H., Kasheverov, I.E., Mordvintsev, D.Y., Hogg, R.C., van Nierop, P., van Elk, R., van Rossum-Fikkert, S.E., Zhmak, M.N., Bertrand, D., Tsetlin, V., Sixma, T.K., Smit, A.B., 2005a. Crystal structure of nicotinic acetylcholine receptor homolog AChBP in complex with an α-conotoxin PnIA variant. Nat Struct Mol Biol 12, 582-588.

Celie, P.H., Klaassen, R.V., van Rossum-Fikkert, S.E., van Elk, R., van Nierop, P., Smit, A.B., Sixma, T.K., 2005b. Crystal structure of acetylcholine-binding protein from Bulinus truncatus reveals the conserved structural scaffold and sites of variation in nicotinic acetylcholine receptors. J Biol Chem 280, 26457-26466.

Celie, P.H., van Rossum-Fikkert, S.E., van Dijk, W.J., Brejc, K., Smit, A.B., Sixma, T.K., 2004. Nicotine and carbamylcholine binding to nicotinic acetylcholine receptors as studied in AChBP crystal structures. Neuron 41, 907-914.

Chang, Y., Weiss, D.S., 2002. Site-specific fluorescence reveals distinct structural changes with GABA receptor activation and antagonism. Nat Neurosci 5, 1163-1168.

Chung, S.Y., Subbiah, S., 1996. A structural explanation for the twilight zone of protein sequence homology. Structure 4, 1123-1127.

Corringer, P.J., Le Novere, N., Changeux, J.P., 2000. Nicotinic receptors at the amino acid level. Annu Rev Pharmacol Toxicol 40, 431-458.

Derry, J.M., Dunn, S.M., Davies, M., 2004. Identification of a residue in the γ-aminobutyric acid type A receptor alpha subunit that differentially affects diazepam-sensitive and -insensitive benzodiazepine site binding. J Neurochem 88, 1431-1438.

Dutertre, S., Ulens, C., Buttner, R., Fish, A., van Elk, R., Kendel, Y., Hopping, G., Alewood, P.F., Schroeder, C., Nicke, A., Smit, A.B., Sixma, T.K., Lewis, R.J., 2007. AChBP-targeted α-conotoxin correlates distinct binding orientations with nAChR subtype selectivity. EMBO J 26, 3858-3867.

Ernst, M., Bruckner, S., Boresch, S., Sieghart, W., 2005. Comparative models of $GABA_A$ receptor extracellular and transmembrane domains: important insights in pharmacology and function. Mol Pharmacol 68, 1291-1300.

Fiser, A., Do, R.K., Sali, A., 2000. Modeling of loops in protein structures. Protein Sci 9, 1753-1773.

Goldin, A.L., 1992. Maintenance of *Xenopus* laevis and oocyte injection. Methods Enzymol 207, 266-279.

Hansen, S.B., Sulzenbacher, G., Huxford, T., Marchot, P., Taylor, P., Bourne, Y., 2005. Structures of Aplysia AChBP complexes with nicotinic agonists and

antagonists reveal distinctive binding interfaces and conformations. EMBO J 24, 3635-3646.

Kash, T.L., Trudell, J.R., Harrison, N.L., 2004. Structural elements involved in activation of the gamma-aminobutyric acid type A ($GABA_A$) receptor. Biochem Soc Trans 32, 540-546.

Katoh, K., Kuma, K., Toh, H., Miyata, T., 2005. MAFFT version 5: improvement in accuracy of multiple sequence alignment. Nucleic Acids Res 33, 511-518.

Khatri, A., Sedelnikova, A., Weiss, D.S., 2009. Structural rearrangements in loop F of the GABA receptor signal ligand binding, not channel activation. Biophys J 96, 45-55.

Lape, R., Colquhoun, D., Sivilotti, L.G., 2008. On the nature of partial agonism in the nicotinic receptor superfamily. Nature 454, 722-727.

Lee, W.Y., Free, C.R., Sine, S.M., 2009. Binding to gating transduction in nicotinic receptors: Cys-loop energetically couples to pre-M1 and M2-M3 regions. J Neurosci 29, 3189-3199.

Miller, P.S., Smart, T.G., 2010. Binding, activation and modulation of Cys-loop receptors. Trends Pharmacol Sci 31, 161-174.

Mokrab, Y., Bavro, V.N., Mizuguchi, K., Todorov, N.P., Martin, I.L., Dunn, S.M., Chan, S.L., Chau, P.L., 2007. Exploring ligand recognition and ion flow in comparative models of the human GABA type A receptor. J Mol Graph Model 26, 760-774.

Mukhtasimova, N., Lee, W.Y., Wang, H.L., Sine, S.M., 2009. Detection and trapping of intermediate states priming nicotinic receptor channel opening. Nature 459, 451-454.

Newell, J.G., Czajkowski, C., 2003. The $GABA_A$ receptor α 1 subunit Pro174-Asp191 segment is involved in GABA binding and channel gating. J Biol Chem 278, 13166-13172.

Noda, M., Takahashi, H., Tanabe, T., Toyosato, M., Furutani, Y., Hirose, T., Asai, M., Inayama, S., Miyata, T., Numa, S., 1982. Primary structure of α-subunit precursor of *Torpedo californica* acetylcholine receptor deduced from cDNA sequence. Nature 299, 793-797.

Olsen, R.W., Tobin, A.J., 1990. Molecular biology of $GABA_A$ receptors. FASEB J 4, 1469-1480.

Rost, B., 1999. Twilight zone of protein sequence alignments. Protein Eng 12, 85-94.

Russell, R.B., Barton, G.J., 1994. Structural features can be unconserved in proteins with similar folds. An analysis of side-chain to side-chain contacts secondary structure and accessibility. J Mol Biol 244, 332-350.

Sali, A., Blundell, T.L., 1993. Comparative protein modelling by satisfaction of spatial restraints. J Mol Biol 234, 779-815.

Shi, J., Blundell, T.L., Mizuguchi, K., 2001. FUGUE: sequence-structure homology recognition using environment-specific substitution tables and structure-dependent gap penalties. J Mol Biol 310, 243-257.

Sieghart, W., Sperk, G., 2002. Subunit composition, distribution and function of $GABA_A$ receptor subtypes. Curr Top Med Chem 2, 795-816.

Simon, J., Wakimoto, H., Fujita, N., Lalande, M., Barnard, E.A., 2004. Analysis of the set of $GABA_A$ receptor genes in the human genome. J Biol Chem 279, 41422-41435.

Sine, S.M., Engel, A.G., 2006. Recent advances in Cys-loop receptor structure and function. Nature 440, 448-455.

Thompson, A.J., Padgett, C.L., Lummis, S.C., 2006. Mutagenesis and molecular modeling reveal the importance of the 5-HT3 receptor F-loop. J Biol Chem 281, 16576-16582.

Ulens, C., Hogg, R.C., Celie, P.H., Bertrand, D., Tsetlin, V., Smit, A.B., Sixma, T.K., 2006. Structural determinants of selective α-conotoxin binding to a nicotinic acetylcholine receptor homolog AChBP. Proc Natl Acad Sci U S A 103, 3615-3620.

Unwin, N., 2005. Refined structure of the nicotinic acetylcholine receptor at 4Å resolution. J Mol Biol 346, 967-989.

Wang, H.L., Toghraee, R., Papke, D., Cheng, X.L., McCammon, J.A., Ravaioli, U., Sine, S.M., 2009. Single-channel current through nicotinic receptor produced by closure of binding site C-loop. Biophys J 96, 3582-3590.

Wu, C.H., Apweiler, R., Bairoch, A., Natale, D.A., Barker, W.C., Boeckmann, B., Ferro, S., Gasteiger, E., Huang, H., Lopez, R., Magrane, M., Martin, M.J., Mazumder, R., O'Donovan, C., Redaschi, N., Suzek, B., 2006. The Universal Protein Resource (UniProt): an expanding universe of protein information. Nucleic Acids Res 34, D187-191.

CHAPTER 4[1]

D-Loop Arginine and its Role in Receptor Function in the α1β2γ2 and α4β3δ $GABA_AR$s

[1] Manuscript in preparation

INTRODUCTION

γ-Aminobutyric acid (GABA), the major inhibitory neurotransmitter in the central nervous system (CNS), mediates inhibition via $GABA_A$ receptors ($GABA_ARs$). The $GABA_AR$ belongs to the Cys-loop family of ligand-gated ion channels (LGICs); other members of this family include the anion-selective inhibitory glycine receptors (GlyRs), and the cationic-selective, excitatory, nicotinic acetylcholine receptor (nAChR) and serotonin type-3 receptor ($5\text{-}HT_3R$). The $GABA_AR$ is a pentamer of homologous subunits that are arranged pseudosymmetrically in a rosette conformation surrounding a GABA-gated central chloride-selective ion pore. To date, we know of 19 different genes coding for $GABA_AR$ subunits (Simon et al., 2004), these include 16 subunits (α1-6, β1-3, γ1-3, δ, ε, π, θ) which combine to form heteropentameric $GABA_ARs$. In addition 3 rho(ρ) subunits contribute to the formation homopentameric $GABA_ARs$ (Olsen and Sieghart, 2008; Collingridge et al., 2009). With such subunit heterogeneity, it is not surprising that $GABA_AR$ complexes display diverse pharmacological profiles (Sieghart, 1995). Despite such diversity, four types of subunits (α, β, γ, and δ) usually comprise the prominent $GABA_ARs$ expressed in the mammalian brain (McKernan et al., 2000). In addition, it seems likely that only a minor fraction of possible receptor combinations are actually present in the brain and the predominant receptor has a stoichiometry of two α, two β and one γ subunit, though the γ subunit may be exchanged for δ subunit (Hartvig et al., 2000).

Recently, interest has focused on the diverse characteristics displayed by γ and δ subunit-containing receptors, and the roles that they play in $GABA_AR$-mediated phasic and tonic inhibition. In 2005, Farrant and Nusser reviewed phasic and tonic inhibition. Phasic inhibition involves the rapid and precise transmission of presynaptic activity into a postsynaptic signal. Phasic inhibition is defined by a short duration (100-500μs) exposure to millimolar concentrations of GABA in the synaptic cleft (Mody et al., 1994; Mozrzymas, 2004). Previous studies indicate that receptors containing the γ2 subunit in association with the α1, α2, α3, β2 and β3 subunits (α1β2/3γ2, α2β2/3γ2 and α3β2/3γ2) are predominantly involved in mediating phasic inhibition (Farrant and Nusser, 2005) with the α1β2γ2 receptor playing a significant role. Tonic inhibition involves the activation of a subset of $GABA_ARs$ in a manner that is temporally and spatially dissociated from phasic synaptic events. Receptors expressed in the extrasynaptic space can be tonically activated by low ambient concentrations of GABA that are released from either glial cells, or "spilled over" from the synaptic cleft (Farrant and Nusser, 2005). $GABA_ARs$ containing the α4 and δ subunits have been implicated in mediating tonic inhibition. One of the most prominent extrasynaptic receptors is the α4β3δ subtype (Wisden et al., 1992; Adkins et al., 2001; Stell et al., 2003; Chandra et al., 2006). Currently, there is a mounting interest in the development of agonists which possess the ability to preferentially modulate one of these two forms of inhibitory transmission. The natural agonist GABA appears to be a full agonist at the synaptic α1β2γ2 receptor, while THIP (also known as gaboxadol), a conformationally restricted analogue of GABA, is a partial agonist (Ebert et al.,

1994). Interestingly, at the extrasynaptic α4β3δ receptor, THIP is considered to be a "super agonist" (Sundstrom-Poromaa et al., 2002), having an efficacy greater then GABA. Clinically, THIP exhibits sedative/hypnotic properties which appear to be distinct from the current most widely used drugs, which act as allosteric modulators of the $GABA_AR$ via interactions at the benzodiazepine binding site (Krogsgaard-Larsen et al., 2004). A better understanding of how these two agonists interact with the α1β2γ2 and α4β3δ receptors and the types of conformational changes that these interactions induce, is key to understanding their clinical effects.

Each subunit in the $GABA_AR$ is composed of a large extracellular N-terminal domain, composed of a sandwich of 10 β-sheets, followed by four transmembrane domains (TMDs, M1-M4), of which M2 lines the channel pore, and an extracellular C-terminus. Ligand binding sites are positioned at the subunit-subunit interfaces where there are six conserved stretches ("loops") of amino acids, known as binding loops A-F (Corringer et al., 2000). Binding loops A, B and C are provided by the so-called "principal subunit" while loops D, E, and F are provided by the neighboring, or "complementary subunit". The GABA binding sites at the $GABA_AR$ occurs at the β-α interface, with β being the "principal subunit" and α being the "complementary subunit".

Mokrab et al, previously described a model of the α1β2γ2 $GABA_AR$ (Mokrab et al., 2007) generated by homology modeling with the *Torpedo* nAChR

(Unwin, 2005). Using a similar protocol, we have obtained a model of the α4β3δ $GABA_AR$ (unpublished data). Previous work has shown that a highly conserved arginine residue in binding loop D of the complementary α subunit (figure 4-1) plays a key role in both agonist binding and channel gating (Hartvig et al., 2000; Holden and Czajkowski, 2002; Wagner et al., 2004; Melis et al., 2008). *In silico* docking studies of the agonists GABA and THIP performed on current working models of the α1β2γ2 and α4β3δ $GABA_AR$s suggest that α1Arg94 and α4Arg100 may interact in an agonist and receptor specific manner. In the current study, I observe that both mutant receptors, α1R94Kβ2γ2 and α4R100Kβ3δ, display similar potencies to wild-type receptors with regard to activation by GABA. However, there is a significant decrease in the potency of THIP. In addition, the efficacy of THIP does not change in the α4R100Kβ3δ mutant receptor compared to the wild-type α4β3δ receptor retaining its "super agonist" properties, whereas the α1R94Kβ2γ2 receptor displays a statistically significant reduction in the efficacy of THIP. These findings suggest that this arginine residue may play a role in stabilizing the agonist in the binding pocket, or in obtaining the agonist bound conformational state of the receptor. In addition, this residue appears to have a receptor specific effect on potency and efficacy, suggesting a subunit specific ability to transmit the information generated by agonist binding to the channel gate.

MATERIALS AND METHODS

Materials

GABA and THIP were obtained from Sigma (Sigma-Aldrich Canada Ltd, Oakville, ON)

Comparative Modeling

Structural models for the human $\alpha1\beta2\gamma2$ and $\alpha4\beta3\delta$ $GABA_A$ receptors were generated as described in Mokrab et al. (2007). Briefly, amino acid sequences were taken from UniProt (Wu et al., 2006) and a multiple alignment of these sequences, together with structural homologues collected by BLAST (Altschul et al., 1990), was generated with MAFFT (Katoh et al., 2005). A structure-based alignment of all five chains of the nAChR using the atomic coordinates from *Torpedo marmorata*, 2BG9 (protein database number) (Unwin, 2005) was then used to generate a sequence-structure alignment with this $GABA_A$ receptor subtype using FUGUE (Shi et al., 2001).

In 2BG9 (protein database number, Unwin 2005), the intracellular regions between helices M3 and M4 are disordered and, with the exception of the MA helices, no atomic coordinates are available. Sequence alignments with the above $GABA_A$ receptor subunits showed them to be poorly conserved with those of the nAChR in this region and, as a consequence, these segments of the sequence, together with the short variable N-terminal segments, were excised prior to model building. A 'two-gap' alignment was adopted for this region following the discussion of Ernst et al. (2005). Only one template structure was used for each

subunit of the $GABA_A$ receptor; the basis of the following subunit equivalences being the accepted position of the agonist recognition sites within these two receptors:

nAChR	$GABA_A$ receptor
α (2BG9 chain A)	β2/β3
β (2BG9 chain B)	γ2/δ
δ (2BG9 chain C)	α1/α4
α ((2BG9 chain D)	β2/β3
γ (2BG9 chain E)	α1/α4

The target template pairs were extracted from the sequence structure alignment and concatenated to create a single alignment corresponding to the entire receptor. This was used as input to MODELLER (Sali and Blundell, 1993; Fiser et al., 2000) together with all five chains of the 2BG9 Protein Data Base entry as the template. It should be noted that although our models are based on human sequences, experiments were performed using rat recombinant receptors. These species share greater then 70% sequence identity in the $GABA_AR$ subunits at the amino acid level.

Ligand Docking

The search for putative ligand binding sites is commonly carried out using efficient algorithms to explore the energy landscape of the protein-ligand interaction. In this work, easyDock, based on the method of quantum stochastic tunneling, was used (Todorov et al., 2003; Mancera et al., 2004). This docking was performed by Dr. N.P. Todorov and searched for both GABA and THIP

recognition sites at the interface between chains A and E in the models of both the $\alpha1\beta2\gamma2$ and $\alpha4\beta3\delta$ $GABA_A$ receptor subtypes and their mutants, $\alpha1R94K\beta2\gamma2$ and $\alpha4R100K\beta3\delta$, respectively. 100 simulations were performed for each ligand-receptor complex, several binding modes being generated with each docking simulation. The binding modes were ordered according to their binding scores and, starting from the lowest energy solution the root mean square deviation of each pose (binding mode) with respect to all previous lower energy poses was calculated. If this deviation was higher than a 3 Å threshold, it was added to a list of distinct solutions. Subsequently all docking solutions were assigned to their nearest distinct binding mode and then re-ranked according to the number of docking solutions they attract. These docking studies were performed by Dr. P-L. Chau. It has been shown that selection of a small set of such clusters increases the probability of the correct binding mode being identified (Kallblad et al., 2004).

Mutagenesis

Site directed mutagenesis was performed as described previously described (Derry et al., 2004). Briefly, the QuickChange protocol (Stratagene, La Jolla, CA) was performed to introduce specific substitutions into the rat wild-type $\alpha1$ and $\alpha4$ cDNA sequences. The individual subunit cDNA sequences had been previously subcloned into pcDNA3.1(+) (Invitrogen, San Diego, CA) and these plasmids were used as templates in separate PCR-mediated mutagenesis protocols. The presence of the mutations was then verified by restriction endonuclease digestion and double-stranded cDNA sequencing.

In Vitro Transcription

Plasmid cDNAs encoding the wild-type and mutant $GABA_AR$ subunits were linearized via digestion with *Xba*I (α1, α4, δ and γ2 subunit), FsPI (β3 subunit) and BamHI (β2 subunit). *In vitro* transcription of cRNA was performed using methods previously described (Goldin, 1992). Briefly, the linearized cDNA templates (5µg) were transcribed *in vitro* by T7 RNA polymerase (Invitrogen) in the presence of RNA capping analogue (New England Biolabs) and ribonucleotide triphosphates (NTP mix, Invitrogen). RNA transcripts were then extracted using a 25:24:1 (v/v) phenol:chloroform:isoamyl alcohol mixture. cRNA pellets were resuspended in diethylpyrocarbonate-treated water to a final concentration of 1 µg/µl and aliquots were stored at –80°C until use.

Expression in *Xenopus* Oocytes and Electrophysiology

Isolated follicle-free oocytes from *Xenopus laevis* were microinjected with a total of 50 ng of wild-type and mutant subunit cRNAs in the ratio of 2β:2α:1γ (ratio by weight). Oocytes were incubated in ND96 buffer (5 mM HEPES, 96 mM NaCl, 1.8 mM $CaCl_2$, 2 mM KCl, 1 mM $MgCl_2$, pH 7.6) supplemented with 50 µg/ml gentamicin at 14°C for at least 48 hours prior to recording. Currents elicited by bath application of agonist were measured using standard two-electrode voltage clamp techniques and a GeneClamp500 amplifier (Axon Instruments, Foster City, CA) at a holding potential of -60 mV. Electrodes were filled with 3 M KCl and only electrodes with resistances of 0.5-1.5 MΩ were

used. The recording chamber was continuously perfused (at a rate of ~5 ml/min) with frog Ringer's solution (110 mM NaCl, 2 mM KCl, 1.8 mM$CaCl_2$, 5 mM HEPES, pH 7.4). Agonist-evoked responses were measured by applying drug (via a gravity flow perfusion system) for 10-20 seconds unless otherwise indicated. Drugs were washed out for 12-min between applications to ensure complete recovery from desensitization. Oocytes were only used for experiments when current responses were stable (±5%) between successive applications of agonist. All compounds were dissolved in perfusion buffer.

Statistical Analysis

Statistical analysis of the EC_{50} data was performed, after log transformation, by two-way ANOVA with Bonferroni post-test using GraphPad Prism version 4.00 for Windows, GraphPad Software, San Diego California USA, (Prism). The columns contained the wild type receptors $\alpha1\beta2\gamma2$and $\alpha4\beta3\delta$ together with their mutants $\alpha1R94K\beta2\gamma2$and $\alpha4R100K\beta3\delta$ while the rows contained the two agonists GABA and THIP. Statistical analysis of THIP efficacy was performed using the one-way ANOVA with Bonferroni post-test.

RESULTS

In Silico Modeling of the α1β2γ2 and α4β3δ $GABA_A$Rs Docked with GABA and THIP

In silico docking of the agonists GABA and THIP to the α1β2γ2 $GABA_A$R (figure 4-2) shows that the residue of interest α1R94 points down towards the membrane and is situated closer to the agonist GABA (cyan) than THIP (green). *In silico* docking of the agonists GABA and THIP at the α4β3δ $GABA_A$R (figure 4-3) shows that in the residue of interest, α4R100, the side chain points towards the N-terminus of the receptor and is situated in such an orientation that it could interact with the agonist THIP (green) more closely than GABA (cyan).

Potency of GABA on Wild-Type and Mutant Receptors

α1Arg94/α4Arg100 is located in binding loop D on the complementary subunit of the binding interface. This arginine is conserved in all $GABA_A$R α subunits (figure 4-1). We performed a conservative mutation of this residue to lysine in the α1 and α4 subunits i.e., α1R94K/α4R100K. This charge-conserving mutation alters side chain volume and thus may be predicted to change its specific spatial orientation and its ability to interact with agonists.

Full length mRNAs were injected into *Xenopus* oocytes, and sufficient time was given for protein expression (48 hours), after which I constructed GABA concentration-effect curves. Both mutant receptors displayed a rightward shift in

their concentration-effect relationships compared to their wild-type receptors showing a decrease in potency of GABA (see figure 4-4 and table 4-1). The EC_{50}s for the endogenous agonist GABA on wild-type $\alpha1\beta2\gamma2$ and $\alpha4\beta3\delta$ receptors were 46.6±5.6 and 6.3±0.3μM, respectively (figure 4-4, table 4-1), thus demonstrating that the δ subunit-containing extrasynaptic receptor has a higher apparent affinity for GABA (You and Dunn, 2007). The mutations α1R94K/α4R100K decreased the potency of GABA at each mutant receptor compared to their respective wild-type. This decrease was ~1.7-fold in the $\alpha1\beta2\gamma2$ to $\alpha1R94K\beta2\gamma2$ receptors (figure 4-5, table 4-1)). A larger change in potency was observed with the mutation in the extrasynaptic receptor where an ~7.8-fold shift was seen for the $\alpha4\beta3\delta$ to $\alpha4R100K\beta3\delta$ receptors (figure 4-6, table 4-1). Both of these shifts in agonist potency were statistically significant using Bonferroni post-test analysis which indicated that the EC_{50} for GABA activation of the $\alpha1\beta2\gamma2$ receptor was significantly increased in the mutant $\alpha1R94K\beta2\gamma2$ ($p<0.05$) (figure 4-10). Homologous mutations in $\alpha4\beta3\delta$ to produce $\alpha4R100K\beta3\delta$ again significantly increased the EC_{50} value for GABA ($p<0.001$) (figure 4-10).

Potency of THIP on wild-type and mutant receptors

THIP has a higher potency for the extrasynaptic $\alpha4\beta3\delta$ receptor than the synaptic $\alpha1\beta2\gamma2$ receptor (figure 4-7). The EC_{50}s of THIP on wild-type $\alpha1\beta2\gamma2$ and $\alpha4\beta3\delta$ receptors were 69.5±6.0 and 9.8±2.3 μM, respectively (figure 4-7, table 4-1), thus demonstrating that the δ subunit-containing receptor has a higher

apparent affinity for THIP. THIP also displays a loss of potency on mutant receptors when compared to wild-type where there is an approximate 4.0-fold shift in potency at the $\alpha1\beta2\gamma2$ and $\alpha1R94K\beta2\gamma2$ receptors (figure 4-8, table 4-1). The extrasynaptic receptor displayed a much greater shift in potency with a 19-fold decrease at the $\alpha4\beta3\delta$to $\alpha4R100K\beta3\delta$receptors (figure 4-9). As with GABA, there appears to be a larger shift in potency seen in the extrasynaptic receptor than the synaptic receptor. Both of these shifts in agonist potency were statistically significant with the results of Bonferroni post-test analysis indicating that the EC_{50} for THIP at $\alpha1\beta2\gamma2$ was significantly increased in the mutant $\alpha1R94K\beta2\gamma2$ ($p<0.001$) (figure 4-10). Homologous mutations in $\alpha4\beta3\delta$ to produce $\alpha4R100K\beta3\delta$ again significantly increased the EC_{50} value for THIP ($p<0.001$) (figure 4-10).

Efficacy of THIP at Wild-Type and Mutant Receptors

The efficacy of THIP at wild-type and mutant receptors was determined relative to the response to GABA acting at each receptor (I_{Max} THIP/I_{Max} GABA), where I_{Max} is defined as the maximal amplitude current evoked by a saturating concentration of agonist. THIP behaves as a partial agonist at the wild-type $\alpha1\beta2\gamma2$ receptor with an efficacy of 85.5±4.4%, the $\alpha1R94K$ mutation causes a 64% decrease with THIP having an efficacy of only 31.7±7.2% on the mutant receptor (figure 4-11, table 4-1). Statistical analysis of the change in efficacy of THIP at this mutant receptor using the one-way ANOVA and Bonferroni post-test analysis indicate the change in efficacy of THIP at this mutant receptor is

statistically significant ($p<0.001$***) (figure 4-11). In contrast, THIP behaves as a super agonist at the wild-type $\alpha4\beta3\delta$ receptor with an efficacy of 135.6±4.7%, with no significant change in the efficacy of THIP seen in the $\alpha4R100K\beta3\delta$ mutant receptor (figure 4-11, table 4-1).

DISCUSSION

Previous work suggests that the elucidation of the role of specific amino acid residues in ligand binding and channel gating through mutational analysis is not a trivial process (Colquhoun, 1998). Commonly, the mutant receptor's ability to bind agonist and respond to the binding of agonist are measured by determining the agonist's K_D and EC_{50} at the mutant receptor, respectively. The binding of agonist produces conformational changes in the receptor. Making a distinction between the mutation's effect on ligand binding and its effect on the conformational changes of the receptor is a fundamental problem of modern molecular studies (Colquhoun, 1998). One tool that has been shown to be effective in attempting to differentiate between binding and/or gating is the use of partial agonists. Classically, endogenous neurotransmitters such as glycine and acetylcholine were termed "full agonists". Using single channel analyses, when a full agonist is bound to the receptor, the probability of the channel gate being open, P_{open} (the fraction of time for which the channel is open; that is, the ratio between total open time per cluster and cluster length) is approximately 95-98% (Song and Hatton, 2003; Burzomato et al., 2004). During the 1950s, partial agonists were described. These were agonists that, despite saturating all of the

available binding sites, produced only a fraction of the response elicited by a full agonist. In 1957, del Castillo and Katz (Del Castillo and Katz, 1957) proposed that when an LGIC is occupied by a partial agonist, the gating equilibrium between the open and the closed state lies more towards the closed state then it does for a full agonist. Agonists with greater efficacy were thought to possess a higher affinity for the open state, thus shifting the equilibrium towards channel opening (Monod et al., 1965). This view had been accepted and remained essentially unchanged for almost half a century. However, recent data suggest that there may be another possibility. Current work suggests that after agonist binding, receptors move through a "conformational wave" (Grosman et al., 2000; Chakrapani et al., 2004) that is composed of brief intermediate closed states prior to channel opening. Recent work on the α1 homomeric GlyR and the *Torpedo* nAChR suggests that it is possible to detect and analyze the properties of one of these conformations and this has been termed the "flipped" or "primed" conformation (Burzomato et al., 2004; Mukhtasimova et al., 2009). This work suggests that agonist binding at one site on the receptor is transmitted in an allosteric manner, thus increasing the affinity for the subsequent binding of agonist at other agonist binding sites. The primed conformation of the receptor is thought to be an activated pre-open state. This altered affinity seen in the primed state could be the result of a domain closure around the agonist, essentially trapping it in the binding site. This phenomenon is thought to occur in the extracellular domain of ionotropic glutamate receptors (Jin et al., 2003) and recent

evidence suggests it can also occur in the Cys-loop family of LGICs (Hansen et al., 2005).

The $GABA_A$ receptor is a large, complex, multi-subunit molecule containing subdomains that undergo dynamic conformational changes upon interaction with agonist. Receptor activation involves a global allosteric rearrangement that not only opens the gate but also changes the molecular structure of the binding region. In the $GABA_AR$, ligand binding sites are proposed to be located at the β-α subunit interfaces. Upon agonist binding, the C-loop of the β subunit may approach the α-subunit while the inter-subunit cleft constricts around the agonist (Wagner and Czajkowski, 2001; Hansen et al., 2005). This dynamic process could essentially trap the agonist in the binding pocket, producing the primed/flipped conformational state of the receptor. Recent data suggest that once the receptor is in this transitional state, the steric hindrance at the M2-M3 region of the receptor is somewhat reduced, therefore lowering the energy needed for the opening of the gate. According to this theory, amino acid residues that line the binding pocket in the α subunit could play a role in promoting/stabilizing the receptor in the agonist bound state. α1R94/α4R100 are situated in loop D in which their side chains are predicted (by modeling) to lie toward the binding pocket. This orientation puts this residue in an appropriate position to interact with dynamic processes in the binding site following agonist interaction.

Based on *in silico* modeling and ligand docking data, I proposed that the α1R94K mutation would have a larger effect on the activation properties of GABA than those of THIP (figure 4-2). I expected to observe the opposite effects with the α4R100K mutation i.e., a greater effect on the activation properties of THIP than GABA (figure 4-3). Upon completion of the experiments, I observed that the conserved R-K mutation significantly decreased the potency of each agonist in the mutant receptors when compared to their respective wild-types. In addition, I observed that there was a significantly greater loss in THIP potency at each receptor compared to GABA (figure 4-10). The shift in GABA potency was 1.7-fold in the α1R93K and 7.5-fold in the α4R100K, whereas the shift in THIP potency was over twice that in each receptor, 4.0- and 19.0-fold respectively. However, in our docking studies, the side chain of α1R93 appeared to play a larger role in stabilizing GABA in the binding pocket, while it did not associate with THIP (see figure 4-2, table 4-1).

Previous studies suggested that the positive charge of this loop-D arginine plays a role in stabilizing the negative charge localized in the carboxylate group of GABA (Melis et al., 2008). In our docking studies, this residue appeared to interact with GABA in the α1β2γ2 receptor, but to a lesser extent in the α4β3δ receptor (see figures 4-2 and 4-3). By performing the conservative R-K mutation we have not lost this stabilizing charge; however, the specific location of this charge has changed. It is possible that this alteration in the location of stabilizing charge in the binding pocket could be responsible for the observed loss of potency

of GABA at the mutant receptors. Although this can potentially explain the changes in potency observed with GABA, to date, little is known of the orientation of THIP in the binding pocket. In our docking studies, this loop-D arginine appears only to interact with THIP in the $\alpha4\beta3\delta$ receptor. However, there was a decrease in THIP potency observed in both mutant receptors. These data suggest that THIP may assume additional orientations in the binding pocket other then those proposed in our model. Alternatively, there may be an allosteric effect introduced in the binding site of the mutated receptor, altering receptor-ligand interactions. In addition, it should be taken into consideration that our models of the $\alpha1\beta2\gamma2$ and $\alpha4\beta3\delta$ $GABA_A$Rs are generated via homology modeling with the *Torpedo* nAChR (Unwin, 2005) that possesses two non-equivalent binding sites located at the α-γ and α-δ subunit interfaces. The homology models of the $\alpha1\beta2\gamma2$ and $\alpha4\beta3\delta$ $GABA_A$Rs were generated by aligning the $GABA_A$R α subunits (either $\alpha1$ or $\alpha4$) with the γ and δ subunits from the *Torpedo* nAChR (see methods). This method produces $GABA_A$R models with two non-equivalent binding sites at the β-α subunit interfaces. *In silico* docking studies in this work were carried out at the bindings site homologous to the α-γ *Torpedo* nAChR binding site. Further docking studies are required at the GABA binding sites homologous to the α-δ *Torpedo* nAChR binding site. This future work may provide us with a more complete picture of GABA and THIP docking at the $\alpha1\beta2\gamma2$ and $\alpha4\beta3\delta$ $GABA_A$Rs.

Another interesting finding of the current investigation are those regarding the efficacy of THIP. Classically THIP is considered to be a partial agonist at the synaptic $\alpha1\beta2\gamma2$ receptor while it has been suggested to be a "super agonist" at the extrasynaptic $\alpha4\beta3\delta$ receptor (Ebert et al., 1994; Sundstrom-Poromaa et al., 2002). The current data suggest a receptor-specific effect with regard to efficacy. In the $\alpha1\beta2\gamma2$ wild-type receptor THIP efficacy is 85.5±4.4% that of GABA and in the $\alpha1R94K\beta2\gamma2$ mutant receptor this value is reduced to 31.7±7.2% (see figure 4-11, table 4-1). In contrast, there is no significant loss of efficacy at the extrasynaptic receptor. At the wild-type $\alpha4\beta3\delta$ receptor, the efficacy of THIP is 135.6±4.7% of GABA, while in the $\alpha4R100K\beta3\delta$ receptor it is 129.0±7.1% (see figure 4-11, table 4-1). This receptor-specific loss in the efficacy of THIP may be explained by alterations in the receptor's ability to assume the flipped/primed conformation. This arginine residue may play a role in the stabilization of the agonist bound state, which once reached, may relieve structural restraints at the M2-M3 linker allowing channel activation. Assuming conformational changes in the binding site occur in an efficacy-dependent manner it would suggest that the conformational change upon interaction with THIP would be different from that induced by GABA. My data suggest that this loop-D arginine may play a greater role in achieving and/or maintaining this activated pre-open conformation in the $\alpha1\beta2\gamma2$ receptor, as mutation of this residue significantly reduces the efficacy of THIP. No change in the efficacy of THIP is observed at the $\alpha_4\beta_3\delta$ receptor, suggesting that this residue may play a lesser role in the extrasynaptic receptor. According to our model, the side chains of the loop-D arginine residues are

present in substantially different orientations in each receptor. In the α1β2γ2 receptor this residue points towards the membrane and may interact with the neighboring α1F92 residue (see figure 4-2). However, in the α4β3δ receptor this residue points towards the N-terminus and away from the neighboring α4F98 residue (see figure 4-4). This change in orientation may explain this residues receptor specific role regarding the efficacy of THIP.

Although the data suggest that this arginine residue may play a role in agonist stabilization in the binding pocket and/or agonist induced conformational changes in the ligand binding site, further work is needed. Many residues have been implicated to play a role in ligand binding and channel gating which are not conserved throughout the Cys-loop family. Some investigators have proposed it is not simply single residue pairings that are crucial for receptor function, but the overall charge distribution conservation in distinct subdomains (Xiu et al., 2005).

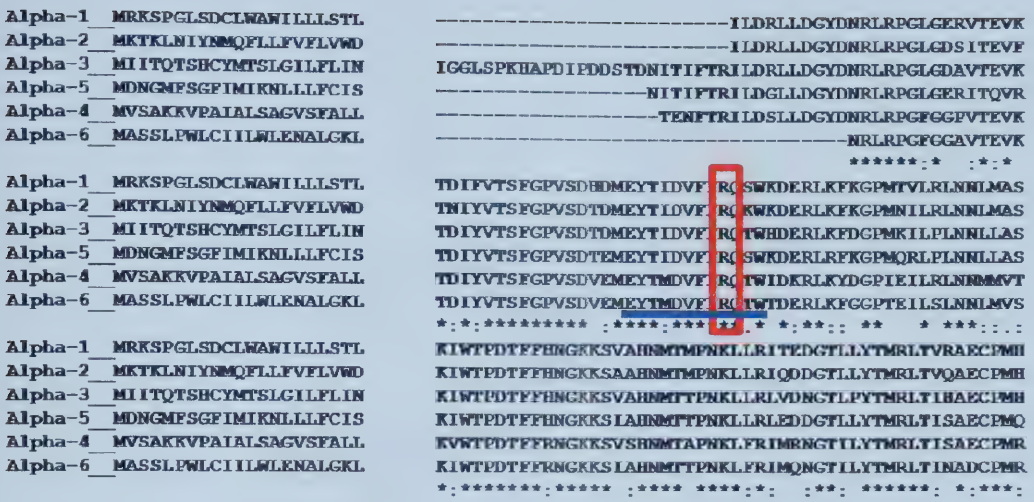

Figure 4-1: Protein sequence alignment of the human $GABA_AR$ α subunits. The location of mutated arginine residues is surrounded by the red box. Conserved amino acids are shown on the bottom line denoted by asterisks. Binding loop D residues are indicated by blue underlining.

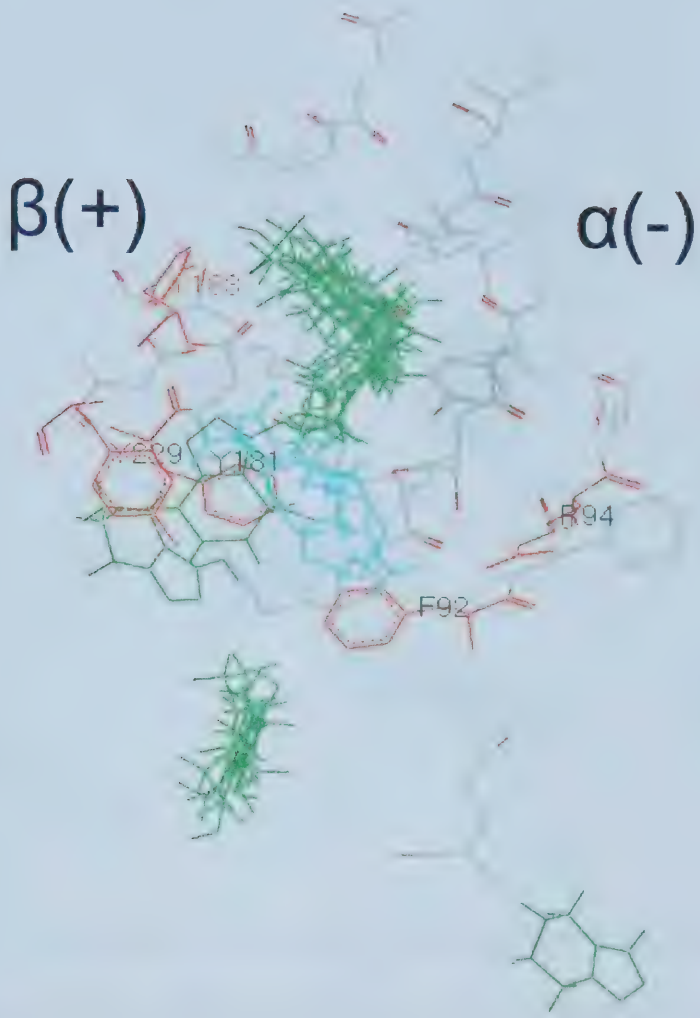

Figure 4-2: Docked clusters of the agonists GABA and THIP in the agonist binding pockets of the α1β2γ2 $GABA_AR$. The α subunit is denoted as (-) while the β subunit is denoted as (+). The recognition site for the α1β2γ2 receptor is shown with pertinent amino acid residues labeled. The binding site is oriented with the long axis of the receptor in the plane of the paper with the extracellular space at the top and viewed from the external face. The GABA clusters are shown in cyan while those for THIP are shown in green.

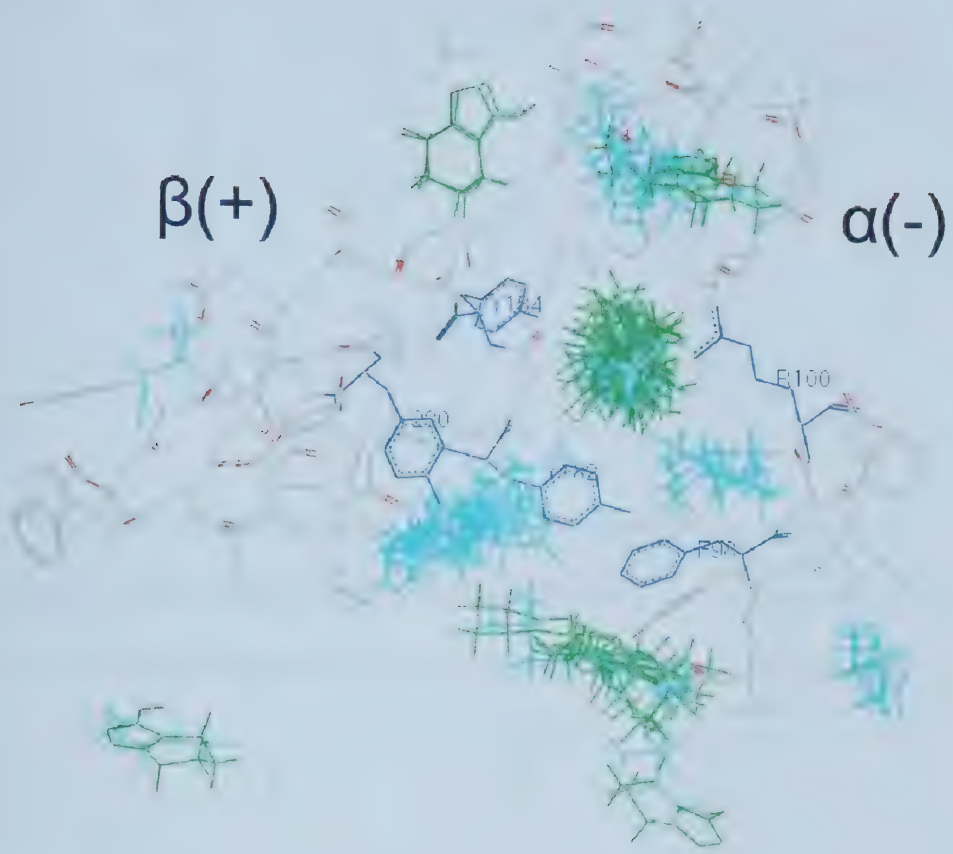

Figure 4-3: Docked clusters of the agonists GABA and THIP in the agonist binding pockets of the α4β3δ $GABA_AR$. The α subunit is denoted as (-) while the β subunit is denoted as (+). The recognition site for the α4β3δ receptor is shown with pertinent amino acid residues labeled. The binding site is oriented with the long axis of the receptor in the plane of the paper with the extracellular space at the top and viewed from the external face. The GABA clusters are shown in cyan while those for THIP are shown in green.

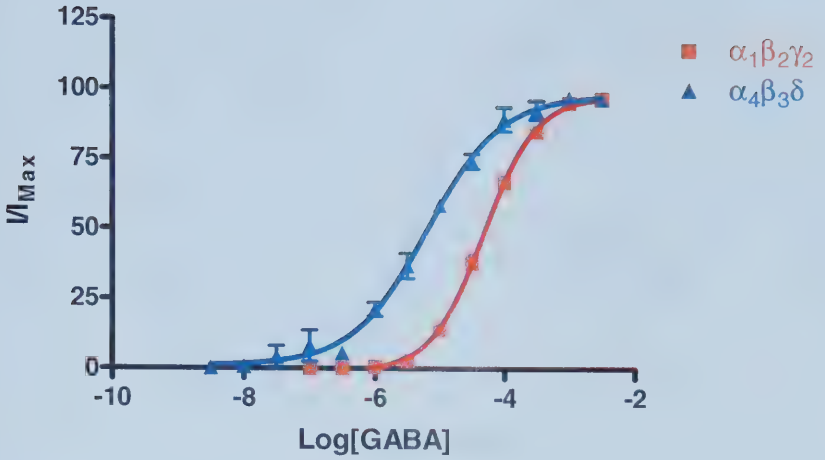

Figure 4-4: Concentration-effect curves for the agonist GABA at wild-type α1β2γ2 (red) and α4β3δ $GABA_A$Rs (blue). The EC_{50} for GABA at α1β2γ2 (red) and α4β3δ $GABA_A$Rs (blue) was 46.6±5.6 and 6.3±0.3 μM, respectively.

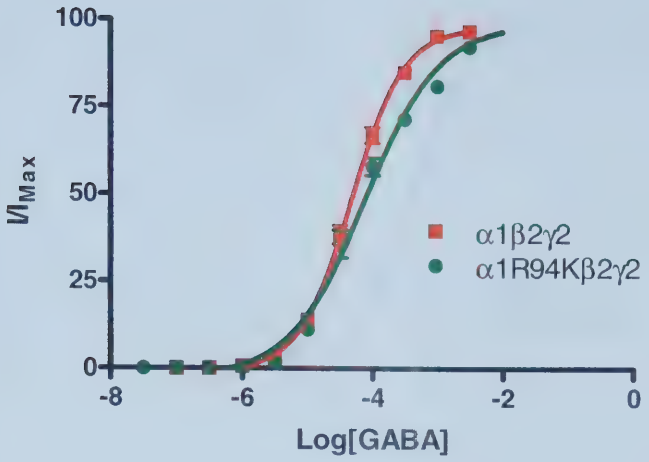

Figure 4-5: Concentration-effect curves for the agonist GABA at the wild-type α1β2γ2 (red) and mutant α1R94Kβ2γ2 (green) $GABA_A$Rs. The EC_{50} for GABA at the α1β2γ2 $GABA_A$R (red) and the mutant α1R94Kβ2γ2 (green) $GABA_A$Rs were 46.6±5.6 and 77.7±10.0 μM respectively. There was an approximately 1.7-fold decrease in potency for GABA observed at the mutant receptor.

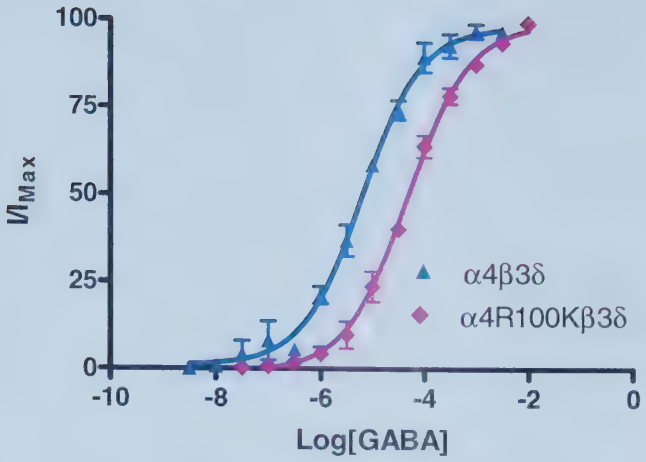

Figure 4-6: Concentration-effect curves for the agonist GABA at the wild-type α4β3δ (blue) and mutant α4R100Kβ3δ (purple) $GABA_A$Rs. The EC_{50} for GABA at the α4β3δ $GABA_A$R (blue) and the mutant α4R100Kβ3δ (purple) $GABA_A$Rs were 6.3±0.3 and 49.2±11.3 μM respectively. There was an approximately 7.8-fold decrease in potency for GABA observed at the mutant receptor.

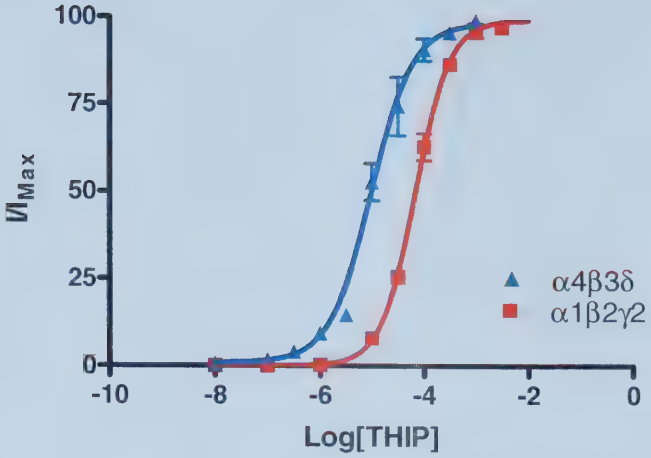

Figure 4-7: Concentration-effect curves for the agonist THIP at wild-type α1β2γ2 $GABA_AR$ (red) and α4β3δ $GABA_ARs$ (blue). The EC_{50} for THIP at α1β2γ2 $GABA_AR$ (red) and α4β3δ $GABA_ARs$ (blue) was 69.5±6.0 and 9.8±2.3 μM, respectively.

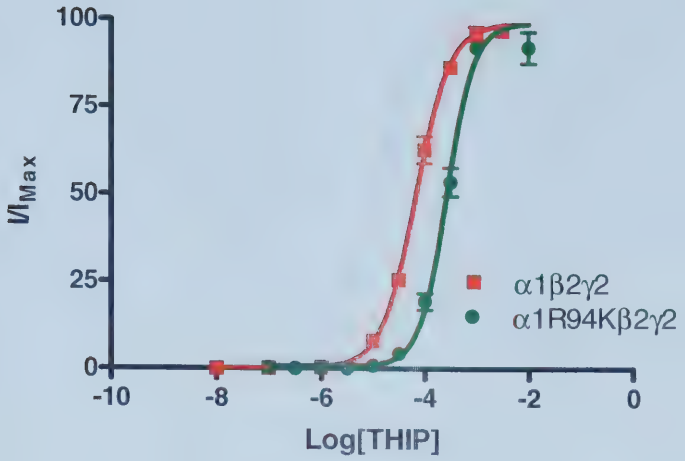

Figure 4-8: Concentration-effect curves for the agonist THIP at the wild-type α1β2γ2 (red) and mutant α1R94Kβ2γ2 (green) $GABA_A$Rs. The EC_{50} for THIP at the wild-type α1β2γ2 (red) and the mutant α1R94Kβ2γ2 (green) $GABA_A$Rs was 69.5±6.0 and 276.7±25.5 μM respectively. There was an approximately 4.0-fold decrease in potency observed for THIP at the mutant receptor.

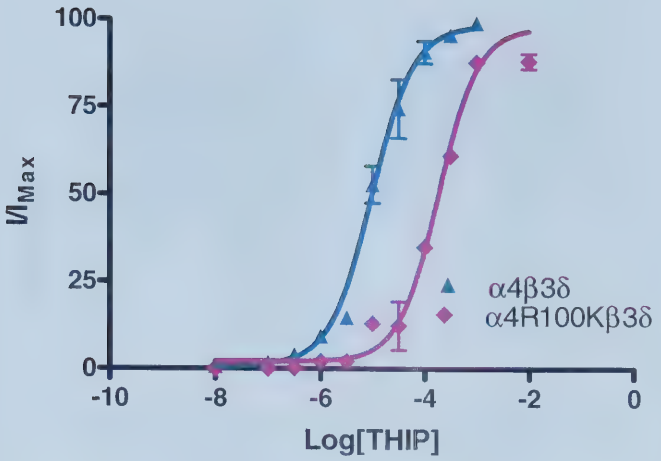

Figure 4-9: Concentration-effect curves for the agonist THIP at the wild-type α4β3δ (blue) and mutant α4R100Kβ3δ (purple) $GABA_A$Rs. The EC_{50} for THIP at the α4β3δ (blue) and the α4R100Kβ3δ (purple) $GABA_A$Rs were 9.8±2.3 and 186.4±3.0 μM respectively. There was an approximately 19.0-fold decrease in potency observed for THIP at the mutant receptor.

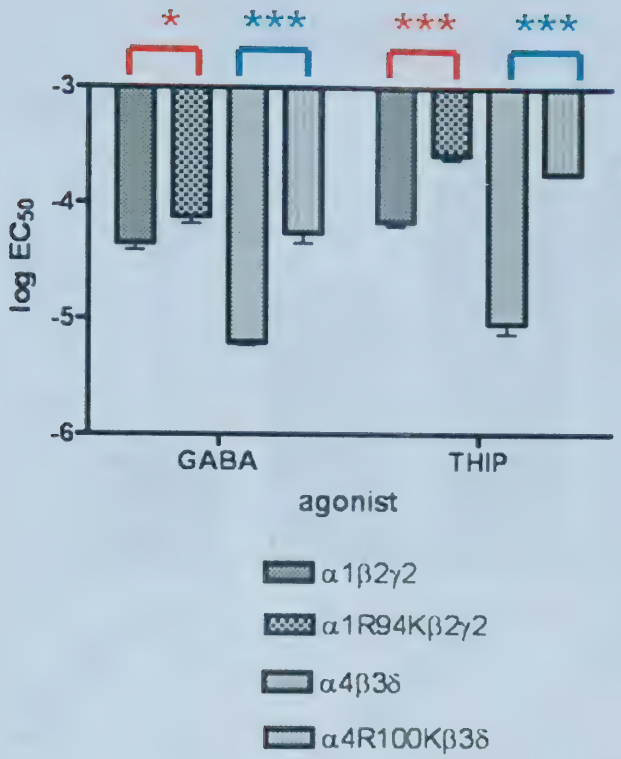

Figure 4-10: Statistical analysis of the EC_{50} data was performed, after log transformation, by two-way ANOVA with Bonferroni post test using GraphPad Prism version 4.00 for Windows, GraphPad Software, San Diego California USA, (Prism). The individual comparisons are summarized graphically. The results of Bonferroni post-test analysis indicates that the EC_{50} for GABA at $\alpha1\beta2\gamma2$ was significantly increased in the mutant $\alpha1R94K\beta2\gamma2$ ($p<0.05$*); a similar increase was found for the agonist THIP ($p<0.001$***). Homologous mutations in $\alpha4\beta3\delta$ to produce $\alpha4R100K\beta3\delta$ again significantly increased the EC_{50} values for both GABA ($p<0.001$***) and THIP ($p<0.001$***).

Figure 4-11: Statistical analysis of the efficacy data was performed by one-way ANOVA with Bonferroni post test using GraphPad Prism version 4.00 for Windows, GraphPad Software, San Diego California USA, (Prism). The columns contained the wild type receptors α1β2γ2 and α4β3δ together with their mutants α1R94Kβ2γ2 and α4R100Kβ3δ and the rows contained the THIP efficacy in relation to GABA, Imax THIP: Imax GABA. The results of Bonferroni post-test analysis indicates that THIPs efficacy at α1β2γ2 was significantly reduced in the mutant α1R94Kβ2γ2 ($p<0.001$***). In contrast, there was no statistically significant reduction in THIPs efficacy between the α4β3δ and α4R100Kβ3δ receptors ($p>0.05$ n.s.).

Table 4-1: Summary of functional data for the effects of GABA and THIP at recombinant α1β2γ2, α1R94Kβ2γ2, α4β3δ and α4R100Kβ3δ $GABA_A$Rs expressed in *Xenopus* oocytes.

Receptor	Agonist	Potency, EC50 (μM)	Efficacy I_{Max}THIP/I_{Max}GABA (%)
α1β2γ2	GABA	46.6±5.6	-
	THIP	69.5±6.0	85.5±4.4
α1R94Kβ2γ2	GABA	77.7±10.0	-
	THIP	276.7±25.5	31.7±7.2
α4β3δ	GABA	6.3±0.3	-
	THIP	9.8±2.3	135.6±4.7
α4R100Kβ3δ	GABA	49.2±11.3	-
	THIP	186.4±3.0	129.0±7.1

REFERENCES

Adkins, C.E., Pillai, G.V., Kerby, J., Bonnert, T.P., Haldon, C., McKernan, R.M., Gonzalez, J.E., Oades, K., Whiting, P.J., Simpson, P.B., 2001. α4β3δ $GABA_A$ receptors characterized by fluorescence resonance energy transfer-derived measurements of membrane potential. J Biol Chem 276, 38934-38939.

Altschul, S.F., Gish, W., Miller, W., Myers, E.W., Lipman, D.J., 1990. Basic local alignment search tool. J Mol Biol 215, 403-410.

Burzomato, V., Beato, M., Groot-Kormelink, P.J., Colquhoun, D., Sivilotti, L.G., 2004. Single-channel behavior of heteromeric α1β glycine receptors: an attempt to detect a conformational change before the channel opens. J Neurosci 24, 10924-10940.

Chakrapani, S., Bailey, T.D., Auerbach, A., 2004. Gating dynamics of the acetylcholine receptor extracellular domain. J Gen Physiol 123, 341-356.

Chandra, D., Jia, F., Liang, J., Peng, Z., Suryanarayanan, A., Werner, D.F., Spigelman, I., Houser, C.R., Olsen, R.W., Harrison, N.L., Homanics, G.E., 2006. $GABA_A$ receptor α 4 subunits mediate extrasynaptic inhibition in thalamus and dentate gyrus and the action of gaboxadol. Proc Natl Acad Sci U S A 103, 15230-15235.

Collingridge, G.L., Olsen, R.W., Peters, J., Spedding, M., 2009. A nomenclature for ligand-gated ion channels. Neuropharmacology 56, 2-5.

Colquhoun, D., 1998. Binding, gating, affinity and efficacy: the interpretation of structure-activity relationships for agonists and of the effects of mutating receptors. Br J Pharmacol 125, 924-947.

Corringer, P.J., Le Novere, N., Changeux, J.P., 2000. Nicotinic receptors at the amino acid level. Annu Rev Pharmacol Toxicol 40, 431-458.

Del Castillo, J., Katz, B., 1957. Interaction at end-plate receptors between different choline derivatives. Proc. R. Soc. Lond. B. Biol. Sci. 146, 369-381.

Derry, J.M., Dunn, S.M., Davies, M., 2004. Identification of a residue in the γ-aminobutyric acid type A receptor α subunit that differentially affects diazepam-sensitive and -insensitive benzodiazepine site binding. J Neurochem 88, 1431-1438.

Ebert, B., Wafford, K.A., Whiting, P.J., Krogsgaard-Larsen, P., Kemp, J.A., 1994. Molecular pharmacology of γ-aminobutyric acid type A receptor agonists and partial agonists in oocytes injected with different alpha, β, and γ receptor subunit combinations. Mol Pharmacol 46, 957-963.

Ernst, M., Bruckner, S., Boresch, S., Sieghart, W., 2005. Comparative models of $GABA_A$ receptor extracellular and transmembrane domains: important insights in pharmacology and function. Mol Pharmacol 68, 1291-1300.

Farrant, M., Nusser, Z., 2005. Variations on an inhibitory theme: phasic and tonic activation of $GABA_A$ receptors. Nat Rev Neurosci 6, 215-229.

Fiser, A., Do, R.K., Sali, A., 2000. Modeling of loops in protein structures. Protein Sci 9, 1753-1773.

Goldin, A.L., 1992. Maintenance of *Xenopus laevis* and oocyte injection. Methods Enzymol 207, 266-279.

Grosman, C., Zhou, M., Auerbach, A., 2000. Mapping the conformational wave of acetylcholine receptor channel gating. Nature 403, 773-776.

Hansen, S.B., Sulzenbacher, G., Huxford, T., Marchot, P., Taylor, P., Bourne, Y., 2005. Structures of *Aplysia* AChBP complexes with nicotinic agonists and antagonists reveal distinctive binding interfaces and conformations. EMBO J 24, 3635-3646.

Hartvig, L., Lukensmejer, B., Liljefors, T., Dekermendjian, K., 2000. Two conserved arginines in the extracellular N-terminal domain of the $GABA_A$ receptor α5 subunit are crucial for receptor function. J Neurochem 75, 1746-1753.

Holden, J.H., Czajkowski, C., 2002. Different residues in the $GABA_A$ receptor α 1T60-α 1K70 region mediate GABA and SR-95531 actions. J Biol Chem 277, 18785-18792.

Jin, R., Banke, T.G., Mayer, M.L., Traynelis, S.F., Gouaux, E., 2003. Structural basis for partial agonist action at ionotropic glutamate receptors. Nat Neurosci 6, 803-810.

Kallblad, P., Mancera, R.L., Todorov, N.P., 2004. Assessment of multiple binding modes in ligand-protein docking. J Med Chem 47, 3334-3337.

Katoh, K., Kuma, K., Toh, H., Miyata, T., 2005. MAFFT version 5: improvement in accuracy of multiple sequence alignment. Nucleic Acids Res 33, 511-518.

Krogsgaard-Larsen, P., Frolund, B., Liljefors, T., Ebert, B., 2004. $GABA_A$ agonists and partial agonists: THIP (Gaboxadol) as a non-opioid analgesic and a novel type of hypnotic. Biochem Pharmacol 68, 1573-1580.

Mancera, R.L., Kallblad, P., Todorov, N.P., 2004. Ligand-protein docking using a quantum stochastic tunneling optimization method. J Comput Chem 25, 858-864.

McKernan, R.M., Rosahl, T.W., Reynolds, D.S., Sur, C., Wafford, K.A., Atack, J.R., Farrar, S., Myers, J., Cook, G., Ferris, P., Garrett, L., Bristow, L., Marshall,

G., Macaulay, A., Brown, N., Howell, O., Moore, K.W., Carling, R.W., Street, L.J., Castro, J.L., Ragan, C.I., Dawson, G.R., Whiting, P.J., 2000. Sedative but not anxiolytic properties of benzodiazepines are mediated by the $GABA_A$ receptor α1 subtype. Nat Neurosci 3, 587-592.

Melis, C., Lummis, S.C., Molteni, C., 2008. Molecular dynamics simulations of GABA binding to the $GABA_C$ receptor: the role of Arg104. Biophys J 95, 4115-4123.

Mody, I., De Koninck, Y., Otis, T.S., Soltesz, I., 1994. Bridging the cleft at GABA synapses in the brain. Trends Neurosci 17, 517-525.

Mokrab, Y., Bavro, V.N., Mizuguchi, K., Todorov, N.P., Martin, I.L., Dunn, S.M., Chan, S.L., Chau, P.L., 2007. Exploring ligand recognition and ion flow in comparative models of the human GABA type A receptor. J Mol Graph Model 26, 760-774.

Monod, J., Wyman, J., Changeux, J.P., 1965. On the Nature of Allosteric Transitions: A Plausible Model. J Mol Biol 12, 88-118.

Mozrzymas, J.W., 2004. Dynamism of $GABA_A$ receptor activation shapes the "personality" of inhibitory synapses. Neuropharmacology 47, 945-960.

Mukhtasimova, N., Lee, W.Y., Wang, H.L., Sine, S.M., 2009. Detection and trapping of intermediate states priming nicotinic receptor channel opening. Nature 459, 451-454.

Olsen, R.W., Sieghart, W., 2008. International Union of Pharmacology. LXX. Subtypes of γ-aminobutyric acid A receptors: classification on the basis of subunit composition, pharmacology, and function. Update. Pharmacol Rev 60, 243-260.

Sali, A., Blundell, T.L., 1993. Comparative protein modelling by satisfaction of spatial restraints. J Mol Biol 234, 779-815.

Shi, J., Blundell, T.L., Mizuguchi, K., 2001. FUGUE: sequence-structure homology recognition using environment-specific substitution tables and structure-dependent gap penalties. J Mol Biol 310, 243-257.

Sieghart, W., 1995. Structure and pharmacology of γ-aminobutyric acid A receptor subtypes. Pharmacol Rev 47, 181-234.

Simon, J., Wakimoto, H., Fujita, N., Lalande, M., Barnard, E.A., 2004. Analysis of the set of $GABA_A$ receptor genes in the human genome. J Biol Chem 279, 41422-41435.

Song, Z., Hatton, G.I., 2003. Taurine and the control of basal hormone release from rat neurohypophysis. Exp Neurol 183, 330-337.

Stell, B.M., Brickley, S.G., Tang, C.Y., Farrant, M., Mody, I., 2003. Neuroactive steroids reduce neuronal excitability by selectively enhancing tonic inhibition mediated by δ subunit-containing $GABA_A$ receptors. Proc Natl Acad Sci U S A 100, 14439-14444.

Sundstrom-Poromaa, I., Smith, D.H., Gong, Q.H., Sabado, T.N., Li, X., Light, A., Wiedmann, M., Williams, K., Smith, S.S., 2002. Hormonally regulated α4β2δ $GABA_A$ receptors are a target for alcohol. Nat Neurosci 5, 721-722.

Todorov, N.P., Mancera, R.L., Monthoux, P.H., 2003. A new quantum stochastic tunneling optimisation method for proein-ligand. Chem. Phys. Lett. 369, 257-263.

Unwin, N., 2005. Refined structure of the nicotinic acetylcholine receptor at 4Å resolution. J Mol Biol 346, 967-989.

Wagner, D.A., Czajkowski, C., 2001. Structure and dynamics of the GABA binding pocket: A narrowing cleft that constricts during activation. J Neurosci 21, 67-74.

Wagner, D.A., Czajkowski, C., Jones, M.V., 2004. An arginine involved in GABA binding and unbinding but not gating of the $GABA_A$ receptor. J Neurosci 24, 2733-2741.

Wisden, W., Laurie, D.J., Monyer, H., Seeburg, P.H., 1992. The distribution of 13 $GABA_A$ receptor subunit mRNAs in the rat brain. I. Telencephalon, diencephalon, mesencephalon. J Neurosci 12, 1040-1062.

Wu, C.H., Apweiler, R., Bairoch, A., Natale, D.A., Barker, W.C., Boeckmann, B., Ferro, S., Gasteiger, E., Huang, H., Lopez, R., Magrane, M., Martin, M.J., Mazumder, R., O'Donovan, C., Redaschi, N., Suzek, B., 2006. The Universal Protein Resource (UniProt): an expanding universe of protein information. Nucleic Acids Res 34, D187-191.

Xiu, X., Hanek, A.P., Wang, J., Lester, H.A., Dougherty, D.A., 2005. A unified view of the role of electrostatic interactions in modulating the gating of Cys loop receptors. J Biol Chem 280, 41655-41666.

You, H., Dunn, S.M., 2007. Identification of a domain in the δ subunit (S238-V264) of the $\alpha4\beta3\delta$ $GABA_A$ receptor that confers high agonist sensitivity. J Neurochem 103, 1092-1101.

CHAPTER 5

General Discussion

GENERAL DISCUSSION

The Cys-loop family of LGICs are multi-subunit allosteric proteins that undergo agonist-induced conformational changes between the closed and open state. The earliest explanation of agonist action described receptor activation and agonist binding as separate events. These assumptions led to a separation between the two classical properties of agonists: affinity and efficacy (Stephenson, 1956). At this point it was suggested that receptors existed in the conformationally and functionally distinct states, active or inactive (Wyman and Allen, 1951b). Upon interaction with agonist it was proposed the equilibrium between the open and closed states shifted towards the open conformation of the protein (Del Castillo and Katz, 1957). These fundamental receptor concepts contributed to the creation of the Monod-Wyman-Changeux (MWC) model of allosteric proteins (Monod et al., 1965). The WMC model suggests partial agonists may be less efficient then full agonists at shifting the equilibrium from the inactive to the active state (Monod et al., 1965). In contrast to the MWC model description of partial agonism, the Koshland-Nemethy-Filmer (KNF) model states that receptors undergo sequential non-concerted structural changes (Koshland et al., 1966), based on this model, different ligands possess the ability to induce distinct receptor conformations.

Previous work has elucidated some key ideas regarding the process of Cys-loop receptor activation, in relation to structure (Brejc et al., 2001;

Unwin et al., 2002; Miyazawa et al., 2003; Celie et al., 2004; Hansen et al., 2005; Dellisanti et al., 2007a) and function (Colquhoun and Sakmann, 1985; Sine et al., 1990; Grosman et al., 2000). These studies have suggested that a conformational change of the binding site may precede channel opening. In addition, these two events must be linked via a series of conformational changes in a successive manner in which discrete subdomains between the binding site and the channel gate move in a concert of rigid body movements (Chakrapani et al., 2004).

In the Cys-loop family of LGICs there is an emerging theme of ligand-specific induced conformational changes and of particular interest is agonist-induced C-loop closure (Hansen et al., 2005). A "conformational wave" hypothesis has been proposed for this family of proteins (Grosman et al., 2000; Chakrapani et al., 2004), where ligand-induced structural changes in the LBD are transmitted to the TMDs. This hypothesis is supported by experimental data suggesting a dynamic role of several loop structures in the N-terminal LBD, including the C-loop, loop 7 (the characteristic Cys-loop), loop 2 and loop 9 play a role in receptor activation (Bera et al., 2002; Kash et al., 2003; Leite et al., 2003; Chakrapani et al., 2004; Kash et al., 2004a; Kash et al., 2004b; Lobo et al., 2004; Hansen et al., 2005; Pless and Lynch, 2009a, b). The dynamic motion of these loops alters interactions between the N-terminal domain and the M2-M3 linker of the TMDs, allowing M2 rotation

and channel gating (Lee and Sine, 2005; Sine and Engel, 2006; Lee et al., 2009).

In 2004, Burzomato et al. analyzed single channel behavior of the heteromeric α1β GlyR attempting to detect conformational changes of the receptor preceding channel opening (Burzomato et al., 2004). The authors attempted to fit 30 different reaction schemes to the steady-state single channel activity evoked by a full range of agonist concentrations. They observed the binding of a second molecule of agonist did so with apparent higher affinity then the first, and the third with higher affinity then the second (Burzomato et al., 2004). According to their data, the third molecule of agonist binds with an equilibrium constant 1400 times less than the first (Burzomato et al., 2004). This work suggests the binding of agonist at one binding site is transmitted allosterically to other binding sites on the receptor molecule. This occurs even in the closed state of the receptor, despite the distance separating these two sites. These observations are similar to those seen with hemoglobin's increase in affinity for the binding of subsequent molecules of oxygen (Wyman and Gill, 1990), which represents a basis for the property of co-opertivity (Wyman and Allen, 1951a).

In 1951, Wyman and Allen suggested a mechanism for the apparent co-operativity of binding between enzymes and substrates (Wyman and Allen, 1951a). This mechanism stated; if a protein could exist in two

conformational states, of which one possessed a higher affinity for ligand, the binding of ligand would cause a shift to the higher affinity form (Wyman and Allen, 1951a), though no direct interaction between multiple binding sites takes place. This mechanism suggests ligand binding changes the conformation of the protein, determining the affinity for ligand. In the heteromeric α1β GlyR it has been suggested the high affinity state of the receptor may be achieved via the receptor changing from the resting state to the "flipped" conformation (Burzomato et al., 2004), after which the receptor can undergo further conformational changes to reach the open state. Current work suggests C-loop closure may be the conformational change responsible for achieving the flipped state of the receptor (Miller and Smart 2010; Hansen et al., 2005; Lape et al., 2008; Mukhtasimova et al., 2009).

In 1957, in order to explain partial agonism, Del Castillo and Katz proposed it was necessary to consider the binding and gating steps independently (Del Castillo and Katz, 1957). The flipped mechanism separates the agonist-induced conformational change of the LBD from channel gating. In 2009 Mukhtasimova et al. used single channel analysis in an attempt to describe the mechanism by which this flipped state of the receptor affects channel gating in the *Torpedo* nAChR (Mukhtasimova et al., 2009). In that study the authors suggest the transition from the closed to open state is dependent on the conformational state of the receptor, i.e. in the primed/flipped state the receptor is more likely to open, independent of the

presence of agonist (Mukhtasimova et al., 2009). Taking this evidence into account, agonist efficacy may be determined by the ability of the agonist-receptor complex to achieve the primed/flipped state, i.e., the degree of C-loop closure caused by the agonist. In addition, crystallization studies of AChBP in the presence of agonists suggest the magnitude of C-loop closure is dependent on agonist efficacy (Hansen et al., 2005).

Chapter 2 described the apparent affinity and efficacy of a series of bis-quaternary agonists at the *Torpedo* nAChR. Compounds of shorter length (interonium distances < 16Å) bound with high affinity to the receptor, though they behaved as weak partial agonists. Though the interaction of these compounds with the binding site are thought to be complex, their chemistry may offer an explanation. Due to the shorter distance separating the ligands two positively charged quaternary nitrogens, these two positive charges may be in close enough proximity to experience a certain amount of repulsion from each other. In theory, this may lead to increased rigidity in the shorter compounds. Although the shorter compounds display high affinity binding to the receptor, their rigid structure could impede C-loop closure. If the receptor cannot achieve C-loop closure this may be interpreted as weak partial agonism. Increasing the distance between the two positively charged quaternary nitrogen atoms may allow for a greater degree of flexibility in the ligand. Increased flexibility in the agonist molecule

may provide less steric hindrance to C-loop closure and receptor priming, resulting in an increase in agonist efficacy.

As the C-loop closes into the capped, or primed, position it is thought to interact with residues on the complimentary subunit of the binding interface (Sine and Engel, 2006). Chapter 4 looked at a highly conserved arginine residue in binding loop-D, located on the complimentary α-subunit in the $GABA_AR$ GABA binding site (Hartvig et al., 2000). I suggest, upon agonist binding, this residue may play a role in achieving and/or stabilizing the primed state of the receptor via interactions of the C-loop of the primary β-subunit. In this study Iobserved a decrease in the potency of the agonists GABA and THIP at the α1R94Kβ2γ2 and α4R100Kβ3δ mutant $GABA_ARs$ in comparison to their relative wild-type receptors. There appeared to be a greater decrease in the potency of THIP than the natural agonist GABA in both receptors. This data suggests this particular residue may play a greater role in the stabilization of THIP than GABA in the binding pocket. In addition, the efficacy of THIP was significantly reduced at the α1R94Kβ2γ2 receptor compared to wild-type. This data suggests an alteration in the receptor's ability to achieve/maintain the agonist bound, C-loop capped conformation (see above).

Chapter 3 describes an attempt to trap the C-loop in the capped position using calculations based on a current model of the α1β2γ2 $GABA_AR$

(Mokrab et al., 2007). The homology model was constructed by aligning the primary amino acid sequence of the $\alpha1\beta2\gamma2$ $GABA_AR$ with the *Torpedo* nAChR, which has been solved to a 4 Å resolution (Unwin, 2005). The aim of comparative/homology protein structural modeling is to develop a three-dimensional working model of a protein of unknown structure via sequence alignment with a protein of known structure (Blundell et al., 1987; Bajorath et al., 1993). Building a successful model requires; (1) similarity between the two sequences and (2) the calculation of a correct alignment between the two sequences. Comparative protein modeling is possible based on the theory that small changes in the proteins sequence equate to small changes in the proteins three-dimensional structure (Chothia and Lesk, 1986). In addition, it has been observed that the three-dimensional structures of proteins within a family may be more conserved then their primary sequences. Therefore, if similarity between two proteins is detected at the primary sequence level, structural similarity may be present (Lesk and Chothia, 1980). Proteins with sequence identity of 40%, or greater, produce reliable alignments, at values less than this regions of low local sequence similarity start to become common (Saqi et al., 1999). Alignments become increasingly difficult once the sequence identity falls to less than 30%, termed the proverbial "twilight zone" of homology modeling (Rost, 1999). As the similarity in sequence decreases, alignments contain an increasingly large number of gaps and alignment errors regardless of the preparation method. Evidence suggests, sequence identities below 30% display a rapid

decrease in the conservation of side-chain packing. Therefore, although protein folding may be maintained the pattern of side-chain interactions is lost (Russell and Barton, 1994; Chung and Subbiah, 1996). Additional sources of error are introduced if segments of the target sequence have no equivalent region in the template structure, this may be represented as insertions, deletions or loops. (van Vlijmen and Karplus, 1997).

I faced two challenges working with the model of the $\alpha1\beta2\gamma2$ $GABA_AR$. This model (Mokrab et al., 2007) was constructed via sequence alignment with the *Torpedo* nAChR, previously resolved to a 4 Å resolution (Unwin, 2005). Sequence homology between subunits of these two receptors is 20-40% (Cheng et al., 2009). In addition, the extracellular region in Unwin's nAChR structure was modeled by alignment with AChBP (Brejc et al., 2001; Unwin, 2005). AChBP shares only a 24% sequence homology with the $\alpha7$ nAChR LBD, 20-24% with other nAChRs subunits and only 15-18% with subunits of other members of the Cys-loop receptor family (Brejc et al., 2001). In addition, AChBP is homopentamer comprised of only the N-terminus LBD, lacking TMDs and an intracellular region. It may be possible that our estimate of the distances separating and/or side chain orientation of the cystienes on the C- and F-loops in the apo- and agonist-bound states of the receptor were inaccurate due to low levels of sequence homology (see chapter 3). Alternatively, our estimate of dynamic movements in these loops may be inaccurate.

CONCLUSIONS AND FUTURE DIRECTIONS

Although we have obtained data on the binding and/or gating of the *Torpedo* nAChR , $\alpha1\beta2\gamma2$ and $\alpha4\beta3\delta$ $GABA_A$Rs there is still much to be determined in this area. Though each chapter of this thesis investigated different hypotheses, there remains one unifying and recurring theme, i.e., the functional effects resulting from agonist interaction with members of the Cys-loop receptor family. Despite not introducing structural alterations in the *Torpedo* nAChR, manipulating the chemical structure of the ligand has provided us with insight into agonist-receptor interactions and possible protein dynamics.

Despite multiple crystal structures of homopentameric proteins related to the N-terminal LBDs of Cys-loop receptors (Brejc et al., 2001; Celie et al., 2004; Bourne et al., 2005; Celie et al., 2005a; Celie et al., 2005b; Ulens et al., 2006; Dellisanti et al., 2007b; Dutertre et al., 2007) and their prokaryotic ancestors (Bocquet et al., 2009; Hilf and Dutzler, 2009b, a) we still lack a complete structure of a heteropentameric Cys-loop receptor at a resolution above 4Å (Unwin, 2005). Nigel Unwin's 4 Å resolution structure of the *Torpedo* nAChR has provided insight into this family of proteins, allowing us to view the α-carbon backbone, overall folding pattern and indication as to which dynamic structures may play a role in ligand binding (Unwin, 2005).

To date, we have yet to obtain a high-resolution crystal structure of a complete receptor from the Cys-loop family. Crystal structures of the *Torpedo* nAChR in the presence of bis-quaternary agonists would provide us with complete understanding of ligand stabilization in the binding pocket as well as conformational changes occurring in the receptor upon agonist recognition. At this point in time, this it is only wishful thinking.

Similar conclusions may be drawn with regard to chapters 3 and 4. Improvements in the structural model of the $\alpha1\beta2\gamma2$ and $\alpha4\beta3\delta$ $GABA_AR$ may provide a more accurate estimate as to which residues in the binding pocket provide stabilization energy to THIP and GABA and help stabilize the C-loop in the capped position. In addition, refinements to the structural model may elucidate which residues come into closer proximity following agonist interaction and C-loop closure. A high-resolution crystal structure of a member of the Cys-loop receptor family may provide us with this information. Though structural alterations introduced via site-directed mutagenesis combined with the electrophysiological measurement of agonist properties provide us with insight into receptor-ligand interaction we are still at a disadvantage. It has been suggested that the interpretation of the structure-activity relationship for agonists at mutated receptors can be complicated task (Colquhoun, 1998) as correct assessment of alterations in the receptors activation parameters at the macroscopic level may be difficult to interpret. Though there are no crystal structures of a anionic member of

the Cys-loop family of receptors there are multiple molecular dynamic simulations and theoretical models (Khatri and Weiss 2010; Trudell and Bertaccini, 2004; Grudzinska et al., 2005; Harrison and Lummis, 2006; Campagna-Slater and Weaver, 2007; Mokrab et al., 2007; Abdel-Halim et al., 2008; Vogel et al., 2009) based on structures of various AChBP's and the *Torpedo* nAChR (Brejc et al., 2001; Unwin, 2005). Although these studies provide structural insight into the Cys-loop receptors they share below 30% sequence homology and fall into the "twilight zone" of homology modeling (Rost, 1999). Obtaining a high-resolution crystal structures of the $\alpha1\beta2\gamma2$ and $\alpha4\beta3\delta$ $GABA_A$Rs, alone or in complex with the agonists GABA or THIP may elucidate the receptor-specific role of the conserved loop-D arginine.

In addition to obtaining high-resolution crystal structures of these proteins, single channel analysis could further the understanding of my work. Single channel analysis of the series of bis-quaternary agonists at the *Torpedo* nAChR as well as GABA and THIP at wild-type and mutant $\alpha1\beta2\gamma2$ and $\alpha4\beta3\delta$ $GABA_A$Rs may provide a more detailed characterization of the receptor-agonist interactions. *Xenopus* oocytes may be utilized for the collection of single channel data (Stuhmer and Parekh, 1995) providing a more detailed kinetic characterization.

In conclusion, there remain many unresolved issues in the area of Cys-loop receptors and the relationship between ligand recognition and receptor

activation. Cys-loop receptors possess a rich pharmacology making it imperative that we fully elucidate ligand-receptor interactions and provide understanding for both the basic and medical sciences.

REFERENCES

Abdel-Halim, H., Hanrahan, J.R., Hibbs, D.E., Johnston, G.A., Chebib, M., 2008. A molecular basis for agonist and antagonist actions at $GABA_C$ receptors. Chem Biol Drug Des 71, 306-327.

Bajorath, J., Stenkamp, R., Aruffo, A., 1993. Knowledge-based model building of proteins: concepts and examples. Protein Sci 2, 1798-1810.

Bera, A.K., Chatav, M., Akabas, M.H., 2002. $GABA_A$ receptor M2-M3 loop secondary structure and changes in accessibility during channel gating. J Biol Chem 277, 43002-43010.

Blundell, T.L., Sibanda, B.L., Sternberg, M.J., Thornton, J.M., 1987. Knowledge-based prediction of protein structures and the design of novel molecules. Nature 326, 347-352.

Bocquet, N., Nury, H., Baaden, M., Le Poupon, C., Changeux, J.P., Delarue, M., Corringer, P.J., 2009. X-ray structure of a pentameric ligand-gated ion channel in an apparently open conformation. Nature 457, 111-114.

Bourne, Y., Talley, T.T., Hansen, S.B., Taylor, P., Marchot, P., 2005. Crystal structure of a Cbtx-AChBP complex reveals essential interactions between snake alpha-neurotoxins and nicotinic receptors. EMBO J 24, 1512-1522.

Brejc, K., van Dijk, W.J., Klaassen, R.V., Schuurmans, M., van Der Oost, J., Smit, A.B., Sixma, T.K., 2001. Crystal structure of an ACh-binding protein reveals the ligand-binding domain of nicotinic receptors. Nature 411, 269-276.

Burzomato, V., Beato, M., Groot-Kormelink, P.J., Colquhoun, D., Sivilotti, L.G., 2004. Single-channel behavior of heteromeric $\alpha 1\beta$ glycine receptors: an

attempt to detect a conformational change before the channel opens. J Neurosci 24, 10924-10940.

Campagna-Slater, V., Weaver, D.F., 2007. Molecular modelling of the $GABA_A$ ion channel protein. J Mol Graph Model 25, 721-730.

Celie, P.H., Kasheverov, I.E., Mordvintsev, D.Y., Hogg, R.C., van Nierop, P., van Elk, R., van Rossum-Fikkert, S.E., Zhmak, M.N., Bertrand, D., Tsetlin, V., Sixma, T.K., Smit, A.B., 2005a. Crystal structure of nicotinic acetylcholine receptor homolog AChBP in complex with an α-conotoxin PnIA variant. Nat Struct Mol Biol 12, 582-588.

Celie, P.H., Klaassen, R.V., van Rossum-Fikkert, S.E., van Elk, R., van Nierop, P., Smit, A.B., Sixma, T.K., 2005b. Crystal structure of acetylcholine-binding protein from *Bulinus truncatus* reveals the conserved structural scaffold and sites of variation in nicotinic acetylcholine receptors. J Biol Chem 280, 26457-26466.

Celie, P.H., van Rossum-Fikkert, S.E., van Dijk, W.J., Brejc, K., Smit, A.B., Sixma, T.K., 2004. Nicotine and carbamylcholine binding to nicotinic acetylcholine receptors as studied in AChBP crystal structures. Neuron 41, 907-914.

Chakrapani, S., Bailey, T.D., Auerbach, A., 2004. Gating dynamics of the acetylcholine receptor extracellular domain. J Gen Physiol 123, 341-356.

Cheng, J., Ju, X.L., Chen, X.Y., Liu, G.Y., 2009. Homology modeling of human α1β2γ2 and house fly β3 GABA receptor channels and Surflex-docking of fipronil. J Mol Model 15, 1145-1153.

Chothia, C., Lesk, A.M., 1986. The relation between the divergence of sequence and structure in proteins. EMBO J 5, 823-826.

Chung, S.Y., Subbiah, S., 1996. A structural explanation for the twilight zone of protein sequence homology. Structure 4, 1123-1127.

Colquhoun, D., 1998. Binding, gating, affinity and efficacy: the interpretation of structure-activity relationships for agonists and of the effects of mutating receptors. Br J Pharmacol 125, 924-947.

Colquhoun, D., Sakmann, B., 1985. Fast events in single-channel currents activated by acetylcholine and its analogues at the frog muscle end-plate. J Physiol 369, 501-557.

Del Castillo, J., Katz, B., 1957. Interaction at end-plate receptors between different choline derivatives. Proc. R. Soc. Lond. B. Biol. Sci. 146, 369-381.

Dellisanti, C.D., Yao, Y., Stroud, J.C., Wang, Z.Z., Chen, L., 2007a. Crystal structure of the extracellular domain of nAChR alpha1 bound to alpha-bungarotoxin at 1.94 Å resolution. Nat Neurosci 10, 953-962.

Dellisanti, C.D., Yao, Y., Stroud, J.C., Wang, Z.Z., Chen, L., 2007b. Structural determinants for α-neurotoxin sensitivity in muscle nAChR and their implications for the gating mechanism. Channels (Austin) 1, 234-237.

Dutertre, S., Ulens, C., Buttner, R., Fish, A., van Elk, R., Kendel, Y., Hopping, G., Alewood, P.F., Schroeder, C., Nicke, A., Smit, A.B., Sixma, T.K., Lewis, R.J., 2007. AChBP-targeted α-conotoxin correlates distinct binding orientations with nAChR subtype selectivity. EMBO J 26, 3858-3867.

Grosman, C., Zhou, M., Auerbach, A., 2000. Mapping the conformational wave of acetylcholine receptor channel gating. Nature 403, 773-776.

Grudzinska, J., Schemm, R., Haeger, S., Nicke, A., Schmalzing, G., Betz, H., Laube, B., 2005. The β subunit determines the ligand binding properties of synaptic glycine receptors. Neuron 45, 727-739.

Hansen, S.B., Sulzenbacher, G., Huxford, T., Marchot, P., Taylor, P., Bourne, Y., 2005. Structures of *Aplysia* AChBP complexes with nicotinic agonists and antagonists reveal distinctive binding interfaces and conformations. EMBO J 24, 3635-3646.

Harrison, N.J., Lummis, S.C., 2006. Molecular modeling of the $GABA_C$ receptor ligand-binding domain. J Mol Model 12, 317-324.

Hartvig, L., Lukensmejer, B., Liljefors, T., Dekermendjian, K., 2000. Two conserved arginines in the extracellular N-terminal domain of the $GABA_A$ receptor α5 subunit are crucial for receptor function. J Neurochem 75, 1746-1753.

Hilf, R.J., Dutzler, R., 2009a. A prokaryotic perspective on pentameric ligand-gated ion channel structure. Curr Opin Struct Biol.

Hilf, R.J., Dutzler, R., 2009b. Structure of a potentially open state of a proton-activated pentameric ligand-gated ion channel. Nature 457, 115-118.

Kash, T.L., Dizon, M.J., Trudell, J.R., Harrison, N.L., 2004a. Charged residues in the β2 subunit involved in $GABA_A$ receptor activation. J Biol Chem 279, 4887-4893.

Kash, T.L., Jenkins, A., Kelley, J.C., Trudell, J.R., Harrison, N.L., 2003. Coupling of agonist binding to channel gating in the $GABA_A$ receptor. Nature 421, 272-275.

Kash, T.L., Trudell, J.R., Harrison, N.L., 2004b. Structural elements involved in activation of the γ-aminobutyric acid type A ($GABA_A$) receptor. Biochem Soc Trans 32, 540-546.

Khatri, A., Weiss, D.S., The role of Loop F in the activation of the GABA receptor. J Physiol 588, 59-66.

Koshland, D.E., Jr., Nemethy, G., Filmer, D., 1966. Comparison of experimental binding data and theoretical models in proteins containing subunits. Biochemistry 5, 365-385.

Lape, R., Colquhoun, D., Sivilotti, L.G., 2008. On the nature of partial agonism in the nicotinic receptor superfamily. Nature 454, 722-727.

Lee, W.Y., Free, C.R., Sine, S.M., 2009. Binding to gating transduction in nicotinic receptors: Cys-loop energetically couples to pre-M1 and M2-M3 regions. J Neurosci 29, 3189-3199.

Lee, W.Y., Sine, S.M., 2005. Principal pathway coupling agonist binding to channel gating in nicotinic receptors. Nature 438, 243-247.

Leite, J.F., Blanton, M.P., Shahgholi, M., Dougherty, D.A., Lester, H.A., 2003. Conformation-dependent hydrophobic photolabeling of the nicotinic receptor: electrophysiology-coordinated photochemistry and mass spectrometry. Proc Natl Acad Sci U S A 100, 13054-13059.

Lesk, A.M., Chothia, C., 1980. How different amino acid sequences determine similar protein structures: the structure and evolutionary dynamics of the globins. J Mol Biol 136, 225-270.

Lobo, I.A., Mascia, M.P., Trudell, J.R., Harris, R.A., 2004. Channel gating of the glycine receptor changes accessibility to residues implicated in receptor potentiation by alcohols and anesthetics. J Biol Chem 279, 33919-33927.

Miller, P.S., Smart, T.G., Binding, activation and modulation of Cys-loop receptors. Trends Pharmacol Sci.

Miyazawa, A., Fujiyoshi, Y., Unwin, N., 2003. Structure and gating mechanism of the acetylcholine receptor pore. Nature 423, 949-955.

Mokrab, Y., Bavro, V.N., Mizuguchi, K., Todorov, N.P., Martin, I.L., Dunn, S.M., Chan, S.L., Chau, P.L., 2007. Exploring ligand recognition and ion flow in comparative models of the human GABA type A receptor. J Mol Graph Model 26, 760-774.

Monod, J., Wyman, J., Changeux, J.P., 1965. On the Nature of Allosteric Transitions: A Plausible Model. J Mol Biol 12, 88-118.

Mukhtasimova, N., Lee, W.Y., Wang, H.L., Sine, S.M., 2009. Detection and trapping of intermediate states priming nicotinic receptor channel opening. Nature 459, 451-454.

Pless, S.A., Lynch, J.W., 2009a. Ligand-specific conformational changes in the α1 glycine receptor ligand-binding domain. J Biol Chem 284, 15847-15856.

Pless, S.A., Lynch, J.W., 2009b. Magnitude of a conformational change in the glycine receptor β1-β2 loop is correlated with agonist efficacy. J Biol Chem 284, 27370-27376.

Rost, B., 1999. Twilight zone of protein sequence alignments. Protein Eng 12, 85-94.

Russell, R.B., Barton, G.J., 1994. Structural features can be unconserved in proteins with similar folds. An analysis of side-chain to side-chain contacts secondary structure and accessibility. J Mol Biol 244, 332-350.

Saqi, M.A.S., Russel, R.B., Sternberg, M.J.E., 1999. Misleading local sequence alignments: implications for comparative protein modeling. Protein Eng 11, 627-630.

Sine, S.M., Claudio, T., Sigworth, F.J., 1990. Activation of *Torpedo* acetylcholine receptors expressed in mouse fibroblasts. Single channel current kinetics reveal distinct agonist binding affinities. J Gen Physiol 96, 395-437.

Sine, S.M., Engel, A.G., 2006. Recent advances in Cys-loop receptor structure and function. Nature 440, 448-455.

Stephenson, R.P., 1956. A modification of receptor theory. Br J Pharmacol Chemother 11, 379-393.

Stuhmer, W., Parekh, A.B., 1995. Electrophysiological recordings from *Xenopus* oocytes. Single-Channel Recording, Second Edition, . Plenum Press, New York, pp. 341-356.

Trudell, J.R., Bertaccini, E., 2004. Comparative modeling of a $GABA_A$ α1 receptor using three crystal structures as templates. J Mol Graph Model 23, 39-49.

Ulens, C., Hogg, R.C., Celie, P.H., Bertrand, D., Tsetlin, V., Smit, A.B., Sixma, T.K., 2006. Structural determinants of selective α-conotoxin binding to a nicotinic acetylcholine receptor homolog AChBP. Proc Natl Acad Sci U S A 103, 3615-3620.

Unwin, N., 2005. Refined structure of the nicotinic acetylcholine receptor at 4Å resolution. J Mol Biol 346, 967-989.

Unwin, N., Miyazawa, A., Li, J., Fujiyoshi, Y., 2002. Activation of the nicotinic acetylcholine receptor involves a switch in conformation of the α subunits. J Mol Biol 319, 1165-1176.

van Vlijmen, H.W., Karplus, M., 1997. PDB-based protein loop prediction: parameters for selection and methods for optimization. J Mol Biol 267, 975-1001.

Vogel, N., Kluck, C.J., Melzer, N., Schwarzinger, S., Breitinger, U., Seeber, S., Becker, C.M., 2009. Mapping of disulfide bonds within the amino-terminal extracellular domain of the inhibitory glycine receptor. J Biol Chem 284, 36128-36136.

Wyman, J., Allen, D.W., 1951a. The problem of the heme interactions in hemoglobin and the basis of the Bohr effect. J. Polymer. Sci. VII, 499-518.

Wyman, J., Gill, S.J., 1990. Binding and linkage of functional chemistry of biological macromolecules. University Science Books, Mill Valley, CA.

Wyman, J.W., Allen, D.W., 1951b. The problem of the heme interactions in hemoglobin and the basis of the bohr effect. J. Polymer. Sci. VII, 499-518.

C12329